NOVEL BIODEGRADABLE AND BIOCOMPATIBLE ELASTOMERS FOR ENDOSTATIN DELIVERY

HANY ELLABOUDY

NOVEL BIODEGRADABLE AND BIOCOMPATIBLE ELASTOMERS FOR ENDOSTATIN DELIVERY

By

© Hany Ellaboudy

A thesis submitted to the

School of Graduate Studies

in partial fulfilment of the

requirements for the degree of

Master of Science in Pharmacy

School of Pharmacy

Memorial University of Newfoundland

May 2008

St. John's Newfoundland Canada

Abstract

Long term, localized continuous release of Endostatin (END) in the vicinity of tumour bed represents a new strategy for neoplastic treatment. The main reason of localization is to maximize the therapeutic outcome and at the same time to reduce the toxic effects on the surrounding tissues due to the exposure to the angiogenesis inhibitory effect of END. The main objective of this study was to design and formulate a biodegradable and biocompatible polymeric device for delivering END at a sustained and constant rate, and at a concentration within its therapeutic window by utilizing the osmotic release mechanism. The new device was prepared by mixing of END with osmotically active excipients and incorporate the mixture as solid particles within a rubbery polyermic matrix. The results demonstrated that this new device achieved a constant and sustained release rate for END for a certain period.

Acknowledgments

During the preparation of this thesis, many people supported me directly and indirectly, so I would like to express my deep gratitude and appreciation to all of them. In particular, Pharmacy, Chemistry and Biochemistry faculty members, staff and graduate students.

I would like also to acknowledge my research supervisor Dr. Husam Younes for his guidance during my program. My thanks are extended to my co-supervisor Dr. Mohsen Daneshtalab, and supervisory committee member Dr. Ken Kao for their constructive comments through this thesis.

A special thank-you goes to Dr. Karen Hattenhauer, Dr. Christina Bottaro, and Ms. Margaret Connors for providing continuous advices.

I am highly thankful to Dr. Linda Hensman, Dr. Chet Jablonski, Dr. Mahmoud Haddara and Dr. Noreen Golfman for their endless support, valuable recommendations and constant encouragement during this work.

I sincerely thank Ms. Linda Thompson, Ms. Julie Collins, Mr. Terrence Madhujith and Dr. Najla Ben-Ameur for their assistance and technical support.

I would also like to thank Ms. Denise Burke, Ms. Heather Bugler, Ms. Janet Robinso, Ms. Paula Ryan, and Ms. Sharon Tucker from the School of Pharmacy for their help during this program.

I would like to express my deep gratitude to all my family members and friends, especially my great father, aunt and sister for their love and support through this study.

My exceptional acknowledgement goes to my wife who played an important role to support me in the difficult moments during this research, she was always there when I needed her, and her efforts cannot be forgotten.

Table of Contents

List of Tables

List of Figures

LIST OF ABBREVIATIONS AND SYMBOLS

^{1}H-NMR	Proton Nuclear Magnetic Resonance
ACRL	Acryloyl Chloride
APCI	Atmospheric Pressure Chemical Ionization
APOT	Acrylated Poly(octanediol-tartarate)
Arg	Arginine
AUP	Area Under Peak
BCP	2,2-bis(ε-caprolactone-4-yl)-propane
bFGF	Basic Fibroblast Growth Factor
BSA	Bovine Serum Albumin
CLP	Cationic Liposome Complex
DCM	Dichloromethane
DLS	Dynamic Laser Scattering
DMAP	4-Dimethyl Amionpyridine
DMPA	2,2-Dimethoxy-2-Phenyl-Acetophenone
DNA	Deoxyribonucleic Acid
DSC	Differential Scanning Calorimetry
DW	Deionized Water
E	Young's Modulus
EC	Endothelial Cells
ELISA	Enzyme-Linked ImmunoSorbent Assay
END	Endostatin
FDA	Food and Drug Administration
FT-IR	Fourier Transfer Infrared
GPC	Gel Permeation Chromatography
IA	Intraarterial
IC	Intracerebral
IM	Intratumoral
IP	Intraperitoneal

IU	International Unit
IV	Intravenous
KDA	Kilo Dalton
LC-MS	Liquid Chromatography with Mass Spectrometry
LWUV	Low Wave Ultra Violet
mCPBA	m-Chloroperoxybenzoic Acid
MHz	Megahertz
mm	Millimetre
MMP	Matrix Metalloproteinase
MPa	Mega Pascal
MS	Mass Spectroscopy
N	Newton
PBS	Phosphate Buffer Saline
pCPP:SA	polyanhydride-poly-(bis-[carboxyphenoxy-propane]–sebacic acid) polymer
PD	Precision Detector
PDA	Personal Digital Assistant
PEG	Polyethylene Glycol
PK	Pharmacokinetics
PLGA	Poly(DL-lactic-*co*-glycolic Acid)
PN	Pilocarpine Nitrate
POT	Poly(octanediol-tartarate)
PPM	Part Per Million
rEND	Recombinant Endostatin
rhEND	Recombinant Human Endostatin
SC	Subcutaneous
SnOct	Stannous Octoate
TEA	Triethylamine
Tg	Glass Transition Temperature
THF	Tetrahydrofuran

Tm	Melting Temperature
TMS	Tetramethylsilane
UV	Ultra Violet
UV/VIS	Ultraviolet-Visible
V/V	Volume Per Volume
VEGF	Vascular Endothelial Growth Factor
W/O/W	Water in Oil in Water
W/W	Weight Per Weight
ε	Strain
λ_b	Extension Ratio
σ	Tensile Stress

Chapter 1.

1.1 Overview

Over the past few decades, and with the development of recombinant protein technology, there has been wide interest in using therapeutic proteins for the treatment of viral and neoplastic diseases. Endostatin (END) is one of the powerful angiogenic inhibitors that has been investigated for cancer therapy. The use of END for long-term and localized delivery has been hindered by the lack of a delivery vehicle that can release active END at a sustainable rate within the therapeutic window. The most widely used route of administration for protein drugs is systemical, via multiple injections. This route has been reported to have many problems. As a result, it is a highly desirable goal to prepare and develop a device that can provide a persistently high dosage at a continuous release rate locally within the target area, with minimal systemic exposure to the systemic circulation. The following review of literature outlines the mechanism of action, physiochemical properties, pharmacokinetics and different modes of delivery of END. The advantages and disadvantages of delivery systems of END have been evaluated in order to determine the optimal method to administer this polypeptide drug. The following chapters describe the synthesis and characterization of a novel biodegradable elastomeric delivery system to deliver this drug with a constant and sustained release. Two hydrophilic drugs were used in the study. Pilocarpine Nitrate (PN) was used as a model drug as it is a peptidomimetic, and Endostatin (END) was used as a model protein drug.

Chapter 2. Endostatin: Evaluation of Delivery Systems and Routes of Administration Used in Cancer Therapy

2.1 ABSTRACT

Over the past two decades, Endostatin (END), one of the potent angiogenesis inhibitors has become a treatment for a variety of tumors and viral diseases. Several routes and delivery strategies have been reported to deliver END, however, few of them have been successful in the reduction of side effects and the optimization of the therapeutic outcome. The mechanism of action, physiochemical properties, pharmacokinetics and different modes of delivery of END are discussed in this review. The advantages and disadvantages of the delivery systems of END have been discussed to direct the study and determine the most appropriate method to administer this drug. To conclude, a long-term, site localized delivery and sustained release of END are very important strategies for the delivery of this polypeptide drug.

2.2 INTRODUCTION

The clinical use of anti-angiogenic agents developed following the introduction of the angiogenesis theory by Folkman in 1971.[1] Many clinical studies have demonstrated them to be effective in the treatment of viral, neoplastic, and metastatic diseases.[2-4] Many excellent research papers have reviewed their stability, immunobiological properties, amino acid sequence, classification and the mechanisms by which they exert their anti-tumoral activities.[5-10]

Angiogenesis is a normal process in the body, and involves the production of new blood vessels from existing ones. The angiogenesis process is characterized by a number of chronological events. Prior to neovascularization, endothelial cells exist in a near inert state with only about 1 in every 10,000 undergoing division at a given time.[11] The turnover rate of endothelial cells increases up to 50-fold during the formation of a new vascular bud.[12] These events require the remodeling of the extracellular matrix, which can also promote angiogenesis by angiogenic stimulators. The extracellular matrix surrounds the vessels and growth factors combine to promote endothelial cell migration towards the tumor mass. These endothelial cells supply the framework for the new vessels. Endothelial cell sprouts organize into tubular structures and connect to the vascular network.[13] Generally, newly formed capillaries are composed of two cell types, endothelial cells and pericytes, which have the capacity to produce entire capillary networks.

This process is needed to provide the cells with the necessary nutrients and oxygen required for their survival. Angiogenesis is also required whenever there is growth of new tissues, such as during fetal development, wound healing, and the menstrual cycle. Vessel growth is normally controlled by a finely tuned balance between angiogenic inhibitors and stimulators.[14-15] When new capillary growth is desired, the angiogenic stimulators launch signals to the endothelial cells (EC) that line blood vessels. The activated EC will then produce enzymes that break down the surrounding tissue, which permits the EC to proceed beyond the confines of the blood vessel. The EC continue to divide and differentiate, until sprouting and new capillary branch formation is completed.[16] It is also reported that tumor growth affects this equilibrium between stimulators and inhibitors to stimulate new capillary growth, needed for

their nourishment to continue to grow. With access to the circulatory system, the tumors can metastasize to other parts of the body.[1]

According to the mechanism of action, there are two main classes of angiogenesis inhibitors, designated as direct and indirect inhibitors.[17] Direct inhibitors such as END and Angiostatin target EC rather than the tumor cells themselves.[18] In addition, they seem to preferentially target tumor EC versus normal EC by inhibiting the EC proliferation, migration, and tube formation of the tumor and induce apoptosis.[19-21] Indirect angiogenic factors, such as Interferon-alpha and Ribavirin, target tumor cells by preventing the expression of angiogenic growth factors and their receptors.[22] It has been suggested by Hanahan *et al* that direct inhibitors of angiogenesis may be subdivided into three other subgroups.[23] The first group is the pure angiogenesis inhibitors, which inhibit the new vessel growth but have no effect on existing tumor vessels. The second group is the tumor vessels toxins which damage existing tumor vasculature and, the third group to which END belongs is called the dual action agents, which combine these two effects.

In cancer treatment, END is administered as a combined therapy to tumor cells. It acts as an adjuvant and enhances the delay in tumor growth. END possesses several properties related to tumor neovascularization that makes it different from the other anti-angiogeneic factors. First, it is a potent inhibitor of EC proliferation, migration, tube formation, and tumor growth. Second, it directly induces apoptosis. Finally and the most important, it does not develop drug resistance which prevents EC from responding to various proangiogenic stimuli.[17,24,25]

Since its discovery, END has been reported to have many applications in the treatment of a number of immunological, viral and neoplastic diseases. These include endometriotic lesions,[26] a number of different ectopic tumors,[27-29] coronary artery diseases,[30] atherosclerosis,[31] rheumatoid arthritis,[32] proliferative diabetic retinopathy,[33] obesity,[34] Down Syndrome,[35] ectopic tumors,[36] gliosarcoma,[37,38] metastatic breast cancer,[39] and different types of carcinomas.[40-42] A sustained and high dose of END was always needed on the target site in cases where reaching the tumor site by the systemic route is impossible, as in the case of brain tumors.[38] For the treatment of the diseases mentioned above, END has attracted extensive attention and, in the last two decades, scientists have been exploring its clinical uses and therapeutic potential. Now, angiogenesis inhibitors are being studied in over 100 laboratories and 40 biotechnology companies. A detailed list of angiogenic agents currently under study may be found in many other reviews.[43-45]

The first human clinical trials using END began in 1999. This trial was a phase I trial that was designed to study the safety of the drug rather than its effectiveness. This type of trial typically uses small numbers of patients; in this case, the patients were in advanced stages of metastatic pancreatic and colorectal and other solid tumors.[46-47] Even though, END has been shown to be remarkably safe and non-toxic compared to chemotherapy, and many patients have shown an arrest in tumor growth, the actual determination of effectiveness took place during follow-up trials.[48] Phase II trials, that directly lead to Food and Drug Administration (FDA) approval for marketing of the drugs, began in 2002 and ended in 2006 for neuroendocrine tumor patients. The results were disappointing for Folkman's team and many

other researchers, and showed no significant tumor regression in these patients. The drug was not advanced to phase III studies because phase II studies showed no tumor response.

Folkman and Luo Yongzhang made a few amino acid alterations that made END more potent and longer lasting in the blood. This new version of END, Endostar, has returned END back to the attention of researchers,[49] and the promising results of a phase III study for Endostar have been published in a peer-reviewed journal.[50]

Although END has been extensively investigated for a broad range of indications, it possesses properties that have limited its clinical use. Systemic delivery, which is the major route used to administer END, has inherent disadvantages. These disadvantages include the necessity of repeated injections due to the short half-life of END, the fact that treatment needs to be continuous to sustain tumor dormancy, the risk of toxicity and the high expense. Additionally, dosages used in preclinical studies are not feasible for prolonged patient therapy.[51-53] These limitations have inspired the investigation of novel modes to deliver this angiogenesis inhibitor to enhance either targeting or delivery in order to achieve higher therapeutic outcomes while minimizing its shortcoming. In the following sections, focus will be placed on the different strategies to optimize the angiogenic therapy of END by describing its physiochemical, pharmacokinetic (PK), and physiological aspects. Furthermore, emphasis will be placed on the best routes and delivery systems used in the local delivery of END.

2.3 MECHANISMS OF ACTION OF ENDOSTATIN

As with other FDA-approved angiogenesis inhibitors such as Avastin, researchers still do not know the exact biological mechanism of END. Many theories were introduced to describe the anti-angiogenic and antitumor activities of either angiogenesis inhibitors in general or END in particular. These hypotheses include the prevention of tumor spread and metastasis through the same mechanism that is involved in chemotherapy and radiotherapy[54,55] and/or it exerts its action as growth control regulations of the cancer cells[56] and/or it is acting on the immune system.[49,57] Until now, most of the issues relating to how END exerts its effect are unclear. Research to determine the exact molecular mechanisms for END are still ongoing.

Many studies support the idea that tumor cell growth is controlled by a dynamic balance between angiogenic factors [such as vascular endothelial growth factor (VEGF) and basic fibroblast growth factor (bFGF) and angiostatic factors (such as angiostatin or END)].[58-59] Imbalance between angiogenic promoters and inhibitors produces the intense angiogenesis which is characteristic of many pathological processes, including diabetic retinopathy,[60] rheumatoid arthritis,[61] endometriosis[62] and malignant tumors.[63,64] Factors influencing angiogenesis are derived both from tumor cells and infiltrating cells, such as macrophages and fibroblasts.[65] The change in the balance between angiogenic and angiostatic factors, the angiogenic switch, has increasingly become recognized in the field of tumor biology as a critical step in tumor propagation and progression.[66,67]

Migration of tumor and endothelial cells through the tissue extracellular matrix is facilitated by a group of enzymes known as matrix metalloproteinases (MMPs). These

enzymes, which are secreted by the same cells that produce angiogenic factors, are responsible for the breakdown of the tissue matrix surrounding the growing vessels and tumor.[68] Inhibition of the catalytic activity of MMP catalyzing the proteolysis of extracellular matrix and mediating tumor cell invasion into adjacent tissues and endothelial cell migration during formation of new capillaries is one of the mechanisms underlying anti-angiogenic and antitumor effects of END.[54] Some of the classical cellular pathways of END are shown in Figure 2.1.

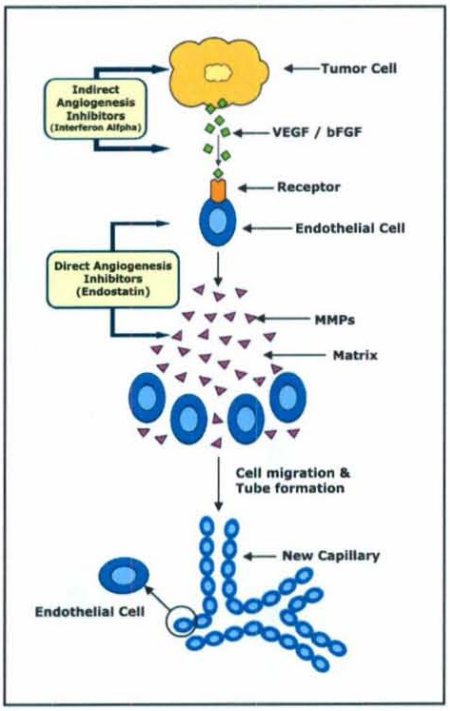

Figure 2.1 A proposed mechanism of direct and indirect action of angiogenesis inhibitors on the endothelial cells. (Diagrams drawn by Hany Ellaboudy) VEGF: vascular endothelial growth factor, bFGF: basic fibroblast growth factor, and MMPs: matrix metalloproteinases.

In another attempt to determine the mechanism of action of END, it was revealed that the study of the crystal structure of human and murine END showed that END has a zinc

binding site and a potent heparin binding site. This zinc binding of END was reported to be essential for its anti-angiogenic activity and molecular stability.[69] In addition, structure–function studies have implicated heparin/heparan-sulfate binding as being important for the activity of END, leading to speculation that END may bind the endothelial cell surface via heparin/heparan-sulfated proteoglycans.[70] Whether END exerts it effect following cell surface receptor binding or, as was recently reported, by internalization, remains to be elucidated. The END treatment of endothelial cells has been correlated to a S to G1 block in the cell cycle and to specific tyrosine phosphorylation activity suggesting that downstream effects of END may be mediated by specific tyrosine phosphorylation events.[70] Another manner by which END elicits its antitumor action is through the indirect stimulation of the immune system causing a sequence of immunological reactions and stimulation of some of the immune system components. Both humoral and cellular effects are produced and these may depend on the dose of END administrated and its timing in relation to the immune process.[71]

END also exerts its indirect cytotoxic and direct cytostatic action via inhibition of the blood supply to tumor tissue. Therefore, the prolonged administration of an anti-angiogenic therapy may be necessary to obtain long-term suppression of tumor growth. Consequently, the local delivery of a potent angiogenic inhibitor would be a valuable treatment strategy for solid tumors such as glioblastoma, leading to an accumulation of the anti-angiogenic proteins at the tumor site in the brain.[72]

More basic scientific research still needs to be done to characterize and trace the pathway of the END to ascertain its mechanism of action. There are many other proposed mechanisms,[73-75] but the understanding of how END works is still unclear.

2.4 STRUCTURE & PHYSIOCHEMICAL PROPERTIES OF ENDOSTATIN

END is a 20 kDA C-terminal proteotically cleaved fragment of collagen XVIII. It is reported to be composed of 184 amino acids and is naturally present in many adult and embryonic human tissues.[76] As a proteolytically cleaved fragment of collagen XVIII, END shares the identical amino acid sequences and secondary structure as the corresponding fragment of collagen XVIII.

The structure of END is different from other angiogenesis inhibitors. Its structure is unique as its secondary structure is mainly irregular loops of β-sheets and contains only a small fraction of α-helices with two pairs of disulfide bonds in a nested pattern.[10] Mismatch of disulfide bond may result in protein aggregation, and multimer formation, however the anti-angiogenesis activity does not change, as the multimer exerts its higher activity by providing a more suitable molecular structure for molecular interaction with heparin sulfate proteoglycans.[77]

The ultra-structure scanning of recombinant murine and human END has been carried out,[78,79] and it predicts a compact globular protein that probably exists as an extracellular module even prior to cleavage from collagen XVIII. Furthermore, its structure reveals a large basic sequence made up of a cluster of arginine residues and predicts for Arg 193/Arg 194 and

Arg 259/Arg 260 to be the putative heparin binding site. There are two interesting and unique characters of END. The first one is that small fragments of END, with or without cysteine, have remarkable anti-angiogenesis activity.[80-83] Unlike cytokines, END has no single locus for its bioactivity and it functions in a different manner. The second one has a great advantage, its lack of toxicity and the fact that, unlike other commonly used chemotherapeutic agents, it does not lead to the development of acquired drug resistance.[81]

END was originally obtained by purifying and isolating the naturally occurring protein from the supernatant of cultured murine hemangioendothelioma cell line or from hemofiltrate of patients with chronic renal failure.[84] Currently, recombinant END (rEND) is produced via recombinant protein technology from different sources including human embryonic cells,[78] *baculovirus,*[85] *Escherichia coli*, *Pichia pastoris*[73] and *Hansenula Polymorpha* expression systems.[76] There is a high degree of amino acid identity and homology reaching up to 99% between human and murine rEND.[86]

Recombinant END produced by an eukaryotic system (yeast, *Pichia pastoris*)[73] was found to be soluble and showed both *in vitro* and *in vivo* anti-angiogenic activities in various tumor animal models. However, the low yield and high cost limited the use of this technique of expression for large-scale production. On the other hand, although the use of prokaryotic systems (bacteria, *Escherichia coli*)[87] demonstrated angiostatic activity and was more economical than the eukaryotic system, the END produced by this method was insoluble. It was found that bacterial rEND forms insoluble amyloid fibers which aggregate as the β-sheets of the polypeptide backbones and are stacked via intermolecular rather than intramolecular

hydrogen bonds, thus forming a cross-β-sheet and therefore rendering it insoluble.[88] The soluble and aggregated (insoluble) forms of rEND have similar physiochemical properties, molecular weight, heparin binding ability, and anti-angiogenesis activity,[85,89,90] and demonstrated no cytotoxicity to primary human umbilical vein endothelial cells or to human dermal microvascular endothelial cells.[91]

Recombinant END has been reported to have the same biological activity as naturally occuring END[76] but, as with many other recombinant proteins, it possesses some differences in its glycosylation.[92] It is recognized that, in contrast to the naturally occurring END, rEND partially or completely lacks the carbohydrate moieties attached to its structure which decreases the half-life of the rEND in the blood stream.[93-95] The carbohydrate chains in END are of mucin type with galactose N-acetylglactosamine core unit of *O*-glycans,[96] and usually, this disaccharide is substituted by one or two sialic acid moites.[84] The sugar moiety in END is assumed to increase its solubility, it protects the END from undesirable digestion by enzymes and regulates the interactions of END with cell receptors.[84] It was found that different glycosylation levels regulate intracellular signaling cascades relevant to tumorigenesis.[97-98] Furthermore, the level of glycosylation differs between the *in vitro* and the *in vivo* which can be attributed to the fact that the growth conditions of cells in a living organism promote the glycosylation in a way that has not been reproduced *in vitro*.[92]

END is basic, with an isoelectric point at about pH 8.93.[99] It is reported to be one of the acid-resistant polypeptides that tolerates acidic conditions. It was found that END remains stable and keeps its activity and native structure at a pH as low as 3.5. Such acid resistance

might be attributed to its tightly packed structure and/or due to its lower accessibility to protons and/or due to its stable conformation. Recently, trifluoroethanol has proven to stabilize the helical structure of native END by strengthening the hydrogen bonds. Therefore it makes END more acidic resistant in the lower pH region. However, it is found that END partially or completely degrades at pH values less that 2.0.[10] On the other hand, END, like other polypeptides is very sensitive to heat. The triple helix of cleaved collagen molecules undergoes thermal melting at 37°C and thermal denaturation and unfolding of intact collagen molecules at temperatures greater than 42°C.[100]

2.5 THE PHARMACOKINETICS OF ENDOSTATIN

The maximum level of END concentration in the bloodstream is dependant on its physiochemical properties which include size, molecular weight, degree of glycosylation, [84] dosage form, and its route of administration.[47,101] The intravenous (iv) route has been used for END delivery,[101,102] however, other routes of administration have been used in various clinical studies which include intratumoral (im),[103,104] intraarterial (ia),[105] intraperitoneal (ip),[106] intracerebral (ic),[107] and subcutaneously (sc). [108]

Recombinant human Endostatin (rhEND) has a short elimination half-life time after iv administration in rats.[109] END given by the sc route to Rhesus monkeys has a longer half-life.[110] The sc and im routes result in a more extended half-life because these two routes form a depot after injection that allows a slower release of END. Simultaneously, other researchers attempted to prolong the half-life of END using an antibody moiety and achieved a four fold increase.[111]

Pegylation technology is a particularly attractive approach to increasing the utility and efficacy of injectable drugs.[112,113] The term pegylation refers to the conjugating of protein drugs with the polymer poly-ethylene glycol (PEG). Because altering the drug molecule can improve both the pharmacokinetic and the pharmacodynamic properties of the drug, pegylated drugs generally have longer plasma half-lives and durations of bioactivity than their nonpegylated ones. Pegylation provides the drug with many benefits such as greater biologic activity, longer circulating half-life, less enzymatic degradation, less immunogenicity and antigenicity, less toxicity, greater solubility, less-frequent administration, better patient adherence and improved quality of life.[112,114]

Whether given by iv, sc or im, END requires a relatively frequent and repeated regimen of administration. For example, the dosing schedule for the treatment of adenocarcinoma is iv bolus 300 $mg/m^2/day$.[101] This dosing schedule requires a health care professional, adding a health care burden, and is hurtful, painful and inconvenient for the patient. Therefore, there is a need for a delivery system that does not require the daily involvement of a health care professional and/or inconvenient lifestyle for patient.

2.6 LOCAL VERSUS SYSTEMIC DELIVERY OF ENDOSTATIN

Local administration might be an excellent solution to overcome the many challenges for the delivery of END.

There are several papers in the literature that emphasize the use of END for the treatment of different metastatic tumors, and other clinical conditions. However, few have reported on the most effective and least toxic routes of delivery. The major route of END delivery to the human body is systemic, (iv, im, sc, and ia).[101,102,105,108] Systemic routes have tremendous disadvantages, such as the uneven and unexpected distribution of END fragments throughout the body tissues and fluids, sometimes at a distance away from the tumor bed.[115] In addition, the concentration of END in the blood stream does not necessarily reflect the therapeutic outcome.[101,110] Furthermore, the dilution effect, hepatic metabolism, and glomerular filtration will reduce the END concentration in a very short time and consequently will reduce the bioavailability of END. Fortunately, the high dose of END to which different organs and tissues are exposed have minimal toxic or side-effects on the function of the organs.[38,51,116]

END has a short half-life in the bloodstream; therefore, this short time would minimize the exposure of many tumor sites that need high doses. Additionally, the high doses used in preclinical studies are not likely to be feasible for prolonged patient therapy.[117] The cost of END production and the painful regimen of delivery is not suitable for cancer patients. The fact that treatment needs to be continuous to sustain tumor dormancy necessitates repeated injections.

END has required doses as high as 20 mg/kg/day to demonstrate antitumor responses in mice.[85] If similar doses are required in humans, systemic administration of END to cancer patients is not feasible.[28] Human END is rapidly cleared from the blood and therefore, to

achieve significant tumor regression, a high amount of END would be required. These challenges have inspired a search for novel delivery systems to enhance either targeting or delivery of END.[43]

Local administration of higher doses of END, up to 20 mg per kg, daily via intracerebral microinfusion caused potent inhibitory effect on Lewis and ovary carcinomas, hemangioma (EOMA), fibrosarcoma T241, melanoma B16F10, and in some cases, END caused total regression of tumors.[118] The antitumor potential of END with the lack of marked nonspecific toxicity and tumor resistance allows it to be considered as a promising antitumor chemotherapeutic agent. However, the development of a stable effect requires the use of high daily doses (from 10 to 100 mg per kg) because of characteristic distribution and excretion of the administered protein.[54] Phase I studies with rhEND given as daily iv bolus injections showed no drug-related toxicity. However, the pharmacokinetic analyses revealed that, at the highest dose that could be practically administered, the drug exposure was lower than that yielding maximum tumor growth inhibition in preclinical studies.[47]

Many research papers have reported on the delivery of angiogenesis inhibitors using different routes of administrations and compared the efficiency and safety issues. Daily systemic administration of 2.5 mg/kg END for more than 16 days resulted in a 53% inhibition in tumor growth in a Lewis lung carcinoma model.[85] In a renal cell carcinoma model, rhEND injected daily sc (10 μg/kg/day) around the tumor for four days led to a 61% inhibition of tumor growth after 20 days.[72] Many researchers have demonstrated that

local or systemic administration of non-viral END plasmid significantly inhibited the growth of several tumor types, including lung, breast, kidney, and sarcoma tumors.[119] However, a sustained local high concentration from paralesional injections resulted in a dose-dependent improvement of the antitumor effect and a cure rate that might be greater than that from a systemic administration.[4,106,117] Therefore, a continuous and local delivery system would provide a significant improvement over the other routes of administration.

Continuous local delivery of END may offer an effective therapeutic approach to the treatment of a variety of tumor types.[72] It provides a high drug concentration around the tumor tissues and at the same time reduces the exposure of the surroundings to this angiogenesis inhibitor. Recently, several strategies including an osmotic pump, cell encapsulation, polymer implants and recombinant technology, have been examined to demonstrate the efficacy of local delivery on the therapeutic outcome.

In studies examining the efficacy of continuous delivery of angiogenesis inhibitors, Giusanni et al., recently showed that continuous local ic delivery via an osmotic mini-pump connected to an intracranial catheter resulted in higher antitumor efficacy against established glioma xenografts compared to continuous systemic administration or daily injections.[120] In a similar study, Kisker et al., have reported that continuous delivery of END could be achieved using osmotic pumps.[106] In another study, Alzet mini osmotic pumps implanted ip and used to administer END continually to sc Lewis lung carcinoma led to 81% inhibition in tumor size compared with a single bolus administration of 100 mg/kg/day for 23 days, which led to 90%

tumor inhibition. However, these mini-pumps had to be refilled every 7 days to achieve this level of inhibition.[107]

Cell encapsulation technology for END presents several advantages including the secretion of de novo produced END,[121] and it overcomes the major problems that confront the systemic delivery of END for use in the treatment of brain tumors.[122] Some studies demonstrated that a single administration of microencapsulated engineered cells that continuously secrete END significantly inhibited human glioblastoma xenografts. Animals treated with encapsulated END cells exhibit a 72% inhibition in tumor growth 21 days post microcapsule injection.[72] The encapsulation delivery system allowed local and continuous release of biologically active human END for the treatment of glioma. This delivery technique may be useful for the treatment of brain tumors, wherein the blood–brain barrier can impede systemic treatment of anti-angiogenic agents. Increasing the amount of encapsulated cells may permit a higher concentration of human END to be obtained, which may lead to higher tumor inhibition.[72]

The above strategy aimed to enhance local delivery of angiogenic inhibitors by the local implantation of encapsulated producer cells engineered to express END. In two studies examining the efficacy of this approach, a reduction in tumor growth of over 70% in orthotopic glioma tumor models was found.[43,72,123] In addition, Dr. Tracy-Ann Read and her colleagues at the University of Bergen have described a method that delivers cells capable of producing END directly to the site of the tumor, but in the form of gel covered beads that are undetected by the immune system. The team injected the beads into the brains of rats that were already

induced to develop a glioblastoma. Dr. Read's team observed that 70% of the beads remained viable, compared with the non-protected control cells, and that END was secreted from the beads for at least four months. The treated rats survived 84% longer than untreated controls.[121]

The utilization of polymers as a drug delivery vehicle has been used in the therapeutic setting, and provides a new method for local delivery of anti-angiogenic agents within the polymer directly to malignant brain tumors.[124] The biodegradable polyanhydride-poly-(bis-[carboxyphenoxy-propane]–sebacic acid) polymer (pCPP:SA), undergoes slow but complete hydrolytic degradation in the presence of water and releases biologically active END in continuous and sustained fashion either *in vivo* or *in vitro*. Biocompatibility studies of pCPP:SA have demonstrated that the original compound and its degradation products are noncytotoxic, nonmutagenic, and nonteratogenic.[125] In addition, the clinical testing demonstrated its safety and efficacy,[126,127] therefore, this drug delivery polymer has become widely used clinically for local drug delivery in patients with malignant tumors. Local drug delivery using polymer has many advantages over other systemic delivery routes of administration.

Another therapeutic approach involves surgical removal of the tumor followed by implantation of a biodegradable controlled-release polymeric device loaded with an antineoplastic agent such as angiostatic steroids, tetracycline derivatives, and amiloride in the resulting cavity. This method would provide a high local drug concentration, effectively destroying surviving malignant cells and would also prevent the systemic side effects of chemotherapy normally associated with its iv administration. It is currently being studied in the

laboratory for local delivery of a variety of anti-angiogenic agents.[128] For example, implantable controlled-release polymers for local drug administration directly into the tumor parenchyma have been developed to achieve therapeutic concentrations of these drugs within the brain while minimizing systemic toxicity. Controlled-release polymers used as a drug delivery strategy provide a clinically practicable method of achieving sustained anti-angiogenic therapy which can be readily used in combination with other treatment modalities such as cytoreductive surgery, radiation, and cytotoxic chemotherapy.[128]

The systemic administration strategy has many disadvantages such as the short half life time, lower drug concentration around the tumor bed and side effects on the other organs, not to mention the pain and patient inconvenience. On the other hand, local delivery would provide an improvement over systemic administration. Various methods for local delivery including osmotic pump, cell encapsulation and polymeric devices have been examined. The polymeric drug delivery technology was shown to be feasible as a tool to localize the drug.

2.7 SUSTAINED VERSUS PULSATILE RELEASE OF ENDOSTATIN

In light of the above discussion, it is necessary to know whether a pulsatile or sustained release of END is required to achieve the maximum therapeutic outcome.

In the pulsatile mode of administration, the cells are exposed to pulses of the delivered END followed by a time- and dose-dependent decrease in the effect. This method of END delivery was the focus of one of the studies conducted by Ding et al.[129] They monitored the

effect of massive pulsatile or multiple and prolonged administration of END by localized im injection of plasmid on murine mammary carcinomas. Although they reported that this strategy of administration was successful and had a potentially active anti-angiogenic effect, it was clear that this method of frequent administration would be an inconvenient and irritating method of drug delivery to the cancer patient.

Kuroiwa et al., used recombinant technology to deliver the rhEND gene. In these experiments, they demonstrated that rhEND was rapidly cleared from the mouse circulation after an intermittent sc dosing regimen of human neuroblastoma xenograft model, which may explain why continuous local delivery was more efficient and improved the END activity. In addition, the constant presence of rhEND around the tumor bed would minimize the acute pathological effect in which the secretion of END would remain active as long as the gene is expressed.[130] They also concluded that continuous administration of rhEND resulted in more significant tumor regression than intermittent administration of the agent in the same model. This indicated that rhEND, if administered in continuous fashion, could become an effective agent for treating patients with neuroblastoma.

In another study, it was documented that high local continuous angiogenesis inhibition therapy was more effective in the treatment of gliosarcoma. The researchers genetically engineered gliosarcoma cells so that they would stably secrete END. END-producing gliosarcoma cells were implanted intracerebrally in rats. The antitumor efficacy of END was evaluated on the basis of survival data and tumor volume comparisons. They confirmed that the continuous release of END by the END-producing cells significantly inhibited tumor

growth. Notably, 40% of the animals in the treatment group experienced long-term survival, without histologically verifiable tumors, seven months after cell implantation. Furthermore, tumor blood plasma volumes were reduced by 71%, microvessel density counts by 84%, and vascular area fractions by 75%.[131]

Reaching and maintaining therapeutically efficacious levels of END could be achieved either by continuous or repeated injections, (i.e. systemic administration) or by a mechanism whereby the protein is continuously secreted by an implanted device (i.e. local administration). By using a local system, lower doses of the effective anti-angiogenic protein may achieve significant tumor suppression.[72] Continuous dosing with anti-angiogenic agents such as END would replace intermittent dosing and would result in a more acceptable endpoint of the mode of administration.

Based on the discussion just presented, it can be concluded that the most efficient and least toxic delivery system for END is a localized and sustained release dosage form. Such a delivery strategy would minimize the exposure of the other cells and organs to the stimulatory and/or angiogenetic inhibitory effects of this potent angiostatic agent.

2.8 COMBINATION THERAPY

An application of the development of a local delivery system for END would be in combination therapy with currently used treatments. The combined application of angiogenetic inhibitors could be a promising strategy for cancer therapy.

Preliminary *in vitro* data described an increased effect when two angiogenic inhibitors were applied in combination. Several studies have reported on the advantages of combining anti-angiogenic agents with immunotherapy, chemotherapy or radiotherapy. The reason for these combinations is the assumption that the various mechanisms of action and various targets could lead to additive antitumoral effects.[132,133] Many other studies suggested that the addition of anti-angiogenic agents to conventional therapeutic strategies such as chemotherapy,[134-137] radiation,[138,139] or other tumor-targeting agents,[140] will increase the clinical efficacy of these different approaches.[141-145] In an attempt to enhance the response to therapy, Mauceri et al., combined radiotherapy with a systemically-administered angiogenic inhibitor via ip injection twice daily at a total dose of 25 mg/kg/day. They reported significantly enhanced antitumor efficacy coinciding with reduced neovascularization in several tumor models including glioblastoma xenografted in mice.[133]

The anti-angiogenic effects of metronomically scheduled chemotherapy (a frequent low-dose schedule regimen) may be enhanced by combining chemotherapeutics with anti-angiogenic inhibitors. Metronomic chemotherapy in combination with the anti-angiogenic compound caused the eradication of drug-resistant Lewis lung carcinoma xenografts. This result was not obtained with conventionally scheduled chemotherapy (long interval between cycles) alone.[43,134]

Enhanced anti-angiogenic effectiveness has been reported for the combination of END with angiostatin,[146,147] and for END with chemotherapeutic agents.[148] Furthermore, the combined therapy with receptor tyrosine kinase and END enhanced the anti-angiogenic effects

in human ECs *in vitro* and enhanced delay of tumor growth of human xenografts of prostate adenocarcinoma, lung cancer, and glioblastoma. The data confirm that combined treatment with direct and indirect inhibitors of angiogenesis may result in synergistic anti-angiogenic activity, improving the overall antitumor efficacy of these agents.[54,141] END not only significantly suppresses tumor growth but also enhances the antitumor efficacy of radiation therapy in human carcinoma xenograft.[149] Ultimately, anti-angiogenic therapy may provide an additional strategy for combination with standard therapies.[150,151]

From the above discussions, it can be concluded that a sustained release and a localized delivery system for END treatment, either alone or in combination with other therapeutic agents, would provide the best therapeutic result.

2.9 ADVANTAGES AND DISADVANTAGES OF VARIOUS DELIVERY SYSTEMS

Several strategies have been investigated to formulate and deliver angiogenesis inhibitors while at the same time trying to achieve two major objectives. The first is to deliver and target those inhibitors, such as END, specifically and safely to their site of action to maximize their therapeutic efficacy while minimizing their toxicity. The other is to overcome stability issues during the preparation of dosage forms containing these angiangiogenic agents and to help in maintaining this stability during storage of the dosage form and after administration to the patient.

Early studies of END were focused on achieving a localized, continuous and controlled release to help in improving the therapeutic outcome. These studies included extension of its

half-life in plasma, and in reducing the amount to which the areas surrounding the tumor were exposed.[10,112] A variety of strategies of achieving localized delivery of END have been explored and investigated including the use of liposomes, biodegradable polymers, encapsulation, and gene therapy, with varying degrees of success.

In gene therapy technology for anti-angiogenesis, a vector is used to insert a gene for the expression of angiogenesis polypeptide inhibitors into a host cell to over express this gene. This process can be conducted using viral vectors including retroviruses, lentiviruses, adenoviruses, and adeno-associated viruses or nonviral vectors including cationic liposomes, microencapsulation, polymers, and naked DNA, and can be accomplished with *in vivo* or *in vitro* settings. The advantages of gene therapy over the direct administration of the inhibitors include the localized delivery and sustained expression of the antiangiogenic molecules, the ability to inhibit multiple angiogenic pathways with the delivery of more than one transgene, the generation of properly folded inhibitor molecules, and the potential for decreasing the cost.[152] This method has been used in several studies to obtain a high concentration of continuous and local END.

Several studies have reported the inhibition of tumor growth and metastasis in mice by adenoviral vector-mediated delivery of END, however, no strong activity against pre-existing tumors was reported via this method.[28,29,153] These results contrast significantly with those observed using repeated injections of high doses of recombinant END protein.[90] As suggested by Sauter *et al.*, this discrepancy can be explained by the insufficient expression levels of END by the adenovirus system, but it is more likely that the inflammatory and immune responses

induced by adenovirus infection caused the loss of transduced cells and thus resulted in transient gene expression. As a result, the reduction in tumor growth stopped once the vector was gone and END expression was lost.[29] Most human tumors are difficult to establish as *in vitro* cell lines, and extensive subcloning and *in vitro* replication might change the original antigenic composition of the original tumor. Moreover, it may take several months to transduce a tumor cell. Such patient-individualized therapy is therefore very cost intensive.

Many researchers have reported on the use of liposomal formulations of END in gene therapy. Liposomal formulations can be viewed as a self-assembled polymer. Some of the more interesting experiments are described below. The END gene could be efficiently transported into the mice with a transferrin-liposome-DNA delivery system utilizing an aerosol spray. Transferrin-liposome-mediated END gene therapy strongly inhibited angiogenesis and the growth of mouse xenograft liver tumors. It also could promote the development of apoptosis of tumor cells indirectly.[154] In another study, the researchers designed an orthotopic osteosarcoma model grafted in immunocompetent rats, a tumor model that reproduces the phenotypic and metastatic characteristics of the osteosarcoma in humans. In this model, they evaluated the therapeutic potential of iv administration of END cDNA complexed to cationic liposomes. The cationic liposomes used in this study possessed a particular affinity for tumor vessels compared to normal vessels. The results showed the ability of iv administered END cDNA/cationic liposomes to delay tumor growth, moreover, it effectively prevented the occurrence of lung metastases, which is the major reason for poor prognosis and death in osteosarcoma patients.[155]

Dutour et al., have demonstrated *in vitro* and *in vivo* that END can be secreted by cDNA/cationic liposome complexed (cDNA/CLP) with plasmid DNA in transfected cells. This complex was used for END gene transfer into orthotopically implanted mice breast tumors. The animals were treated intravenously three times a week. The results demonstrate that therapy using END-cDNA/CLP is associated with a marked delay in tumor growth. Moreover, it effectively prevented the occurrence of lung metastases.[155] High levels of circulating END, resulting in an anti-tumor effect, were achieved when appropriate adenoviral vectors were used.[156] Systemic (iv or im) delivery of non-viral vectors, as described by Chen et al., resulted in very low *in vivo* concentrations of END, though sufficient to exert a therapeutic effect.[27]

Liposomes have the advantage of easy administration by injection or aerosol spray, but they have the disadvantage of having relatively short drug release durations which leads to the need for additional multiple injections which are painful to the patient. Furthermore, the release profiles from liposomes are neither sustained nor controllable. Ma et al., examined the release period of human END with liposome and they found that it is relatively rapid with only a two day release time, therefore long-term END stability in this formulation has yet to be demonstrated.[157] Thus, liposomes do not appear to be optimal for sustained delivery. In addition, liposomes are considered to be a foreign object by the host. As a result, liposomes are recognized by the mononuclear phagocytic system and trapped by the reticuloendothelial system in which macrophage-like cells reside.[158]

Another study has focused on the incorporation and release of END from poly-L-lysine-alginate microcapsules. Rokstad et al., examined the potential of microencapsulation of genetically engineered cells as a delivery system for therapeutic proteins. Parameters that affect capsule integrity such as homogenous and inhomogenous gel cores were evaluated. The transfected cells producing END reached a plateau phase in growth after 23 days post-encapsulation, however, after 30 days a fraction of the microcapsules started to disintegrate.[159] The END release was almost constant. However, release durations were not long, only 23 days. Although alginate-based particles have demonstrated biodegradable, biocompatible properties,[160] further improvements are necessary with regard to capsule integrity as well as controlling the cell growth before this technology can be used for therapy.

Gene therapy has potential, however, there are a number of challenges for using this method as a pharmaceutical drug delivery system. Viral vectors are commonly used as carriers for gene transfer due to their high *in vitro* transfection efficiency, but the safety issues and the toxicity of these viral vectors will likely preclude their use in humans. In contrast, systemically delivered non-viral liposome:DNA complexes have been shown to have low toxicity.[161,162] Nevertheless, as the goal of anti-angiogenic therapy of cancer is the long-term suppression of neovascularization and tumor growth, there is another important challenge for current gene transfer vectors, which either provide only temporary expression (e.g., non viral vectors) or elicit host responses that conspire to eliminate the genetically modified cells (e.g., adenovirus vectors). Another problem associated with anti-angiogenesis gene therapy is the low gene transduction efficiencies that occur with common cancer gene therapy.[44]

Implantable biodegradable polymeric devices provide a unique practical means of localizing angiogenesis inhibitors at the tumor site. The strategy of using a polymeric controlled delivery device reduces the amount of protein needed, relative to systemic administration, to achieve similar angiogenesis inhibition. END fragments were loaded into pCPP:SA biodegradable polymers. The pharmacokinetics of END/polymer formulations were evaluated *in vitro* in rats having gliosarcoma. Biologically active END was delivered from the polymer in a controlled-released and sustained fashion for 19 days without any sign of local or systemic toxicity.[38] The advantages of biodegradable polymers as a delivery vehicle are that they degraded into small biocompatible monomers and could be excreted via normal excretion process in the body and so surgical removal would not be required.

These delivery systems comprise a biodegradable monolithic polymer, throughout which the drug is distributed as separate solid particles. By immersing the device into the medium, the protein drug was released in three stages, an initial burst followed by a diffusion-controlled release, and finally an erosion-controlled release.[163,164] Poly(lactide-co-glycolide) PLG microspheres are among the most extensively studied polymers for the delivery of proteins and cytokines.[165] They have the advantages of not only providing a continuous release, but of being easily delivered to the target site, having a reasonable shelf-life, offering a long-term release duration, and consisting of biocompatible materials. Despite these benefits, the major problem with using a polymeric delivery system in general is keeping the protein stable and active during loading into the devices, storage and during release into the surrounding environment. Polypeptide drugs are susceptible to aggregation, denaturation, deamidation,

cleavage, oxidation, thiol disulfide exchange, and β elimination in aqueous solutions. There are many factors that cause these changes including ionic strength, light, pH, temperature and mechanical stress and presence of oxidizers and radicals. Protein aggregation may result in conformational structural changes in the protein molecule and loss of activity. [166]

Polymeric microspheres are capable of delivering an almost constant amount of an encapsulated polypeptide. Microspheres synthesized from PLG with different co-polymer ratio could be formulated to release their content for different periods of time ranging from weeks to months. This feature enables researchers to design a delivery system to release the whole drug content before microsphere degradation has taken place. It has been reported that anti-angiogenic factors such as hemopexin and platelet factor 4 fragments, have been incorporated into PLG microspheres. The researchers examined the effects of microspheres prepared by water in oil in water emulsion (w/o/w) on the release and bioactivity of these angiogenesis inhibitors after a single local sc injection in nude mice having glioma tumors. The stability and biological activity of these angiogenesis inhibitors were maintained during the fabrication procedure. The results were extremely promising as there was a 88%-95% reduction in glioma tumor volume 30 days post-treatment.[115]

One specific problem of using the PLG microsphere is the central accumulation of acidic degraded monomers within the sphere and the denaturation of the incorporated polypeptide drug. When biodegradable polymers such as PLG degrade in a medium, they produce by-products carrying carboxylic acid end groups that lower the local pH at the surface of the polymer and in the pores and channels of the device.[167,168] Fu et al., has evaluated the pH

at the center of PLG microspheres to be as low as 1.5. This major decline in the pH of the microspheres has been linked to inactivation and aggregation of other proteins within PLG microspheres prior to being released into the surrounding medium.[169] Although END is described as an acid resistant protein at a pH of 1.5 – 2, denaturation and conformational changes are unavoidable and a subsequent loss of activity will take place.

END is a very acid-resistant protein and contains some of its native structure even at pH 2. Stability measurements of END in urea show that END is still in the native structure at pH 3.5 despite the decreased stability.[10] This resistance may be due to its tightly packed structure, its lower accessibility to protons, a result of its stable conformation[10] or from the contribution of the disulfide bonds.[170] The acid-resistance property of END may have biological significance in that it cannot be easily digested by proteases in an acidic environment such as in a lysosome in the cell or acidic monomer in the release medium. Furthermore, rEND, as well as many other recombinant polypeptide drugs, is mostly liable to denaturation and aggregation when presented with a high concentration because when this recombinant protein is formed via genetic engineering, the glycosylation level of the polypeptide molecule changes drastically.[97,171] Therefore, many researchers have attempted to stabilize the proteins in solution, by the addition of carbohydrates, amino acids, and polyols such as trehalose.[172-175]

There does not appear to be a report of END incorporation into PLG microspheres, and subsequent stability of the release. However, instead of using such a device with END, the problem of microspheres degradation could be avoided by using a high osmotic excipient that allows and accelerates the complete END release before significant polymer degradation

occurs. In a study by Gu et al in 2007, it has been proven that a constant drug release rate is achievable from a polymer in which the drug is distributed as discrete particles in an elastomeric monolithic network. As a result of osmotic activity, ruptures and cracks are formed in the polymer matrix and the drug was dissolved out into the surrounding medium.[176] The above delivery system seems promising for END delivery, but the effect of the delivery vehicles and release mechanisms on the stability and activity of this angiogenesis inhibitor are still under investigation.

2.10 CONCLUSIONS

Long-term and localized delivery with sustained release of END alone or in combination with other therapies is a desirable goal for angiogenesis therapy to overcome metastases and tumor outgrowth. In addition, the formulation strategies investigated to date possess a number of desirable properties that make them promising delivery systems, but are limited due to their inability in maintaining END stability and activity prior to being released from the drug delivery device.

It would seem that a biodegradable, biocompatible and implantable polymer would provide a novel strategy to localize drug delivery of END.

2.11 REFERENCES

1. Folkman, J.; Merler, E.; Abernathy, C.; Williams, G. Isolation of a tumor factor responsible for angiogenesis. *J Exp. Med.* 1971, *133,* 275-288.

2. Fardet, L.; Stoebner, P. E.; Bachelez, H.; Descamps, V.; Kerob, D.; Meunier, L.; Dandurand, M.; Morel, P.; Lebbe, C. Treatment with taxanes of refractory or life-threatening Kaposi sarcoma not associated with human immunodeficiency virus infection. *Cancer* 2006, *106,* 1785-1789.

3. Folkman, J. What is the evidence that tumors are angiogenesis dependent? *J. Natl. Cancer Inst.* 1990, *82,* 4-6.

4. Hahnfeldt, P.; Panigrahy, D.; Folkman, J.; Hlatky, L. Tumor development under angiogenic signaling: a dynamical theory of tumor growth, treatment response, and postvascular dormancy. *Cancer Res.* 1999, *59,* 4770-4775.

5. Brannon-Peppas, L.; Blanchette, J. O. Nanoparticle and targeted systems for cancer therapy. *Adv. Drug Deliv. Rev.* 2004, *56,* 1649-1659.

6. Rusnati, M.; Presta, M. Extracellular angiogenic growth factor interactions: an angiogenesis interactome survey. *Endothelium* 2006, *13,* 93-111.

7. He, Y.; Zhou, H.; Tang, H.; Luo, Y. Deficiency of disulfide bonds facilitating fibrillogenesis of endostatin. *J Biol. Chem.* 2006, *281,* 1048-1057.

8. Wickstrom, S. A.; Alitalo, K.; Keski-Oja, J. An endostatin-derived peptide interacts with integrins and regulates actin cytoskeleton and migration of endothelial cells. *J Biol. Chem.* 2004, *279,* 20178-20185.

9. Kutuzova, G. D.; Deluca, H. F. Gene expression profiles in rat intestine identify pathways for 1,25-dihydroxyvitamin D(3) stimulated calcium absorption and clarify its immunomodulatory properties. *Arch. Biochem. Biophys.* 2004, *432,* 152-166.

10. Li, B.; Wu, X.; Zhou, H.; Chen, Q.; Luo, Y. Acid-induced unfolding mechanism of recombinant human endostatin. *Biochemistry* 2004, *43,* 2550-2557.

11. Hobson, B.; Denekamp, J. Endothelial proliferation in tumours and normal tissues: continuous labelling studies. *Br. J. Cancer* 1984, *49,* 405-413.

12. Fox, S. B.; Gatter, K. C.; Bicknell, R.; Going, J. J.; Stanton, P.; Cooke, T. G.; Harris, A. L. Relationship of endothelial cell proliferation to tumor vascularity in human breast cancer. *Cancer Res.* 1993, *53,* 4161-4163.

13. Ingber, D. E. Fibronectin controls capillary endothelial cell growth by modulating cell shape. *Proc. Natl. Acad. Sci. U. S. A* 1990, *87,* 3579-3583.

14. Kerbel, R. S. Vasohibin: the feedback on a new inhibitor of angiogenesis. *J Clin. Invest* 2004, *114,* 884-886.

15. Yoon, S. S.; Segal, N. H.; Olshen, A. B.; Brennan, M. F.; Singer, S. Circulating angiogenic factor levels correlate with extent of disease and risk of recurrence in patients with soft tissue sarcoma. *Ann. Oncol.* 2004, *15,* 1261-1266.

16. Folkman, J. Successful treatment of an angiogenic disease. *N. Engl. J. Med.* 1989, *320,* 1211-1212.

17. Tandle, A.; Blazer, D. G., III; Libutti, S. K. Antiangiogenic gene therapy of cancer: recent developments. *J. Transl. Med.* 2004, *2,* 22.

18. Mi, J.; Sarraf-Yazdi, S.; Zhang, X.; Cao, Y.; Dewhirst, M. W.; Kontos, C. D.; Li, C. Y.; Clary, B. M. A comparison of antiangiogenic therapies for the prevention of liver metastases. *J Surg. Res.* 2006, *131,* 97-104.

19. Yokoyama, Y.; Ramakrishnan, S. Addition of an aminopeptidase N-binding sequence to human endostatin improves inhibition of ovarian carcinoma growth. *Cancer* 2005, *104,* 321-331.

20. Blackhall, F. H.; Merry, C. L.; Lyon, M.; Jayson, G. C.; Folkman, J.; Javaherian, K.; Gallagher, J. T. Binding of endostatin to endothelial heparan sulphate shows a differential requirement for specific sulphates. *Biochem. J* 2003, *375,* 131-139.

21. Bagley, R. G.; Rouleau, C.; Morgenbesser, S. D.; Weber, W.; Cook, B. P.; Shankara, S.; Madden, S. L.; Teicher, B. A. Pericytes from human non-small cell lung carcinomas: An attractive target for anti-angiogenic therapy. *Microvasc. Res.* 2006, *71,* 163-174.

22. Salcedo, X.; Medina, J.; Sanz-Cameno, P.; Garcia-Buey, L.; Martin-Vilchez, S.; Borque, M. J.; Lopez-Cabrera, M.; Moreno-Otero, R. The potential of angiogenesis soluble markers in chronic hepatitis C. *Hepatology* 2005, *42,* 696-701.

23. Hanahan, D. A flanking attack on cancer. *Nat. Med.* 1998, *4,* 13-14.

24. Grosios, K. Endostatin (EntreMed). *IDrugs.* 2000, *3,* 799-810.

25. Tai, K. F.; Chen, P. J.; Chen, D. S.; Hwang, L. H. Concurrent delivery of GM-CSF and endostatin genes by a single adenoviral vector provides a synergistic effect on the treatment of orthotopic liver tumors. *J. Gene Med.* 2003, *5,* 386-398.

26. Becker, C. M.; Wright, R. D.; Satchi-Fainaro, R.; Funakoshi, T.; Folkman, J.; Kung, A. L.; D'Amato, R. J. A novel noninvasive model of endometriosis for monitoring the efficacy of antiangiogenic therapy. *Am. J Pathol.* 2006, *168,* 2074-2084.

27. Chen, C. T.; Lin, J.; Li, Q.; Phipps, S. S.; Jakubczak, J. L.; Stewart, D. A.; Skripchenko, Y.; Forry-Schaudies, S.; Wood, J.; Schnell, C.; Hallenbeck, P. L. Antiangiogenic gene therapy for cancer via systemic administration of adenoviral vectors expressing secretable endostatin. *Hum. Gene Ther.* 2000, *11,* 1983-1996.

28. Feldman, A. L.; Restifo, N. P.; Alexander, H. R.; Bartlett, D. L.; Hwu, P.; Seth, P.; Libutti, S. K. Antiangiogenic gene therapy of cancer utilizing a recombinant adenovirus to elevate systemic endostatin levels in mice. *Cancer Res.* 2000, *60,* 1503-1506.

29. Sauter, B. V.; Martinet, O.; Zhang, W. J.; Mandeli, J.; Woo, S. L. Adenovirus-mediated gene transfer of endostatin in vivo results in high level of transgene expression and inhibition of tumor growth and metastases. *Proc. Natl. Acad. Sci. U. S. A* 2000, *97,* 4802-4807.

30. Liou, J. Y.; Shyu, K. G.; Lu, M. J.; Chao, H. H.; Wang, B. W.; Kuan, P. L. Pericardial fluid and serum levels of vascular endothelial growth factor and endostatin in patients with or without coronary artery disease. *J Formos. Med. Assoc.* 2006, *105,* 377-383.

31. Zeng, X.; Chen, J.; Miller, Y. I.; Javaherian, K.; Moulton, K. S. Endostatin binds biglycan and LDL and interferes with LDL retention to the subendothelial matrix during atherosclerosis. *J Lipid Res.* 2005, *46,* 1849-1859.

32. Yue, L.; Wang, H.; Liu, L. H.; Shen, Y. X.; Wei, W. Anti-adjuvant arthritis of recombinant human endostatin in rats via inhibition of angiogenesis and proinflammatory factors. *Acta Pharmacol. Sin.* 2004, *25,* 1182-1185.

33. Orosz, K. E.; Gupta, S.; Hassink, M.; Abdel-Rahman, M.; Moldovan, L.; Davidorf, F. H.; Moldovan, N. I. Delivery of antiangiogenic and antioxidant drugs of ophthalmic interest through a nanoporous inorganic filter. *Mol. Vis.* 2004, *10,* 555-565.

34. Silha, J. V.; Krsek, M.; Sucharda, P.; Murphy, L. J. Angiogenic factors are elevated in overweight and obese individuals. *Int. J Obes. (Lond)* 2005, *29,* 1308-1314.

35. Zorick, T. S.; Mustacchi, Z.; Bando, S. Y.; Zatz, M.; Moreira-Filho, C. A.; Olsen, B.; Passos-Bueno, M. R. High serum endostatin levels in Down syndrome: implications for improved treatment and prevention of solid tumours. *Eur. J Hum. Genet.* 2001, *9,* 811-814.

36. Read, T. A.; Farhadi, M.; Bjerkvig, R.; Olsen, B. R.; Rokstad, A. M.; Huszthy, P. C.; Vajkoczy, P. Intravital microscopy reveals novel antivascular and antitumor effects of endostatin delivered locally by alginate-encapsulated cells. *Cancer Res.* 2001, *61,* 6830-6837.

37. Huszthy, P. C.; Brekken, C.; Pedersen, T. B.; Thorsen, F.; Sakariassen, P. O.; Skaftnesmo, K. O.; Haraldseth, O.; Lonning, P. E.; Bjerkvig, R.; Enger, P. O. Antitumor efficacy improved by local delivery of species-specific endostatin. *J Neurosurg.* 2006, *104,* 118-128.

38. Pradilla, G.; Legnani, F. G.; Petrangolini, G.; Francescato, P.; Chillemi, F.; Tyler, B. M.; Gaini, S. M.; Brem, H.; Olivi, A.; DiMeco, F. Local delivery of a synthetic endostatin fragment for the treatment of experimental gliomas. *Neurosurgery* 2005, *57,* 1032-1040.

39. Alba, E.; Llombart, A.; Ribelles, N.; Ramos, M.; Fernandez, R.; Mayordomo, J. I.; Tusquets, I.; Gil, M.; Barnadas, A.; Carabante, F.; Ruiz, M.; Vera, R.; Palomero, I.; Soriano, V.; Gonzalez, J.; Colomer, R. Serum endostatin and bFGF as predictive factors in advanced breast cancer patients treated with letrozole. *Clin. Transl. Oncol.* 2006, *8,* 193-199.

40. Schips, L.; Dalpiaz, O.; Lipsky, K.; Langner, C.; Rehak, P.; Puerstner, P.; Pummer, K.; Zigeuner, R. Serum Levels of Vascular Endothelial Growth Factor (VEGF) and Endostatin in Renal Cell Carcinoma Patients Compared to a Control Group. *Eur. Urol.* 2006.

41. Fan, Y. Z.; Chen, C. Q.; Zhao, Z. M.; Sun, W. [Effects of norcantharridin on angiogenesis of human gallbladder carcinoma and its anti-angiogenic mechanisms]. *Zhonghua Yi. Xue. Za Zhi.* 2006, *86,* 693-699.

42. Li, X. P.; Li, C. Y.; Li, X.; Ding, Y.; Chan, L. L.; Yang, P. H.; Li, G.; Liu, X.; Lin, J. S.; Wang, J.; He, M.; Kung, H. F.; Lin, M. C.; Peng, Y. Inhibition of human nasopharyngeal carcinoma growth and metastasis in mice by adenovirus-associated virus-mediated expression of human endostatin. *Mol. Cancer Ther.* 2006, *5,* 1290-1298.

43. Jansen, M.; Witt Hamer, P. C.; Witmer, A. N.; Troost, D.; van Noorden, C. J. Current perspectives on antiangiogenesis strategies in the treatment of malignant gliomas. *Brain Res. Brain Res. Rev.* 2004, *45,* 143-163.

44. Zhang, Z. L.; Wang, J. H.; Liu, X. Y. Current strategies and future directions of antiangiogenic tumor therapy. *Sheng Wu Hua Xue. Yu Sheng Wu Wu Li Xue. Bao. (Shanghai)* 2003, *35,* 873-880.

45. Jubb, A. M.; Oates, A. J.; Holden, S.; Koeppen, H. Predicting benefit from anti-angiogenic agents in malignancy. *Nat. Rev. Cancer* 2006, *6,* 626-635.

46. Ryan, D. P.; Penson, R. T.; Ahmed, S.; Chabner, B. A.; Lynch, T. J., Jr. Reality testing in cancer treatment: the phase I trial of endostatin. *Oncologist.* 1999, *4,* 501-508.

47. Eder, J. P., Jr.; Supko, J. G.; Clark, J. W.; Puchalski, T. A.; Garcia-Carbonero, R.; Ryan, D. P.; Shulman, L. N.; Proper, J.; Kirvan, M.; Rattner, B.; Connors, S.; Keogan, M. T.; Janicek, M. J.; Fogler, W. E.; Schnipper, L.; Kinchla, N.; Sidor, C.; Phillips, E.; Folkman, J.; Kufe, D. W. Phase I clinical trial of recombinant human endostatin administered as a short intravenous infusion repeated daily. *J. Clin. Oncol.* 2002, *20,* 3772-3784.

48. Sorensen, D. R.; Read, T. A. Delivery of endostatin in experimental cancer therapy. *Int. J. Exp. Pathol.* 2002, *83,* 265-274.

49. Whitworth, A. Endostatin: are we waiting for Godot? *J Natl. Cancer Inst.* 2006, *98,* 731-733.

50. Sun, Y.; Wang, J.; Liu, Y.; Song, X.; Zhang, Y.; Li, K.; Zhu, Y.; Zhou, Q.; You, L.; Yao, C. Results of phase III trial of rh-endostatin (YH-16) in advanced non-small cell lung cancer (NSCLC) patients. *J Clin Oncol (Meeting Abstracts)* 2005, *23,* 7138.

51. Hansma, A. H.; Broxterman, H. J.; van, d. H., I; Yuana, Y.; Boven, E.; Giaccone, G.; Pinedo, H. M.; Hoekman, K. Recombinant human endostatin administered as a 28-day continuous intravenous infusion, followed by daily subcutaneous injections: a phase I and pharmacokinetic study in patients with advanced cancer. *Ann. Oncol.* 2005, *16,* 1695-1701.

52. Tsuchida, Y.; Shitara, T.; Kuroiwa, M.; Ikeda, H. Current treatment and future directions in neuroblastoma. *Indian J Pediatr.* 2003, *70,* 809-812.

53. Kamstock, D.; Guth, A.; Elmslie, R.; Kurzman, I.; Liggitt, D.; Coro, L.; Fairman, J.; Dow, S. Liposome-DNA complexes infused intravenously inhibit tumor angiogenesis and elicit antitumor activity in dogs with soft tissue sarcoma. *Cancer Gene Ther.* 2006, *13,* 306-317.

54. Kiselev, S. M.; Lutsenko, S. V.; Severin, S. E.; Severin, E. S. Tumor angiogenesis inhibitors. *Biochemistry (Mosc.)* 2003, *68,* 497-513.

55. Bischof, M.; Abdollahi, A.; Gong, P.; Stoffregen, C.; Lipson, K. E.; Debus, J. U.; Weber, K. J.; Huber, P. E. Triple combination of irradiation, chemotherapy (pemetrexed), and VEGFR inhibition (SU5416) in human endothelial and tumor cells. *Int. J Radiat. Oncol. Biol. Phys.* 2004, *60,* 1220-1232.

56. Janssen, A. P.; Schiffelers, R. M.; ten Hagen, T. L.; Koning, G. A.; Schraa, A. J.; Kok, R. J.; Storm, G.; Molema, G. Peptide-targeted PEG-liposomes in anti-angiogenic therapy. *Int. J. Pharm.* 2003, *254,* 55-58.

57. Kim, S.; Bell, K.; Mousa, S. A.; Varner, J. A. Regulation of angiogenesis in vivo by ligation of integrin alpha5beta1 with the central cell-binding domain of fibronectin. *Am. J. Pathol.* 2000, *156,* 1345-1362.

58. Good, D. J.; Polverini, P. J.; Rastinejad, F.; Le Beau, M. M.; Lemons, R. S.; Frazier, W. A.; Bouck, N. P. A tumor suppressor-dependent inhibitor of angiogenesis is immunologically and functionally indistinguishable from a fragment of thrombospondin. *Proc. Natl. Acad. Sci. U. S. A* 1990, *87,* 6624-6628.

59. Joseph, J. M.; Bouquet, C.; Opolon, P.; Morizet, J.; Aubert, G.; Rossler, J.; Gross, N.; Griscelli, F.; Perricaudet, M.; Vassal, G. High level of stabilized angiostatin mediated by adenovirus delivery does not impair the growth of human neuroblastoma xenografts. *Cancer Gene Ther.* 2003, *10,* 859-866.

60. Murata, T.; Ishibashi, T.; Khalil, A.; Hata, Y.; Yoshikawa, H.; Inomata, H. Vascular endothelial growth factor plays a role in hyperpermeability of diabetic retinal vessels. *Ophthalmic Res.* 1995, *27,* 48-52.

61. Polverini, P. J. Role of the macrophage in angiogenesis-dependent diseases. *EXS* 1997, *79,* 11-28.

62. McLaren, J.; Prentice, A.; Charnock-Jones, D. S.; Millican, S. A.; Muller, K. H.; Sharkey, A. M.; Smith, S. K. Vascular endothelial growth factor is produced by peritoneal fluid macrophages in endometriosis and is regulated by ovarian steroids. *J. Clin. Invest* 1996, *98,* 482-489.

63. Cornali, E.; Zietz, C.; Benelli, R.; Weninger, W.; Masiello, L.; Breier, G.; Tschachler, E.; Albini, A.; Sturzl, M. Vascular endothelial growth factor regulates angiogenesis and vascular permeability in Kaposi's sarcoma. *Am. J. Pathol.* 1996, *149,* 1851-1869.

64. Samoto, K.; Ikezaki, K.; Ono, M.; Shono, T.; Kohno, K.; Kuwano, M.; Fukui, M. Expression of vascular endothelial growth factor and its possible relation with neovascularization in human brain tumors. *Cancer Res.* 1995, *55,* 1189-1193.

65. Takahashi, Y.; Bucana, C. D.; Liu, W.; Yoneda, J.; Kitadai, Y.; Cleary, K. R.; Ellis, L. M. Platelet-derived endothelial cell growth factor in human colon cancer angiogenesis: role of infiltrating cells. *J. Natl. Cancer Inst.* 1996, *88,* 1146-1151.

66. Kopp, H. G.; Hooper, A. T.; Broekman, M. J.; Avecilla, S. T.; Petit, I.; Luo, M.; Milde, T.; Ramos, C. A.; Zhang, F.; Kopp, T.; Bornstein, P.; Jin, D. K.; Marcus, A. J.; Rafii, S. Thrombospondins deployed by thrombopoietic cells determine

angiogenic switch and extent of revascularization. *J Clin. Invest* 2006, *116,* 3277-3291.

67. Nozawa, H.; Chiu, C.; Hanahan, D. Infiltrating neutrophils mediate the initial angiogenic switch in a mouse model of multistage carcinogenesis. *Proc. Natl. Acad. Sci U. S. A* 2006, *103,* 12493-12498.

68. Heissig, B.; Hattori, K.; Friedrich, M.; Rafii, S.; Werb, Z. Angiogenesis: vascular remodeling of the extracellular matrix involves metalloproteinases. *Curr. Opin. Hematol.* 2003, *10,* 136-141.

69. Sasaki, T.; Larsson, H.; Tisi, D.; Claesson-Welsh, L.; Hohenester, E.; Timpl, R. Endostatins derived from collagens XV and XVIII differ in structural and binding properties, tissue distribution and anti-angiogenic activity. *J. Mol. Biol.* 2000, *301,* 1179-1190.

70. Dixelius, J.; Larsson, H.; Sasaki, T.; Holmqvist, K.; Lu, L.; Engstrom, A.; Timpl, R.; Welsh, M.; Claesson-Welsh, L. Endostatin-induced tyrosine kinase signaling through the Shb adaptor protein regulates endothelial cell apoptosis. *Blood* 2000, *95,* 3403-3411.

71. Hu, B.; Wei, Y.; Tian, L.; Zhao, X.; Lu, Y.; Wu, Y.; Yao, B.; Liu, J.; Niu, T.; Wen, Y.; He, Q.; Su, J.; Huang, M.; Lou, Y.; Luo, Y.; Kan, B. Active antitumor immunity elicited by vaccine based on recombinant form of epidermal growth factor receptor. *J. Immunother.* 2005, *28,* 236-244.

72. Joki, T.; Machluf, M.; Atala, A.; Zhu, J.; Seyfried, N. T.; Dunn, I. F.; Abe, T.; Carroll, R. S.; Black, P. M. Continuous release of endostatin from microencapsulated engineered cells for tumor therapy. *Nat. Biotechnol.* 2001, *19,* 35-39.

73. Dhanabal, M.; Ramchandran, R.; Volk, R.; Stillman, I. E.; Lombardo, M.; Iruela-Arispe, M. L.; Simons, M.; Sukhatme, V. P. Endostatin: yeast production, mutants, and antitumor effect in renal cell carcinoma. *Cancer Res.* 1999, *59,* 189-197.

74. Dhanabal, M.; Ramchandran, R.; Waterman, M. J.; Lu, H.; Knebelmann, B.; Segal, M.; Sukhatme, V. P. Endostatin induces endothelial cell apoptosis. *J. Biol. Chem.* 1999, *274,* 11721-11726.

75. Addison, C. L.; Nor, J. E.; Zhao, H.; Linn, S. A.; Polverini, P. J.; Delaney, C. E. The response of VEGF-stimulated endothelial cells to angiostatic molecules is substrate-dependent. *BMC. Cell Biol.* 2005, *6,* 38.

76. Wu, J.; Fu, W.; Luo, J.; Zhang, T. Expression and purification of human endostatin from Hansenula polymorpha A16. *Protein Expr. Purif.* 2005, *42,* 12-19.

77. Wei, D. M.; Gao, Y.; Cao, X. R.; Zhu, N. C.; Liang, J. F.; Xie, W. P.; Zhen, M. Y.; Zhu, M. S. Soluble multimer of recombinant endostatin expressed in E. coli has anti-angiogenesis activity. *Biochem. Biophys. Res Commun.* 2006, *345,* 1398-1404.

78. Hohenester, E.; Sasaki, T.; Olsen, B. R.; Timpl, R. Crystal structure of the angiogenesis inhibitor endostatin at 1.5 A resolution. *EMBO J.* 1998, *17,* 1656-1664.

79. Hohenester, E.; Sasaki, T.; Mann, K.; Timpl, R. Variable zinc coordination in endostatin. *J. Mol. Biol.* 2000, *297,* 1-6.

80. Chillemi, F.; Francescato, P.; Ragg, E.; Cattaneo, M. G.; Pola, S.; Vicentini, L. Studies on the structure-activity relationship of endostatin: synthesis of human endostatin peptides exhibiting potent antiangiogenic activities. *J Med. Chem.* 2003, *46,* 4165-4172.

81. Cattaneo, M. G.; Pola, S.; Francescato, P.; Chillemi, F.; Vicentini, L. M. Human endostatin-derived synthetic peptides possess potent antiangiogenic properties in vitro and in vivo. *Exp. Cell Res* 2003, *283,* 230-236.

82. Morbidelli, L.; Donnini, S.; Chillemi, F.; Giachetti, A.; Ziche, M. Angiosuppressive and angiostimulatory effects exerted by synthetic partial sequences of endostatin. *Clin. Cancer Res* 2003, *9,* 5358-5369.

83. Tjin Tham Sjin, R. M.; Satchi-Fainaro, R.; Birsner, A. E.; Ramanujam, V. M.; Folkman, J.; Javaherian, K. A 27-amino-acid synthetic peptide corresponding to the NH2-terminal zinc-binding domain of endostatin is responsible for its antitumor activity. *Cancer Res* 2005, *65,* 3656-3663.

84. Preissner, J.; Forssman, k.; Standker, W. Novel glycosylated forms of human plasma endostatin and circulating endostatin-related fragments of collagen XV. *Biochemistry* 1999, *38,* 10217-10224.

85. O'Reilly, M. S.; Boehm, T.; Shing, Y.; Fukai, N.; Vasios, G.; Lane, W. S.; Flynn, E.; Birkhead, J. R.; Olsen, B. R.; Folkman, J. Endostatin: an endogenous inhibitor of angiogenesis and tumor growth. *Cell* 1997, *88,* 277-285.

86. Boehle, A.; kurdow, R.; Schulze, M.; Kliche, U.; Sipos, B.; Soondrum, K.; Ebrahimnejad, A.; Dohrmann, P.; Kalthoff, H.; Henne-Bruns, D.; Neumaier, M. Human endostatin inhibits growth of human non-small-cell lung cancer in a murine xenotransplant model. *International Journal of Cancer* 2001, *94,* 420-428.

87. Rochet, J. C.; Lansbury, P. T., Jr. Amyloid fibrillogenesis: themes and variations. *Curr. Opin. Struct. Biol.* 2000, *10,* 60-68.

88. Lansbury, P. T., Jr. In pursuit of the molecular structure of amyloid plaque: new technology provides unexpected and critical information. *Biochemistry* 1992, *31,* 6865-6870.

89. Sim, B. K.; MacDonald, N. J.; Gubish, E. R. Angiostatin and endostatin: endogenous inhibitors of tumor growth. *Cancer Metastasis Rev.* 2000, *19,* 181-190.

90. Boehm, T.; Folkman, J.; Browder, T.; O'Reilly, M. S. Antiangiogenic therapy of experimental cancer does not induce acquired drug resistance. *Nature* 1997, *390,* 404-407.

91. Reijerkerk, A.; Mosnier, L. O.; Kranenburg, O.; Bouma, B. N.; Carmeliet, P.; Drixler, T.; Meijers, J. C.; Voest, E. E.; Gebbink, M. F. Amyloid endostatin induces endothelial cell detachment by stimulation of the plasminogen activation system. *Mol. Cancer Res* 2003, *1,* 561-568.

92. Dong, S.; Cole, G. J.; Halfter, W. Expression of collagen XVIII and localization of its glycosaminoglycan attachment sites. *J. Biol. Chem.* 2003, *278,* 1700-1707.

93. Halfter, W.; Dong, S.; Schurer, B.; Cole, G. J. Collagen XVIII is a basement membrane heparan sulfate proteoglycan. *J. Biol. Chem.* 1998, *273,* 25404-25412.

94. Robert L.Chen and Arthur D.Lander Mechanisms Underlying Preferential Assembly of Heparan Sulfate on Glypican-1*. *J. Biol. Chem.* , 2001, *276,* 7507-7517.

95. Saarela, J.; Ylikarppa, R.; Rehn, M.; Purmonen, S.; Pihlajaniemi, T. Complete primary structure of two variant forms of human type XVIII collagen and tissue-specific differences in the expression of the corresponding transcripts. *Matrix Biol.* 1998, *16,* 319-328.

96. Kobata, A. Structures and functions of the sugar chains of glycoproteins. *Eur. J Biochem.* 1992, *209,* 483-501.

97. Bellis, S. L. Variant glycosylation: an underappreciated regulatory mechanism for beta1 integrins. *Biochim. Biophys. Acta* 2004, *1663,* 52-60.

98. John, H.; Radtke, K.; Standker, L.; Forssmann, W. G. Identification and characterization of novel endogenous proteolytic forms of the human angiogenesis inhibitors restin and endostatin. *Biochim. Biophys. Acta* 2005, *1747,* 161-170.

99. Boehm, T.; Pirie-Shepherd, S.; Trinh, L. B.; Shiloach, J.; Folkman, J. Disruption of the KEX1 gene in Pichia pastoris allows expression of full-length murine and human endostatin. *Yeast* 1999, *15,* 563-572.

100. Davis, G.; Bayless, K.; Davis, M.; Meininger, G. Regulation of Tissue Injury Responses by the Exposure of Matricryptic Sites within Extracellular Matrix Molecules . *The American Journal of Pathology* 2000, *156,* 1489-1498.

101. Herbst, R. S.; Hess, K. R.; Tran, H. T.; Tseng, J. E.; Mullani, N. A.; Charnsangavej, C.; Madden, T.; Davis, D. W.; McConkey, D. J.; O'Reilly, M. S.; Ellis, L. M.; Pluda, J.; Hong, W. K.; Abbruzzese, J. L. Phase I study of recombinant human endostatin in patients with advanced solid tumors. *J. Clin. Oncol.* 2002, *20,* 3792-3803.

102. Thomas, J. P.; Arzoomanian, R. Z.; Alberti, D.; Marnocha, R.; Lee, F.; Friedl, A.; Tutsch, K.; Dresen, A.; Geiger, P.; Pluda, J.; Fogler, W.; Schiller, J. H.; Wilding, G. Phase I pharmacokinetic and pharmacodynamic study of recombinant human endostatin in patients with advanced solid tumors. *J. Clin. Oncol.* 2003, *21,* 223-231.

103. Raikwar, S. P.; Temm, C. J.; Raikwar, N. S.; Kao, C.; Molitoris, B. A.; Gardner, T. A. Adenoviral vectors expressing human endostatin-angiostatin and soluble Tie2: enhanced suppression of tumor growth and antiangiogenic effects in a prostate tumor model. *Mol. Ther.* 2005, *12,* 1091-1100.

104. Luo, X.; Andres, M. L.; Timiryasova, T. M.; Fodor, I.; Slater, J. M.; Gridley, D. S. Radiation-enhanced endostatin gene expression and effects of combination treatment. *Technol. Cancer Res. Treat.* 2005, *4,* 193-202.

105. Barnett, F. H.; Scharer-Schuksz, M.; Wood, M.; Yu, X.; Wagner, T. E.; Friedlander, M. Intra-arterial delivery of endostatin gene to brain tumors prolongs survival and alters tumor vessel ultrastructure. *Gene Ther.* 2004, *11,* 1283-1289.

106. Kisker, O.; Becker, C. M.; Prox, D.; Fannon, M.; D'Amato, R.; Flynn, E.; Fogler, W. E.; Sim, B. K.; Allred, E. N.; Pirie-Shepherd, S. R.; Folkman, J. Continuous administration of endostatin by intraperitoneally implanted osmotic pump improves the efficacy and potency of therapy in a mouse xenograft tumor model. *Cancer Res.* 2001, *61,* 7669-7674.

107. Schmidt, N. O.; Ziu, M.; Carrabba, G.; Giussani, C.; Bello, L.; Sun, Y.; Schmidt, K.; Albert, M.; Black, P. M.; Carroll, R. S. Antiangiogenic therapy by local intracerebral microinfusion improves treatment efficiency and survival in an orthotopic human glioblastoma model. *Clin. Cancer Res.* 2004, *10,* 1255-1262.

108. Abraham, D.; Abri, S.; Hofmann, M.; Holtl, W.; Aharinejad, S. Low dose carboplatin combined with angiostatic agents prevents metastasis in human testicular germ cell tumor xenografts. *J. Urol.* 2003, *170,* 1388-1393.

109. Yang, X. X.; Hu, Z. P.; Chan, E.; Duan, W.; Zhou, S. Pharmacokinetics of recombinant human endostatin in rats. *Curr. Drug Metab* 2006, *7,* 565-576.

110. Song, H. F.; Liu, X. W.; Zhang, H. N.; Zhu, B. Z.; Yuan, S. J.; Liu, S. Y.; Tang, Z. M. Pharmacokinetics of His-tag recombinant human endostatin in Rhesus monkeys. *Acta Pharmacol. Sin.* 2005, *26,* 124-128.

111. Cho, H. M.; Rosenblatt, J. D.; Kang, Y. S.; Iruela-Arispe, M. L.; Morrison, S. L.; Penichet, M. L.; Kwon, Y. G.; Kim, T. W.; Webster, K. A.; Nechustan, H.; Shin, S. U. Enhanced inhibition of murine tumor and human breast tumor xenografts using targeted delivery of an antibody-endostatin fusion protein. *Mol. Cancer Ther.* 2005, *4,* 956-967.

112. Molineux, G. Pegylation: engineering improved pharmaceuticals for enhanced therapy. *Cancer Treat. Rev.* 2002, *28 Suppl A,* 13-16.

113. Reddy, K. R. Controlled-release, pegylation, liposomal formulations: new mechanisms in the delivery of injectable drugs. *Ann. Pharmacother.* 2000, *34,* 915-923.

114. Harrington, K. J.; Mohammadtaghi, S.; Uster, P. S.; Glass, D.; Peters, A. M.; Vile, R. G.; Stewart, J. S. Effective targeting of solid tumors in patients with locally advanced cancers by radiolabeled pegylated liposomes. *Clin. Cancer Res.* 2001, *7,* 243-254.

115. Benny, O.; Duvshani-Eshet, M.; Cargioli, T.; Bello, L.; Bikfalvi, A.; Carroll, R. S.; Machluf, M. Continuous delivery of endogenous inhibitors from poly(lactic-co-glycolic acid) polymeric microspheres inhibits glioma tumor growth. *Clin. Cancer Res.* 2005, *11,* 768-776.

116. Kulke, M. H.; Bergsland, E. K.; Ryan, D. P.; Enzinger, P. C.; Lynch, T. J.; Zhu, A. X.; Meyerhardt, J. A.; Heymach, J. V.; Fogler, W. E.; Sidor, C.; Michelini, A.; Kinsella, K.; Venook, A. P.; Fuchs, C. S. Phase II study of recombinant human endostatin in patients with advanced neuroendocrine tumors. *J Clin. Oncol.* 2006, *24,* 3555-3561.

117. Kerbel, R. S. Clinical trials of antiangiogenic drugs: opportunities, problems, and assessment of initial results. *J. Clin. Oncol.* 2001, *19,* 45S-51S.

118. Sim, B. K. Angiostatin and endostatin: endothelial cell-specific endogenous inhibitors of angiogenesis and tumor growth. *Angiogenesis.* 1998, *2,* 37-48.

119. Wicks, I. P.; Howell, M. L.; Hancock, T.; Kohsaka, H.; Olee, T.; Carson, D. A. Bacterial lipopolysaccharide copurifies with plasmid DNA: implications for animal models and human gene therapy. *Hum. Gene Ther.* 1995, *6,* 317-323.

120. Giussani, C.; Carrabba, G.; Pluderi, M.; Lucini, V.; Pannacci, M.; Caronzolo, D.; Costa, F.; Minotti, M.; Tomei, G.; Villani, R.; Carroll, R. S.; Bikfalvi, A.; Bello, L. Local intracerebral delivery of endogenous inhibitors by osmotic minipumps effectively suppresses glioma growth in vivo. *Cancer Res.* 2003, *63,* 2499-2505.

121. Read, T. A.; Stensvaag, V.; Vindenes, H.; Ulvestad, E.; Bjerkvig, R.; Thorsen, F. Cells encapsulated in alginate: a potential system for delivery of recombinant proteins to malignant brain tumours. *Int. J. Dev. Neurosci.* 1999, *17,* 653-663.

122. Bjerkvig, R.; Read, T. A.; Vajkoczy, P.; Aebischer, P.; Pralong, W.; Platt, S.; Melvik, J. E.; Hagen, A.; Dornish, M. Cell therapy using encapsulated cells producing endostatin. *Acta Neurochir. Suppl* 2003, *88,* 137-141.

123. Read, T. A.; Sorensen, D. R.; Mahesparan, R.; Enger, P. O.; Timpl, R.; Olsen, B. R.; Hjelstuen, M. H.; Haraldseth, O.; Bjerkvig, R. Local endostatin treatment of gliomas administered by microencapsulated producer cells. *Nat. Biotechnol.* 2001, *19,* 29-34.

124. Guerin, C.; Olivi, A.; Weingart, J. D.; Lawson, H. C.; Brem, H. Recent advances in brain tumor therapy: local intracerebral drug delivery by polymers. *Invest New Drugs* 2004, *22,* 27-37.

125. Leong, K. W.; Kost, J.; Mathiowitz, E.; Langer, R. Polyanhydrides for controlled release of bioactive agents. *Biomaterials* 1986, *7,* 364-371.

126. Brem, H.; Piantadosi, S.; Burger, P. C.; Walker, M.; Selker, R.; Vick, N. A.; Black, K.; Sisti, M.; Brem, S.; Mohr, G.; . Placebo-controlled trial of safety and efficacy of intraoperative controlled delivery by biodegradable polymers of chemotherapy for recurrent gliomas. The Polymer-brain Tumor Treatment Group. *Lancet* 1995, *345,* 1008-1012.

127. Valtonen, S.; Timonen, U.; Toivanen, P.; Kalimo, H.; Kivipelto, L.; Heiskanen, O.; Unsgaard, G.; Kuurne, T. Interstitial chemotherapy with carmustine-loaded polymers for high-grade gliomas: a randomized double-blind study. *Neurosurgery* 1997, *41,* 44-48.

128. Sipos, E. P.; Brem, H. Local anti-angiogenic brain tumor therapies. *J. Neurooncol.* 2000, *50,* 181-188.

129. Ding, I.; Sun, J. Z.; Fenton, B.; Liu, W. M.; Kimsely, P.; Okunieff, P.; Min, W. Intratumoral administration of endostatin plasmid inhibits vascular growth and

perfusion in MCa-4 murine mammary carcinomas. *Cancer Res.* 2001, *61,* 526-531.

130. Kuroiwa, M.; Takeuchi, T.; Lee, J. H.; Yoshizawa, J.; Hirato, J.; Kaneko, S.; Choi, S. H.; Suzuki, N.; Ikeda, H.; Tsuchida, Y. Continuous versus intermittent administration of human endostatin in xenografted human neuroblastoma. *J. Pediatr. Surg.* 2003, *38,* 1499-1505.

131. Huszthy, P. C.; Brekken, C.; Pedersen, T. B.; Thorsen, F.; Sakariassen, P. O.; Skaftnesmo, K. O.; Haraldseth, O.; Lonning, P. E.; Bjerkvig, R.; Enger, P. O. Antitumor efficacy improved by local delivery of species-specific endostatin. *J. Neurosurg.* 2006, *104,* 118-128.

132. Cao, Y. Endogenous angiogenesis inhibitors and their therapeutic implications. *Int. J. Biochem. Cell Biol.* 2001, *33,* 357-369.

133. Mauceri, H. J.; Hanna, N. N.; Beckett, M. A.; Gorski, D. H.; Staba, M. J.; Stellato, K. A.; Bigelow, K.; Heimann, R.; Gately, S.; Dhanabal, M.; Soff, G. A.; Sukhatme, V. P.; Kufe, D. W.; Weichselbaum, R. R. Combined effects of angiostatin and ionizing radiation in antitumour therapy. *Nature* 1998, *394,* 287-291.

134. Browder, T.; Butterfield, C. E.; Kraling, B. M.; Shi, B.; Marshall, B.; O'Reilly, M. S.; Folkman, J. Antiangiogenic scheduling of chemotherapy improves efficacy against experimental drug-resistant cancer. *Cancer Res.* 2000, *60,* 1878-1886.

135. Herbst, R. S.; Madden, T. L.; Tran, H. T.; Blumenschein, G. R., Jr.; Meyers, C. A.; Seabrooke, L. F.; Khuri, F. R.; Puduvalli, V. K.; Allgood, V.; Fritsche, H. A., Jr.; Hinton, L.; Newman, R. A.; Crane, E. A.; Fossella, F. V.; Dordal, M.; Goodin, T.; Hong, W. K. Safety and pharmacokinetic effects of TNP-470, an angiogenesis inhibitor, combined with paclitaxel in patients with solid tumors: evidence for activity in non-small-cell lung cancer. *J. Clin. Oncol.* 2002, *20,* 4440-4447.

136. Huang, S. F.; Kim, S. J.; Lee, A. T.; Karashima, T.; Bucana, C.; Kedar, D.; Sweeney, P.; Mian, B.; Fan, D.; Shepherd, D.; Fidler, I. J.; Dinney, C. P.; Killion, J. J. Inhibition of growth and metastasis of orthotopic human prostate cancer in athymic mice by combination therapy with pegylated interferon-alpha-2b and docetaxel. *Cancer Res.* 2002, *62,* 5720-5726.

137. Klement, G.; Baruchel, S.; Rak, J.; Man, S.; Clark, K.; Hicklin, D. J.; Bohlen, P.; Kerbel, R. S. Continuous low-dose therapy with vinblastine and VEGF receptor-2 antibody induces sustained tumor regression without overt toxicity. *J. Clin. Invest* 2000, *105,* R15-R24.

138. Pedley, R. B.; El Emir, E.; Flynn, A. A.; Boxer, G. M.; Dearling, J.; Raleigh, J. A.; Hill, S. A.; Stuart, S.; Motha, R.; Begent, R. H. Synergy between vascular

targeting agents and antibody-directed therapy. *Int. J. Radiat. Oncol. Biol. Phys.* 2002, *54,* 1524-1531.

139. Khan, M. K.; Miller, M. W.; Taylor, J.; Gill, N. K.; Dick, R. D.; Van Golen, K.; Brewer, G. J.; Merajver, S. D. Radiotherapy and antiangiogenic TM in lung cancer. *Neoplasia.* 2002, *4,* 164-170.

140. Baker, C. H.; Solorzano, C. C.; Fidler, I. J. Blockade of vascular endothelial growth factor receptor and epidermal growth factor receptor signaling for therapy of metastatic human pancreatic cancer. *Cancer Res.* 2002, *62,* 1996-2003.

141. Abdollahi, A.; Lipson, K. E.; Sckell, A.; Zieher, H.; Klenke, F.; Poerschke, D.; Roth, A.; Han, X.; Krix, M.; Bischof, M.; Hahnfeldt, P.; Grone, H. J.; Debus, J.; Hlatky, L.; Huber, P. E. Combined therapy with direct and indirect angiogenesis inhibition results in enhanced antiangiogenic and antitumor effects. *Cancer Res.* 2003, *63,* 8890-8898.

142. O'Reilly, M. S. Targeting multiple biological pathways as a strategy to improve the treatment of cancer. *Clin. Cancer Res.* 2002, *8,* 3309-3310.

143. Jain, R. K. Normalization of tumor vasculature: an emerging concept in antiangiogenic therapy. *Science* 2005, *307,* 58-62.

144. Huang, X.; Wong, M. K.; Yi, H.; Watkins, S.; Laird, A. D.; Wolf, S. F.; Gorelik, E. Combined therapy of local and metastatic 4T1 breast tumor in mice using SU6668, an inhibitor of angiogenic receptor tyrosine kinases, and the immunostimulator B7.2-IgG fusion protein. *Cancer Res.* 2002, *62,* 5727-5735.

145. Qian, C. N.; Min, H. Q.; Lin, H. L.; Hong, M. H. Combination of angiogenesis inhibitor TNP-470 with cytotoxic drugs in experimental therapy of nasopharyngeal carcinoma. *Ann. Otol. Rhinol. Laryngol.* 2000, *109,* 641-645.

146. Bergers, G.; Javaherian, K.; Lo, K. M.; Folkman, J.; Hanahan, D. Effects of angiogenesis inhibitors on multistage carcinogenesis in mice. *Science* 1999, *284,* 808-812.

147. Yokoyama, Y.; Dhanabal, M.; Griffioen, A. W.; Sukhatme, V. P.; Ramakrishnan, S. Synergy between angiostatin and endostatin: inhibition of ovarian cancer growth. *Cancer Res.* 2000, *60,* 2190-2196.

148. Te-Velde, E. A.; Vogten, J. M.; Gebbink, M. F.; van Gorp, J. M.; Voest, E. E.; Borel, R., I Enhanced antitumour efficacy by combining conventional chemotherapy with angiostatin or endostatin in a liver metastasis model. *Br. J. Surg.* 2002, *89,* 1302-1309.

149. Zheng, A. Q.; Song, X. R.; Yu, J. M.; Wei, L.; Wang, X. W. Liposome transfected to plasmid-encoding endostatin gene combined with radiotherapy inhibits liver cancer growth in nude mice. *World J. Gastroenterol.* 2005, *11,* 4439-4442.

150. Heere-Ress, E.; Boehm, J.; Thallinger, C.; Hoeller, C.; Wacheck, V.; Birner, P.; Wolff, K.; Pehamberger, H.; Jansen, B. Thalidomide enhances the anti-tumor activity of standard chemotherapy in a human melanoma xenotransplatation model. *J Invest Dermatol.* 2005, *125,* 201-206.

151. Cho, S. W.; Gwak, S. J.; Kang, S. W.; Bhang, S. H.; Song, K. W.; Yang, Y. S.; Choi, C. Y.; Kim, B. S. Enhancement of Angiogenic Efficacy of Human Cord Blood Cell Transplantation. *Tissue Eng* 2006.

152. Liau, G.; Su, E. J.; Dixon, K. D. Clinical efforts to modulate angiogenesis in the adult: gene therapy versus conventional approaches. *Drug Discov. Today* 2001, *6,* 689-697.

153. Kuo, C. J.; Farnebo, F.; Yu, E. Y.; Christofferson, R.; Swearingen, R. A.; Carter, R.; von Recum, H. A.; Yuan, J.; Kamihara, J.; Flynn, E.; D'Amato, R.; Folkman, J.; Mulligan, R. C. Comparative evaluation of the antitumor activity of antiangiogenic proteins delivered by gene transfer. *Proc. Natl. Acad. Sci. U. S. A* 2001, *98,* 4605-4610.

154. Li, X.; Fu, G. F.; Fan, Y. R.; Shi, C. F.; Liu, X. J.; Xu, G. X.; Wang, J. J. Potent inhibition of angiogenesis and liver tumor growth by administration of an aerosol containing a transferrin-liposome-endostatin complex. *World J. Gastroenterol.* 2003, *9,* 262-266.

155. Dutour, A.; Monteil, J.; Paraf, F.; Charissoux, J. L.; Kaletta, C.; Sauer, B.; Naujoks, K.; Rigaud, M. Endostatin cDNA/cationic liposome complexes as a promising therapy to prevent lung metastases in osteosarcoma: study in a human-like rat orthotopic tumor. *Mol. Ther.* 2005, *11,* 311-319.

156. Fenton, B. M.; Paoni, S. F.; Lee, J.; Koch, C. J.; Lord, E. M. Quantification of tumour vasculature and hypoxia by immunohistochemical staining and HbO2 saturation measurements. *Br. J. Cancer* 1999, *79,* 464-471.

157. Ma, C. H.; Zhang, Y.; Wang, X. Y.; Gao, L. F.; Liu, H.; Guo, C.; Liu, S. X.; Cao, Y. L.; Zhang, L. N.; Sun, W. S. Human endostatin gene transfer, either naked or with liposome, has the same inhibitory effect on growth of mouse liver tumor cells in vivo. *World J Gastroenterol.* 2004, *10,* 2874-2877.

158. Medina, O. P.; Zhu, Y.; Kairemo, K. Targeted liposomal drug delivery in cancer. *Curr. Pharm. Des* 2004, *10,* 2981-2989.

159. Rokstad, A. M.; Holtan, S.; Strand, B.; Steinkjer, B.; Ryan, L.; Kulseng, B.; Skjak-Braek, G.; Espevik, T. Microencapsulation of cells producing therapeutic proteins: optimizing cell growth and secretion. *Cell Transplant.* 2002, *11,* 313-324.

160. Aynie, I.; Vauthier, C.; Chacun, H.; Fattal, E.; Couvreur, P. Spongelike alginate nanoparticles as a new potential system for the delivery of antisense oligonucleotides. *Antisense Nucleic Acid Drug Dev.* 1999, *9,* 301-312.

161. Chen, Q. R.; Kumar, D.; Stass, S. A.; Mixson, A. J. Liposomes complexed to plasmids encoding angiostatin and endostatin inhibit breast cancer in nude mice. *Cancer Res.* 1999, *59,* 3308-3312.

162. Xu, M.; Kumar, D.; Srinivas, S.; Detolla, L. J.; Yu, S. F.; Stass, S. A.; Mixson, A. J. Parenteral gene therapy with p53 inhibits human breast tumors in vivo through a bystander mechanism without evidence of toxicity. *Hum. Gene Ther.* 1997, *8,* 177-185.

163. Rahul C.Mehta1, B. C. T. a. P. P. D. Peptide containing microspheres from low molecular weight and hydrophilic poly(*d,l*-lactide-co-glycolide). *J Controlled Release* 1996, *41,* 249-257.

164. Spenlehauer, G.; Spenlehauer-Bonthonneau, F.; Thies, C. Biodegradable microparticles for delivery of polypeptides and proteins. *Prog. Clin. Biol. Res* 1989, *292,* 283-291.

165. Cleland, J. L.; Duenas, E. T.; Park, A.; Daugherty, A.; Kahn, J.; Kowalski, J.; Cuthbertson, A. Development of poly-(D,L-lactide--coglycolide) microsphere formulations containing recombinant human vascular endothelial growth factor to promote local angiogenesis. *J Control Release* 2001, *72,* 13-24.

166. Lee VHL Changing needs in drug delivery in the era of peptide and protein drugs. In Peptide and Protein Drug Delivery; Lee VHL, Ed.; Marcel Dekker: New York, 1990; pp. 1-56.

167. Shenderova, A.; Burke, T. G.; Schwendeman, S. P. The acidic microclimate in poly(lactide-co-glycolide) microspheres stabilizes camptothecins. *Pharm. Res.* 1999, *16,* 241-248.

168. Mader, K.; Gallez, B.; Liu, K. J.; Swartz, H. M. Non-invasive in vivo characterization of release processes in biodegradable polymers by low-frequency electron paramagnetic resonance spectroscopy. *Biomaterials* 1996, *17,* 457-461.

169. Fu, K.; Pack, D. W.; Klibanov, A. M.; Langer, R. Visual evidence of acidic environment within degrading poly(lactic-co-glycolic acid) (PLGA) microspheres. *Pharm. Res.* 2000, *17,* 100-106.

170. Wu, X.; Huang, J.; Chang, G.; Luo, Y. Detection and characterization of an acid-induced folding intermediate of endostatin. *Biochem. Biophys. Res. Commun.* 2004, *320,* 973-978.

171. Moll, M.; Kaufmann, A.; Maisner, A. Influence of N-glycans on processing and biological activity of the nipah virus fusion protein. *J Virol.* 2004, *78,* 7274-7278.

172. Makinen, K. K.; Soderling, E.; Peacor, D. R.; Makinen, P. L.; Park, L. M. Carbohydrate-controlled precipitation of apatite with coprecipitation of organic molecules in human saliva: stabilizing role of polyols. *Calcif. Tissue Int.* 1989, *44,* 258-268.

173. Eckhardt, B. M.; Oeswein, J. Q.; Bewley, T. A. Effect of freezing on aggregation of human growth hormone. *Pharm. Res.* 1991, *8,* 1360-1364.

174. Oeswein JQ., S. SJ.; Peptide and protein drug delivery. In Phsical Biochemistry of Protein Drugs.; Lee VHL, Ed.; Marcel Dekker: New York, 1991; pp. 167-202.

175. Gu, F.; Younes, H. M.; El Kadi, A. O.; Neufeld, R. J.; Amsden, B. G. Sustained interferon-gamma delivery from a photo-crosslinked biodegradable elastomer. *J Control Release* 2005, *102,* 607-617.

176. Gu, F.; Neufeld, R.; Amsden, B. Sustained release of bioactive therapeutic proteins from a biodegradable elastomeric device. *J Control Release* 2007, *117,* 80-89.

Chapter 3. Novel Poly(Octanediol-Tartarate) (POT) Biodegradable Elastomers for Drug Delivery and Biomedical Applications.

3.1 ABSTRACT

Purpose: To synthesize and characterize a series of a novel family of thermal crossliked biodegradable poly(octanediol-tartarate) (POT) elastomers and to modify the mechanical and physical properties by adding a crosslinking agent.

Method: Saturated, aliphatic, low molecular weight, amorphous thermoset, biocompatible and biodegradable polyester elastomers consisting of L-tartaric and 1,8-octanediol were prepared and characterized. The elastomers were produced in two steps. First, the aliphatic saturated polyester prepolymer was synthesized via a polyesterfication polymerization reaction. Following purification, the living poly(octanediol-tartarate) prepolymers (POT) were further thermally crosslinked with different ratios of the crosslinking agent, 2,2-bis(ε-caprolactone-yl)-propane (BCP), to prepare crosslinked elastomers that could be used for implantable drug delivery and tissue engineering applications. The polyester prepolymers were characterized by means of proton nuclear magnetic resonance (^{1}H-NMR), Fourier transform infrared analysis (FT-IR), differential scanning calorimetry (DSC), liquid chromatography with mass spectrometry detection (LC-MS), and molecular weight analysis. The final POT elastomers were also subjected to swelling studies, sol-gel content analysis, mechanical testing, and long term *in vitro* accelerated degradation studies.

Results: ^{1}H-NMR and FT-IR analysis confirmed that a pure preparation of the POT prepolymer was obtained and also confirmed the formation of ester bonds in the backbone. DSC showed that the prepolymer was of semicrystalline nature with a corresponding low glass transition temperature (Tg) of -16.2 °C and a sharp melting endotherm at 57.2 °C. Molecular weight analysis reported a weight average molecular weight of 1250 daltons. The final crosslinked POT elastomers had amorphous structures with Tg ranges from -10 to -5 °C depending on the crosslinking density. Sol content ranged from 2.2 % - 9.8 % and depended on the amount of BCP used. Mechanical properties including Young's modulus, % strain, extension ratio all demonstrated dependence on crosslinking density. The elastomers were soft with physical properties similar to those of natural elastomers such as elastin. Accelerated degradation studies demonstrated linear loss of mechanical properties with time and confirmed bulk hydrolysis as being the predominant mechanism of polymer degradation.

Conclusions: The novel POT biodegradable polyester elastomers have promising use in drug delivery and other biomedical applications including tissue engineering.

3.2 INTRODUCTION

The use of biodegradable polymers in tissue engineering,[1-4] gene therapy,[5,6],and drug delivery systems[7-9] has motivated the development of novel biodegradable elastomers.[10-12] Biodegradable polymers with elastomeric features demonstrate elastic and flexible properties which resemble those of the human soft body organs and tissues such as blood vessels, heart valves, tendons and cartilages,[2,13-15] because of their ability to

adjust to the mechanical environment.[16] Therefore, they can easily adapt to a variety of mechanical stimuli when they are implanted into a non-static part of the body.

Biodegradable elastomers are synthesized as one of two types: thermoplastic or thermoset. Thermoplastics have the advantage of being easily processed by melting. The crystalline crosslinked hard regions of these materials provide regions having a slower and heterogeneous degradation profile. However, the amorphous regions degrade faster than the crystalline regions and produce a material whose physical and mechanical properties degrade in a non-linear fashion.[15] Thermosets are not easily fabricated by heat, but the rate of degradation is more uniform. Therefore, they keep their dimensions for a longer period of time with their physical and mechanical properties changing in a linear fashion. Thermosets, therefore attract the attention of many researchers due to their advantageous properties with respect to controlled drug delivery applications.

Polyesters degrade by simple hydrolysis in an aqueous environment, such as body fluids, because of the hydroxyl, carboxyl, and ester groups of the polymer backbone.[17] It is well known that 1,8-octanediol with long methylene chains shows a certain hydrophilicity. L-tartaric acid is hydrophilic due to its two hydroxyl groups and two carboxylic groups. Furthermore, the promising properties of L-tartaric acid as a backbone unit for building of polytartarate polymers and their potential biomedical applications have been evaluated.[18]

The aliphatic polyesters, in general, do not have the good physical and mechanical properties required for many biomedical applications.[19] Therefore, the goal is to modify the elastomers and to improve their mechanical and physical properties, by adding a crosslinking agent, to develop desirable elastomers for medical applications. To be considered for such applications, the elastomers must be biocompatible to avoid an inflammatory response from the host tissue and provide a suitable substrate for cell attachment and proliferation.

Poly-(octanediol-tartarate) possesses many advantages for use as an agent for controlled release for the following reasons: (i) It is composed of low cost monomers which increases the potential for future commercialization. (ii) It readily degrades in biological systems via hydrolysis of ester bonds to a non-toxic end-product since neither the monomers nor the crosslinking agent used are toxic. (iii) The hydrophilic/hydrophobic (amphiphilic) properties of the elastomers which are desirable in some biomedical applications,[20] can be altered by changing the ratio of BCP and length of the diol chain. In addition, the ability to modify the degree of hydrophilicity of the elastomers facilitates the use with a wide range of drugs and proteins. Therefore, the system can be tailored to suit a specific situation. (iv) The poor physical strengths of the relatively low molecular weight elastomers can be tailored by modulating the BCP ratio. (v) Finally, the POT prepolymer has a low viscosity which facilitates the injection and pouring into molds at moderate temperature. Therefore, their design could be altered to achieve different mechanical properties and degradation rates by incorporation of the tetra-functional crosslinker BCP into the elastomer networks.

The synthesis, characterization, mechanical properties and *in vitro* degradation of a novel synthesized POT biodegradable elastomer are reported in this study. This elastomer was prepared in two stages. The first involved the preparation of the aliphatic chain of the POT prepolymer which is composed of two non-toxic monomers; 1,8-octanediol and L-tartaric acid via a polyesterfication polymerization reaction. The second stage involved the reaction of a POT prepolymer with different ratios of 2,2-bis(ε-caprolactone-4-yl)-propane (BCP) using stannous 2-ethylhexanoate as a catalyst. The idea behind using a BCP as a crosslinking agent for the preparation of biodegradable elastomers stems from the fact that BCP is biocompatible with living tissues,[21] and it increases the crosslinking density of the elastomers. Furthermore, the influence of the molar ratio of BCP to POT used to prepare the elastomers was examined to determine the effect on their physical properties such as mechanical behaviour, water loss, sol content and swelling degree, and to examine the *in vitro* degradation of these elastomers by following the changes in their mechanical properties with time.

3.3 MATERIALS AND METHODS

3.3.1 Materials

The chemicals used in the synthesis and purification of elastomers such as L-tartaric acid and 1,8-octanediol, stannous octoate (SnOct), acetone, chloroform, and ethyl ether were obtained from Sigma-Aldrich. The chemicals used in the preparation of the crosslinker (BCP) such as chromium trioxide, m-chloroperoxybenzoic acid (mCPBA), acetone, and 2-heptanone were obtained from Sigma-Aldrich, and 2,2-bis(4-

hydroxycyclohexyl) propane was purchased from TCI America. Other chemicals used such as 2-propanol, dichloromethane (DCM), glacial acetic acid, and magnesium sulphate ($MgSO_4$) were obtained from Fisher Scientific Inc.

3.3.2 Preparation of 1:1 Poly(Octanediole-L-Tartaric) Prepolymer (POT)

Solvent free polymerization was carried out in sealed silanized 20 ml ampoules. L-tartaric acid and 1,8-octanediol in 1:1 molar ratios were transferred and mixed into a dry ampoule. The ampoule was placed in an oven at 160 °C until complete melting of the reactants. The mix was then stirred using a vortex mixer. The ampoule was filled with nitrogen, flame sealed under vacuum and placed in an oven again at 140 °C for 1 hour. The prepared crude prepolymers were purified by dissolution in chloroform, precipitated in cold anhydrous ethyl ether, and dried in vacuum overnight. The final product of the polyester prepolymer (POT) was dissolved in acetone-d_6 and was characterized using proton nuclear magnetic resonance spectroscopy (^{1}H-NMR), mass spectroscopy (MS), fourier transform infrared (FT-IR) spectrometry, differential scanning calorimetry (DSC), and gel permeation chromatography (GPC). Scheme 3.1 shows a representation of the synthesis of poly(ocatanediol-tartarate) polyester prepolymer (POT).

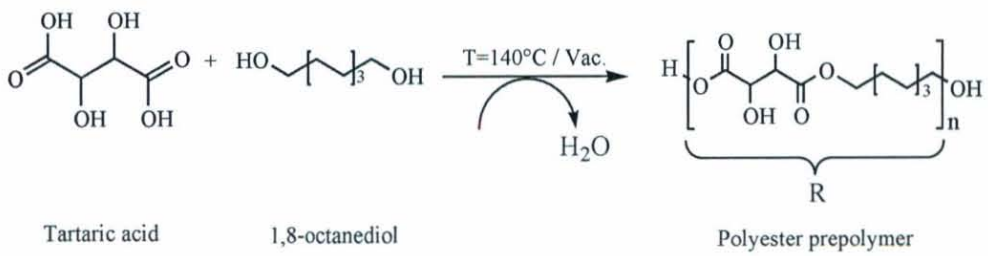

Scheme 3.1

3.3.3 Preparation of 2,2-bis(ε-caprolactone-4-yl)-propane (BCP)

A detailed synthesis procedure has been reported by Palmgren et al.[22] In summary, 5.4 g of 2,2-bis(4-hydroxyhexyl)propane was dissolved in 29.5 ml glacial acetic acid to which a solution of 5.5 g of chromium trioxide in dilute acetic acid (25 ml of glacial acetic acid mixed with 40 ml distilled water) was added in a dropwise fashion over a period of 2 hours under stirring while maintaining a temperature of 17-18 °C. After the complete addition of the reactants, the solution was left to react for another 30 minutes, and then 25 ml of 2-propanol was added to the solution. This solution was covered with aluminium foil and left overnight. Then this solution was uncovered and left under vacuum for another overnight to concentrate. The concentrated solution was then poured into 200 ml of distilled water and a thick violet suspension was formed. The suspension was filtered using whatman no. 1 filter paper and the cake was washed several times with distilled water. The resulting white dicyclohexyl-4,4'-dione (diketone) powder was dried in an oven at 50 °C overnight and characterized.

A Baeyer-Villiger oxidation reaction was then carried out on the prepared diketone as follows: In a round bottom flask, 3.9 g of mCPBA, previously dried with $MgSO_4$/DCM, was added in batches, about 12 batches with one hour between each batch, to a DCM solution of the diketone (4.1 g in 200 ml) under reflux at 50 °C and continuous stirring with a magnetic stirrer. The solution was then left under the same conditions for 24 hours. After the reaction was completed, the solution was filtered using triple filter papers and the filtrate was left in the fume hood under vacuum to evaporate the DCM. White crystals of the BCP appeared after the complete evaporation of the DCM. The final

product was purified and re-crystallized with hot 2-heptanone. The final white powder product was characterized using DSC and MS. Scheme 3.2 summarizes the steps involved in preparing BCP.

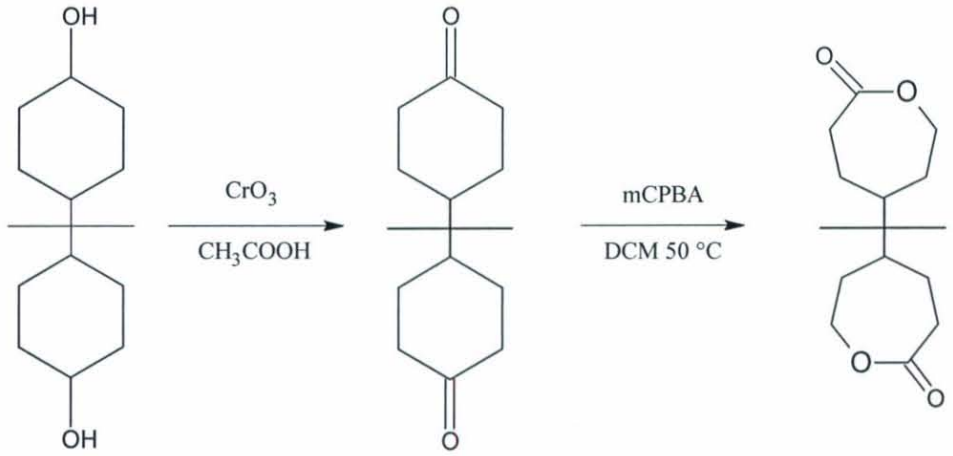

2, 2-bis(4-hydroxycyclohexyl)propane Diketone Bis-Caprolactone Propane (BCP)

Scheme 3.2

3.3.4 Synthesis of the Elastomers

Several different elastomers of varying ratios of BCP (as reported in Table 3.1) were synthesized. The following procedure describes the steps involved in preparing elastomer 1 using the weight ratio of POT to BCP as reported in Table 3.1. In a dry glass ampoule, 1 g of BCP was left in the oven for 5-10 minutes to dissolve at 180°C. A mass of 4 g of POT and an amount of SnOct equivalent to 1.4×10^{-4} mol for each 1 mol of the monomer were added to the ampoule. The contents were mixed using a vortex mixer and the ampoule was sealed under vacuum. The ampoule was left in the vacuum oven at 120 °C for 1 hour and then the seal was broken and the highly viscous liquid was poured into rectangular Teflon moulds (100 x 6 x 3 mm), covered, and left in the oven at 120 °C for

18 hours. The elastomer was then removed from the mould and characterized using DSC, *in vitro* degradation and tensile mechanical testing. Table 3.1 lists the different ratios of both POT and BCP used to prepare elastomers 1-5 and scheme 3.3 summarizes the steps involved in preparing these elastomers.

Table 3.1 Ratios of prepolymer (POT) and BCP used in preparing the elastomers.

Sample ID	**Prepolymer (POT) (g)**	**BCP (g)**	**Prepolymer (POT)/BCP Weight Ratio**
Elastomer 1	4.0	1.00	4.00/1.0
Elastomer 2	4.0	0.75	5.33/1.0
Elastomer 3	4.0	0.50	8.00/1.0
Elastomer 4	4.0	0.25	16.00/1.0
Elastomer 5	4.0	0.00	4.00/0.0

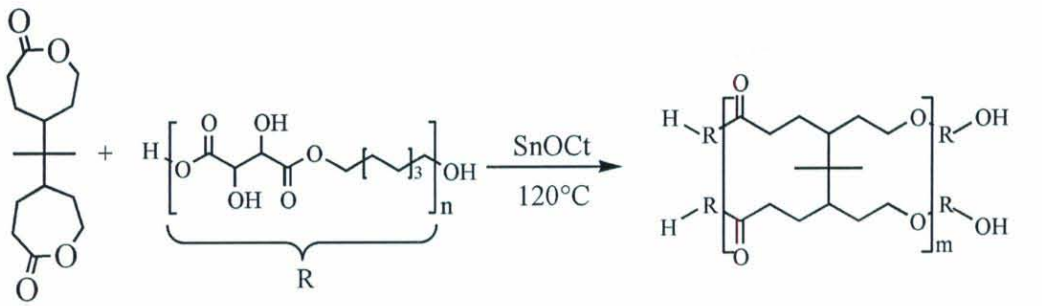

BCP Polyester prepolymer Poly (octanediol-tartarate) POT (Elastomer)

Scheme 3.3

3.3.5 Characterization of BCP and Elastomers

With the exception of the GPC, which is located at the University of Alberta, all equipment used for spectroscopic characterizations were conducted and performed at Memorial University of Newfoundland.

Proton-NMR of the prepolymer was run using acetone-d_6 with a Bruker AVANCE 500MHz Spectophotometer. The chemical shifts in parts-per-million (ppm) for ^{1}H-NMR spectra were referenced relative to tetramethylsilane (TMS, 0.00 ppm) as the internal reference.

To verify the identity of the product, mass spectrometry (MS) was carried out using an Agilent 1100 series LC/MSD system with atmospheric pressure chemical ionization (APCI) positive mode of ionization in flow injection mode. BCP sample was prepared by dissolution in DCM. The MS data was collected and analyzed using Bruker Daltonik and MSD Trap control Version 5.2 software.

GPC was performed using a Hewlett-Packard 1100 system connected to a precision detector (PD) 2000 dynamic laser scattering (DLS) light scattering detector supplied with a Waters 410 differential refractometer. The mobile phase consisted of tetrahydrofuran (THF) at a flow rate of 2 ml/min with the system at a temperature of 35°C. The polymer concentration used was 2 mg/ml and the injection volume was 20 µl. Monodisperse polystyrene standards were used for the initial calibration.

FT-IR spectra were obtained at room temperature using a Bruker TENSOR 27 Fourier transform infrared spectrometer. Prepolymer samples were prepared by pouring over a zinc/selenium crystal. IR data was analyzed using Opus Bruker Optik version 4.0 software.

The thermal properties of the elastomers and prepolymer were characterized using DSC. The experiments were carried out on a Seiko 210 with cooling system machine. The sample (5-8 mg) was placed in an aluminium pan and was run with a heating rate of 10 °C /min using a cycle from ambient to -60°C to 150°C to -60°C to 150°C. The glass transition temperature (Tg) was measured from the second heating cycle. The DSC instrument was calibrated using indium and gallium standards. The enthalpies, glass transition temperatures, and melting endotherm were determined using the internal DSC analysis program.

The sol content of the products and the swelling degree (R) of the corresponding gels were measured in the following way. A small disc sample (3 mm in thickness and 10 mm in diameter) with weight, W1, diameter, D1 and thickness, T1, was placed in 20 ml of DCM for 24 h and was then taken out. The weight of the disk was recorded as W2 and the diameter as D2 and thickness, T2, after the solvent on the surface was absorbed by filter paper. The disk was dried to a constant weight, W3, diameter, D3, and thickness, T3, in a vacuum oven at 40 °C under 4000 Pa for 7 days. The sol content was calculated as follows: (Q) = [(W1-W3) / W1] X 100%. The swelling degree (R) for the

corresponding gel was calculated as (R) = [(W2-W3) / W3] X 100%. Three samples were used for each experiment, and the average value of the three samples was reported.

The equilibrium water uptake in deionized water is defined as the fraction of weight gained by the small disk sample and was calculated as water uptake = [(M2 – M1)/ M1] X 100 %, where M1 is the initial weight of the specimen and M2 is the weight of the sample after it was placed in deionized water for 24 h. Three samples were tested for each product at room temperature and the average value was obtained.

Tensile mechanical testing was conducted with an Instron model In-Spec 2200 tester with Marlin PDA Data Management Software. The Instron was equipped with a 500 newtons (N) load cell. The measurements of the mechanical properties of the elastomers were carried out on slabs (100 x 6 x 3 mm) using an Instron with extensometer. The extensometer gauge length was set to 5 mm while the specimen gauge length was set to 30 mm. The crosshead speed was set at 50 mm/min and the sample rate was set at 0.833 mm/sec. Elastomers 1-5 (having various degree of crosslinking), were tested at room temperature. A Young's modulus was calculated from the initial slope of the stress-strain curve. Three samples of each product were measured and the mean and standard deviation were calculated.

3.3.6 *In Vitro* Degradation Study

Slab specimens of elastomers 1 & 2 as listed in Table 3.1 were subjected to an accelerated *in vitro* degradation study to demonstrate the changes in mechanical

properties during the degradation process. Each specimen was weighed and then placed into a 15 ml tissue culture tube which was filled with 12 ml phosphate buffer saline (PBS) of pH = 7.4. The tubes were attached to a Glas-Col rugged culture rotator. The rotator was set at a rotation speed of 30 % and placed in an oven at 37 ^{o}C. The buffer was replaced every 2-3 days to ensure a constant pH of 7.4 during the whole period of study. Samples of elastomers 1 & 2 (each sample represents 3 specimens) were dried, weighed and subjected to tensile testing at time periods of 0, 1, 2, 4, 6 and 8 weeks. Another set of samples of elastomers 1-5 was left without changing its buffer, to monitor the change in the pH of the medium with respect to time.

After the tensile testing, the broken slabs were collected and washed three times with deionized water and were then dried to a constant weight (G2) in a vacuum oven at 40 ^{o}C under 4000 Pa. The mass loss was calculated as follows: Mass loss = [(G1 - G2) / G1] X 100 %, where G1 is the initial weight of the slab before incubation in the buffer. Three samples for each product were tested at room temperature to achieve the average value.

3.4 RESULTS AND DISCUSSION

The aim of this study was to synthesize amorphous, biodegradable and biocompatible elastomers that would have a Tg lower than body and room temperatures, and that would be utilized as a polymeric drug delivery system, especially for protein drugs. To achieve this goal, the hydroxyl groups of 1,8-ocatanediol were reacted with carboxylic groups of L-tartaric acid in a 1:1 molar ratio using SnOct as a catalyst to form

polyester (octanediol-tartarate) prepolymer (POT). Then, different ratio of BCP were incorporated with the prepolymer to synthesize the biodegradable POT elastomers.

The ^{1}H-NMR spectrum of POT showed peaks at about 1.3, 1.5, and 1.7 ppm, which were assigned to the methylene protons. The peaks at 3.5 ppm can be attributed to the hydroxyl protons at the end of the diol monomer. The protons on the methylene group adjacent to the ester bond were attributed to the peak at 4.2 ppm, and the peak at 4.5 ppm was assigned to the α-hydrogens on the L-tartaric acid as shown in Figure 3.1. A number average molecular weight of 1247 Daltons was estimated using the integrals of the chemical shifts of the ^{1}H NMR spectrum characteristic of the contributing monomers. The estimation was based on the degree of polymerization of both monomers. The ^{1}H-NMR of the POT confirmed the composition as being 52.91 mol % 1,8-octanediol and 47.09 mol % L-tartaric acid measured using the ratio of integrals at the chemical shift of 1.3 ppm which corresponds to the 1,8-octanediol methylene proton resonances to that of 4.5 ppm which corresponds to the L-tartaric acid methine proton resonances.

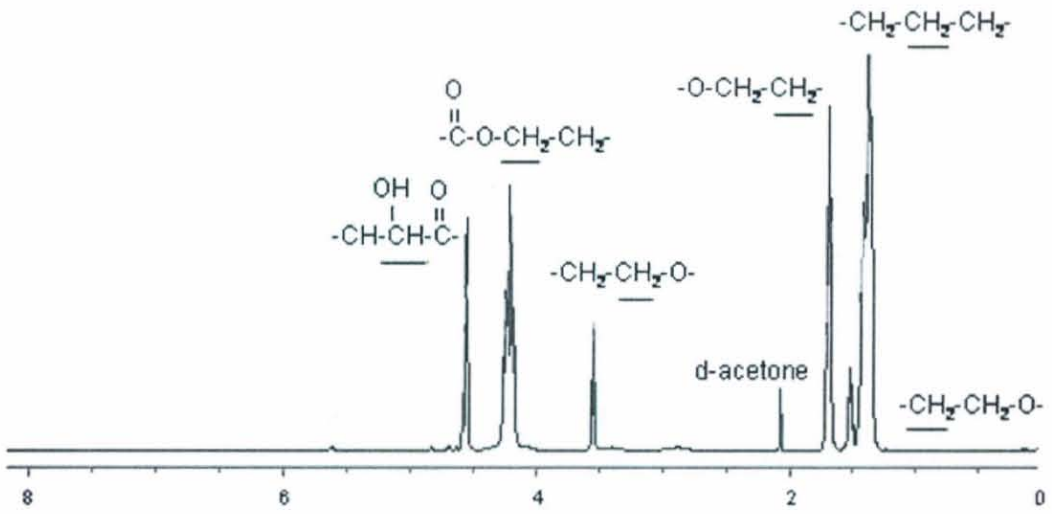

Figure 3.1 ^{1}H-NMR of the prepared prepolymer POT.

Mass spectrometry of the prepared POT prepolymer was performed to characterize the formation of the product and to confirm the molecular weight. The resulting molecular weight was 1241 Daltons, which agrees with the estimated molecular weight obtained using the ^{1}H-NMR spectrum.

The second step in the preparation of the elastomers was the synthesis and characterization of the tetra-functional crosslinking monomer BCP. The crosslinker was characterized by the APCI-MS spectroscopic method. The mass spectrum shown in Figure 3.2 confirmed the molecular weight of the final product. A peak (base peak) corresponding to the protonated molecule (M+1) appears at m/z 269, which is consistent with the molecular mass of the expected BCP product. The prominent peaks observed at m/z 253.1 and m/z 239.1 are likely due to neutral losses of oxygen, $[M-O+H]^{+}$, and CH_2O, respectively.

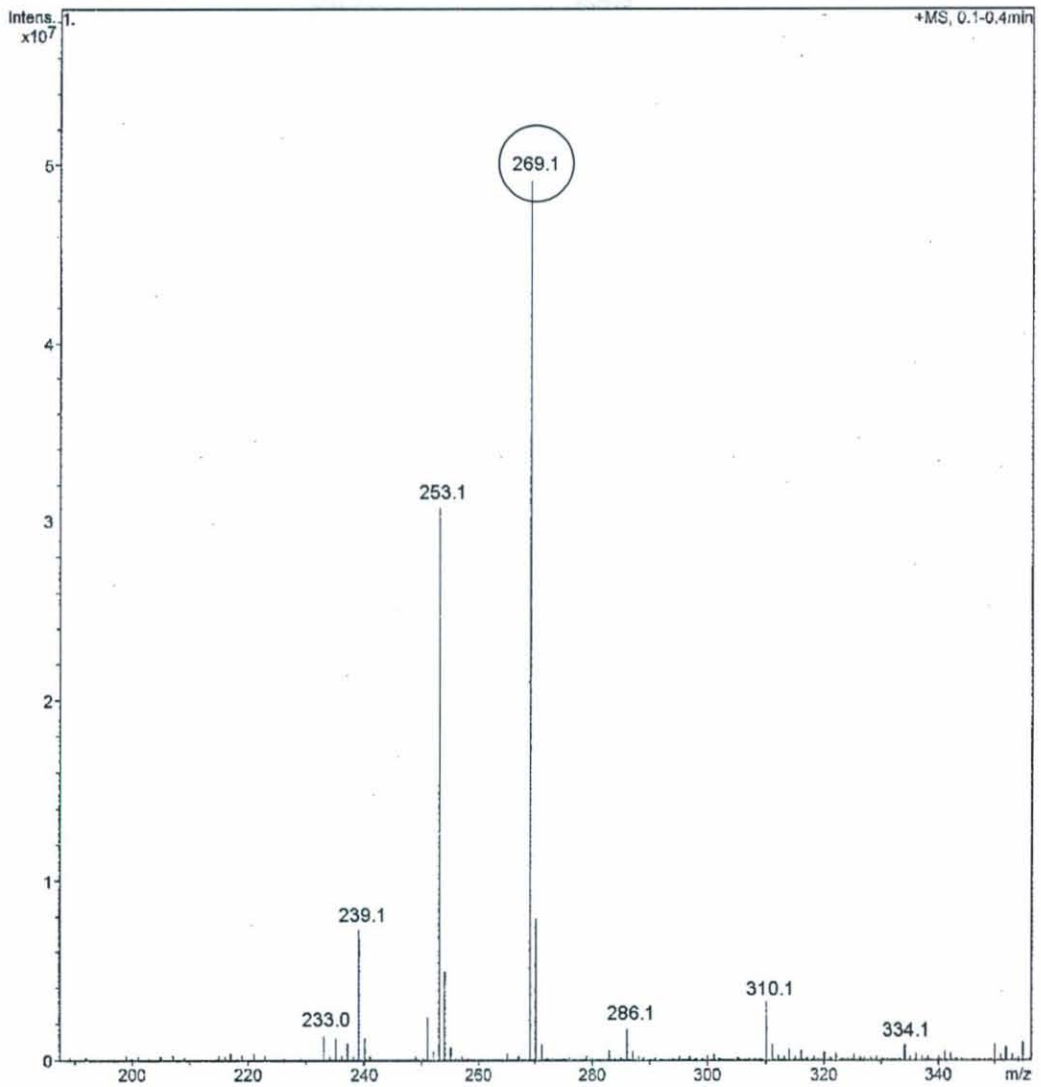

Figure 3.2 Mass spectrum of BCP.

GPC molecular weight analysis of the prepared POT prepolymer resulted in a weight average molecular weight of 1250 Daltons which is similar to the average molecular weight that was calculated using the integral of the chemical shifts of the ^{1}H-NMR spectrum and confirmed the previous molecular weight analysis results.

To confirm the formation of ester linkages in the backbone of the elastomers, FT-IR was conducted. The spectrum of the POT prepolymer is shown in Figure 3.3. A relatively sharp peak at 1734 cm^{-1} was found in the spectrum which was attributed to the (C=O) of the ester group. The broad peak at 3443 cm^{-1} was attributed to the hydroxyl group stretching vibrations and indicating that the hydroxyl groups are hydrogen bonded.[23,24] The non-covalent inter- and intra-molecular interactions of hydrogen bonding and van der Waals attractive forces were expected to enhance the thermal and mechanical properties of the polyester. These bonds are relatively weak and their role is to maintain the strength and elasticity of the polymer.[25-27] The absorption bands at 2928 cm^{-1} and 2856 cm^{-1} were attributed to methine group (CH) vibrations. The peak at 1465 cm^{-1} was attributed to the aliphatic methylene group (CH_2) stretching. Finally, the peak from 1300-1000 cm^{-1} was attributed to (CO) stretching.

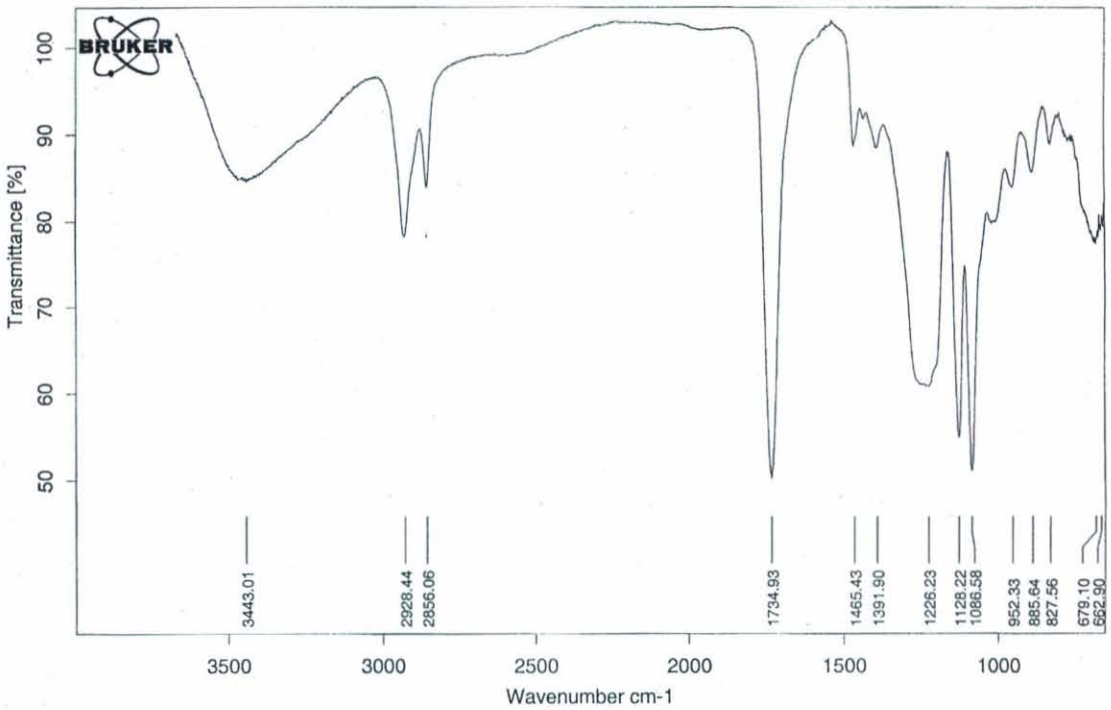

Figure 3.3 FTIR analysis of POT.

DSC was used to investigate the thermal properties of the prepared polymers. A DSC thermogram of the prepared POT prepolymer reported that a semicrystalline prepolymer was prepared with a corresponding glass transition temperature (Tg) of -16.2 °C and melting temperature (Tm) of 57.2 °C. The heat of fusion of the corresponding endotherm was measured to be 36.39 J/g.

The DSC analysis of each batch of diketone and BCP prepared and tested for purity produced sharp endothermic peaks between 160-165°C and 195-205°C, respectively, as shown in figures 3.4 and 3.5. There were no other interfering endotherms, which is an indication of the high purity that was confirmed with the LC-MS data.

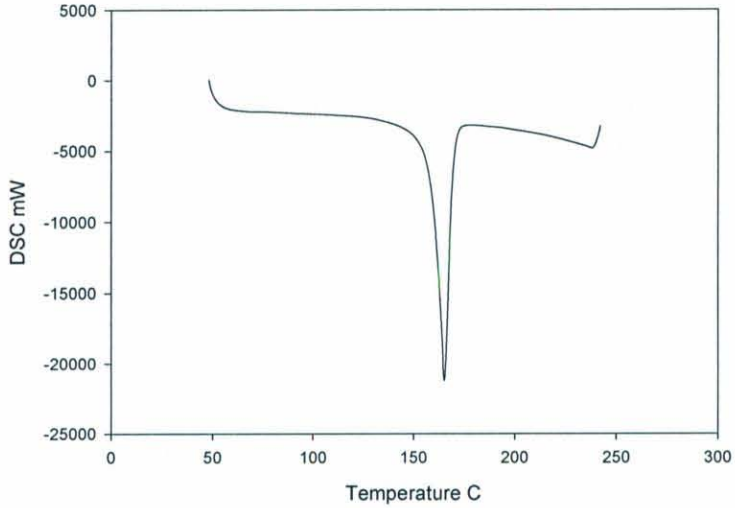

Figure 3.4 DSC thermogram of diketone.

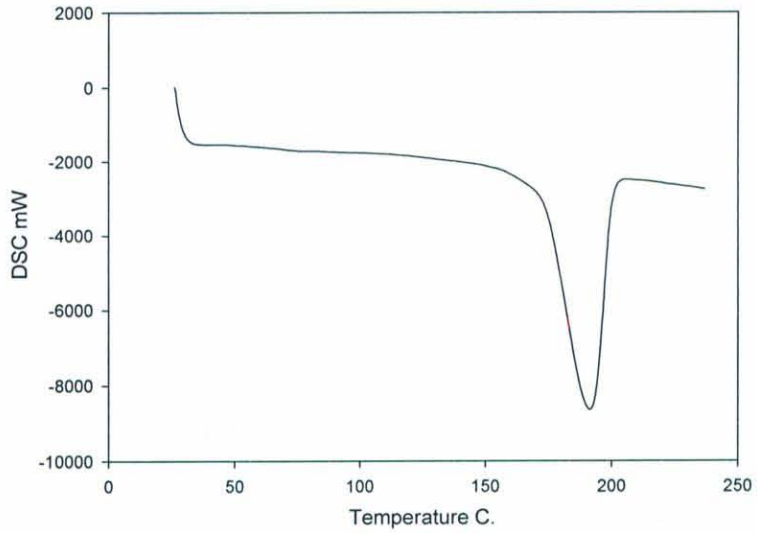

Figure 3.5 DSC thermogram of BCP.

With the structure of the prepolymer and the crosslinking agent confirmed, the elastomers were prepared. The purified POT was crosslinked in different ratios with the BCP monomer, as listed in Table 3.1. Five different elastomers were prepared with

different mechanical properties. A summary of the corresponding Tg, and Tm for each of the prepared elastomers is reported in Table 3.2. The data shows that all elastomeric networks are thermoset amorphous polymers as no melting temperatures were observed in the thermograms of any of the prepared elastomers. Also, it shows that the higher the amount of BCP used in crosslinking the POT prepolymer, the higher the Tg of the elastomer, with a range from -10.1 to -4.8 °C, as would be expected due to the increase in the crosslinking density of the elastomers.

Table 3.2 Thermal properties of the products.

Products	**Tg (°C)**	**Tm (°C)**
POT prepolymer	-16.2	57.2
Elastomer 1	-4.8	-
Elastomer 2	-6.1	-
Elastomer 3	-8.5	-
Elastomer 4	-9.3	-
Elastomer 5	-10.1	-

It was noted that in the presence of crosslinking agent (BCP), the polymerization time was reduced from 36 hours, as in case of elastomer 5, to 18 hours, as in case of elastomers 1-4. On account of the difference in preparation (the absence of a crosslinker in case of elastomer 5), only elastomers 1-4 were compared.

It was observed that when a larger amount of BCP is introduced to L-tartarate and 1,8-octandiol monomers to form polymers, (elastomers 1 & 2), it resulted in a highly crosslinked, amorphous network. On the other hand, elastomers 3 & 4, with a lesser amount of BCP, consisted of soft rubber-like segments with lower Tg. The DSC results showed that Tg was directly proportional to the amount of BCP used. The increase in Tg, upon the use of a higher amount of BCP, was attributed to the restriction in the movement of the highly crosslinked network of the polymer chain segment. In other words, the higher the crosslinking density, the bulkier the segments of polymer and the greater the amount of energy required to move it. Therefore, the Tg of the highly crosslinked elastomers will require a higher temperature than the less crosslinked elastomers.

Swelling Properties, Structure of the Sol and Gel Products, and Water Uptake Studies: Swelling experiments on the elastomers showed that they consisted of crosslinked networks that contained both insoluble parts (gel) and soluble parts (sol) (i.e, the portion of elastomer that had no covalent bonds to other chains in the network). The content of sol was lower than gel and ranged from 2.16 to 9.76 % for elastomer 1 to elastomer 4, respectively. The swelling test results showed relatively low sol content and elastomer network formation was confirmed, as none of the discs of elastomer dissolved in dichloromethane, and each kept its original physical structure after the removal of dichloromethane.

As shown in Table 3.3, the values of the sol content % (Q) of elastomer 1 and elastomer 2 were the lowest. The values for Q of elastomer 3 and elastomer 4 were the

highest, which indicates that the gel content of these products were the lowest. The gel parts of the products gradually increased and the sol parts decreased with the increase in the amount of BCP in the elastomers. Considering the mechanism of condensation polymerization and the presence of the tetra-functional crosslinking BCP, these observations were expected. Upon increasing the amount of BCP of the reactants, more and more living crosslinkable terminals of the crosslinking agent in the chains were formed, as a result, more crosslinking points were generated.

Table 3.3 Sol Contents, R, and Water Uptake of different elastomers in dichloromethane.

Elastomer	**Sol content % (Q)**	**Swelling degree of the corresponding gel % (R)**	**Water uptake %**
Elastomer 1	2.16	161.45	2.22
Elastomer 2	3.29	181.82	3.04
Elastomer 3	6.59	249.43	3.31
Elastomer 4	9.76	264.86	3.99

The degree of swelling for the corresponding gel (R) of the elastomers in dichloromethane is an important property for characterizing the degree of crosslinking of elastomers. The value of R is the total of the degree of swelling of the sol and gel parts of the polymer matrix.

From the R values of the elastomers shown in Table 3.3, the following can be observed. First, all of the values of the swelling percentages ranged between 161 % and 265 %, which implied that the swelling represented by the the gel part, was fairly high. Second, the R values of the elastomers were the lowest with the highest amount of BCP, elastomer 1, and increased when the amount of BCP decreased; furthermore, R reached its highest value when the elastomer had the least amount of BCP, elastomer 4.

By increasing the sol content Q, the swelling degree R increases due to the swelling of the sol part. Therefore a high value for the swelling percentage means less crosslinking, in other words a lower gel content. On the basis of such a model, the R value of the elastomers would be composed of both sol swelling and gel swelling. Therefore, the increase in the crosslinking density of the gel portions was believed to decrease the R, the increases of the sol content of the elastomers lead to an overall increase in R.[23] It was concluded that, increasing the amount of BCP within the elastomer networks would decrease the Q, and R values, and increase the crosslinking degree of the products.

All the elastomers were insoluble in water, and swelled from 2.22 to 3.99 % after soaking in water for 24 hr, for elastomer 1 to elastomer 4, respectively (Table 3.3). The hydrophobicity of BCP influenced the extent of the water uptake. The water uptake of the elastomers was not high because water was prevented from diffusing into the materials due to the highly crosslinked structure, particularly for elastomer 1 and elastomer 2. Water was able to diffuse to a greater extent in elastomers 3 and 4 due to the lower

amount of crosslinking agent. In short, the water uptake increased by decreasing the BCP content; that is to say, decreasing the crosslinking density of the elastomers.[28] The data confirmed that by increasing the crosslinking density using BCP, the sol content and water uptake decreases as a result of more anchoring termini of BCP molecules in the polymer matrices.

Mechanical Properties: For the purpose of determining the mechanical properties of elastomers 1-4, slabs of those elastomers were subjected to tensile testing as detailed in the experimental section of this work. All the elastomeric slabs were completely intact for the tensile testing and were very easy to align in the Instron clamps.

Figure 3.6 shows the stress-strain profiles for elastomers prepared using different BCP:POT ratios. Average values (for triplet samples) for the Young's modulus, E, extension ratio, λ_b, maximum stress, σ, and percent strain at maximum load, ε, obtained for uniaxial tensile measurements are listed in Table 3.4.

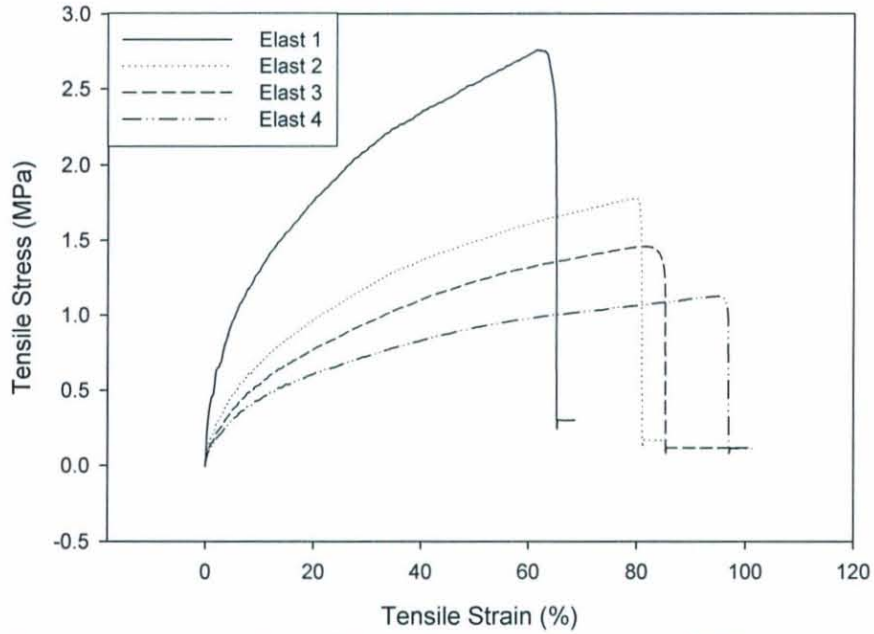

Figure 3.6 Stress-strain behaviour of Poly(Octanediol-Tartarate) POT elastomers.

Table 3.4 Summary of the mechanical properties of the elastomers. Values are means ± (standard deviation).

Elastomer	**Young's Modulus (MPa) (E)**	**Extension Ratio (λ_b)**	**Max Stress (MPa) (σ)**	**% Strain at Max Load (ε)**
Elastomer 1	0.23 ± (0.01)	1.34	2.99 ± (0.02)	66.62 ± (1.87)
Elastomer 2	0.13 ± (0.02)	1.46	1.95 ± (0.08)	80.85 ± (0.74)
Elastomer 3	0.08 ± (0.01)	1.78	1.48 ± (0.01)	84.03 ± (0.53)
Elastomer 4	0.05 ± (0.02)	2.04	1.05 ± (0.05)	95.27 ± (0.71)

The elasticity moduli, E, decreased from a value of 0.23 MPa from elastomer 1 to a value of 0.05 MPa for elastomer 4. These results are mirrored in the results for maximum stress (σ), as the amount of BCP decreased; the maximum stress also decreased from a value of 2.99 to 1.05 MPa for elastomer 1 to elastomer 4, respectively. A decrease in the amount of crosslinking agent resulted in the increase of the extension ratio of 1.34 for elastomer 1 to 2.04 for elastomer 4. Similarily, the percent strain at maximum load increased from 66.62 for elastomer 1 to 95.27 for elastomer 4. Incorporation of higher amounts of the crosslinker, BCP, resulted in a tougher elastomer.

The stress-strain behaviours of all of the elastomers were a reflection of their corresponding Tgs. As expected, incorporation of higher amounts of the BCP crosslinker resulted in a higher crosslinking density and tougher elastomer indicated by higher Young's modulus (E) values and lower percent strain at maximum load (ε) as for elastomer 1. On the other hand, elastomer 4, with less BCP, was a soft and weak elastomeric polymer with a low E and high ε. Therefore, it can be concluded that a consistent correlation was established between the mechanical properties and the amount of BCP added to the polymer matrices.

***In Vitro* Degradation Studies:** To determine the changes in the mechanical properties and the degradation patterns of the prepared elastomers as a function of time, slab specimens of elastomers 1 & 2 were subjected to an accelerated *in vitro* degradation experiment in PBS of pH = 7.4 at 37 ^{o}C. Figure 3.7 shows the percentage mean increase in weight of the slabs with respect to time over a period of 8 weeks. The weight gain of

elastomer 1 and elastomer 2 increased with time, due to the formation of degradation products that drew more water into the polymer matrix via osmosis. The reason for the increase in water content is likely due to the inability of the degradation products to diffuse out from the bulk as a result of the high crosslinked density. By the end of 8 weeks, the elastomeric slabs became paste-like in their consistency but none of the slabs had degraded completely. The weight gain during the incubation of elastomer 1 and elastomer 2 resulted from water penetration into the amorphous network where it is less organized and more accessible to water molecules via diffusion.[29] Such behaviour has been reported for other polymers.[30]

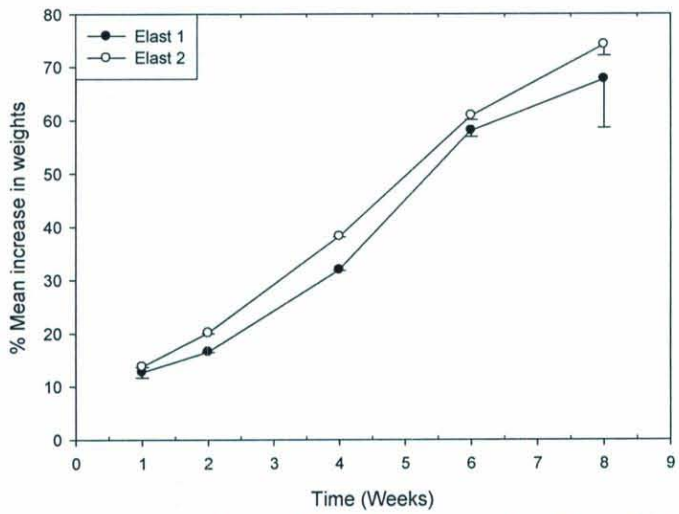

Figure 3.7 Percentage increase in weight of the tested slabs of the corresponding elastomers.

The hydrophiliciy of the elastomer is increased by the formation of free carboxylic and hydroxylic end groups as a result of the nonenzymatic hydrolytic cleavage of ester bonds during the degradation of the elastomer.[31] Furthermore, the hydrophilic moieties acted as a driving force for imbibition of water into the elastomers due to osmotic

activity, therefore the elastomers began to swell. Thus, the increase in weight of the elastomers with time can be used as a measure of the rate of degradation of the products. This pattern of degradation would result in the accumulation of the acidic monomers inside the bulk which contributed to the further autocatalytic acidic degradation, which is comparable to the degradation pattern of poly(DL-lactic-*co*-glycolic acid) (PLGA) copolymer.[32]

It was reported that polymers containing both hydrophobic and hydrophilic segments seem to have a higher biodegradability than those polymers containing either hydrophobic or hydrophilic segments only.[33,34] POT elastomers containing a higher amount of BCP, which is hydrophobic, had a slower rate of degradation than those containing lower amounts of BCP. As such, we can conclude that the elastomeric properties can potentially be tailored by grafting hydrophobic moieties to the hydroxyl groups, such as BCP, which inhibits the attack of the ester groups. The presence of both hydrophilic and hydrophobic segments provides the best characteristics to the polymer during degradation and therefore, is very useful for the controlled release of drugs.[35] Such a pattern has been previously reported with many polymers.[16,36,37] In general, the rate of degradation increased with the increase of the hydrophilic moieties or decrease in the hydrophobic segments in the polymer chain.[38] Increasing the crosslinking density in elastomer 1 over elastomer 2 served to reduce the rate of hydrolytic attack by restricting the segmental motion of the polymer chains and reducing the water penetration into the elastomer network.

The 11 % increase in weight during the first week indicates that degradation began immediately after placement in the buffer. This is likely because of the low molecular weight of the polymer. By the second week, the absorption of water was higher in elastomer 2 than elastomer 1, and this pattern continued for the eight week incubation period. This behavior would be attributed to the lower crosslinking density of elastomer 2 compared to elastomer 1. The higher the crosslinking density, the slower the degradation rate.[10,39]

Changes in the Mechanical Properties during *In Vitro* Degradation: The decrease in the modulus values for elastomer 1 and elastomer 2 during the *in vitro* degradation study period are shown in Figure 3.8. A decrease in the modulus with time during degradation has been reported previously.[21] This behavior is indicative of a homogenous bulk hydrolysis mechanism in which a random chain scission of ester groups occurs along the backbone. The bond cleavage is occurring within the bulk matrix, causing a decrease in modulus as the number of effective elastic chains is reduced with each bond cleavage. Similarly, the percent strain at maximum load, ε, for elastomer 1 and elastomer 2 decreased until the second week and then maintained some elasticity till the end of the incubation period (data not shown). This is may be explained because elastomer 1 and elastomer 2 had elastic behavior due to their high crosslinked density.

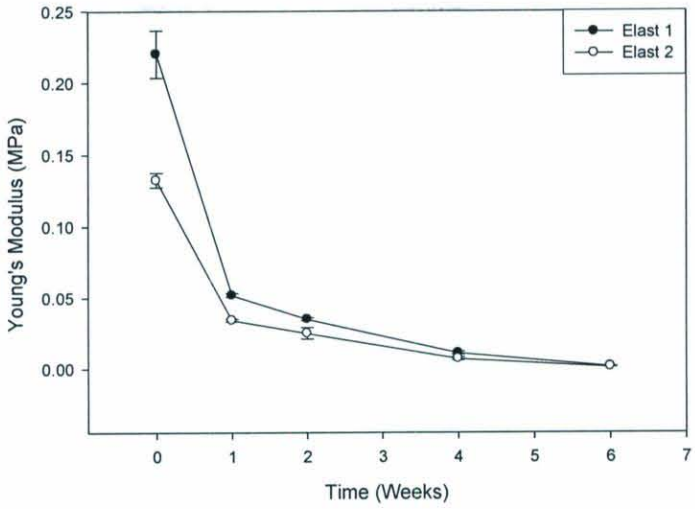

Figure 3.8 Change in Young's Modulus with time.

The changes in the ultimate tensile stress, σ, of the elastomers during the *in vitro* degradation study were expected and were related to the other mechanical properties examined in this study. First, a decrease in the ultimate tensile stress was indicative of the degradation process of elastomer 1 and elastomer 2. In addition, the decrease in the ultimate tensile stress was most significant after two weeks of the *in vitro* study and then declined more slowly until the values approached zero by the end of the degradation study. (Figure 3.9)

The mechanical properties testing was stopped at week 6. The degraded slabs were very weak and hard to align properly in the Instron clamps.

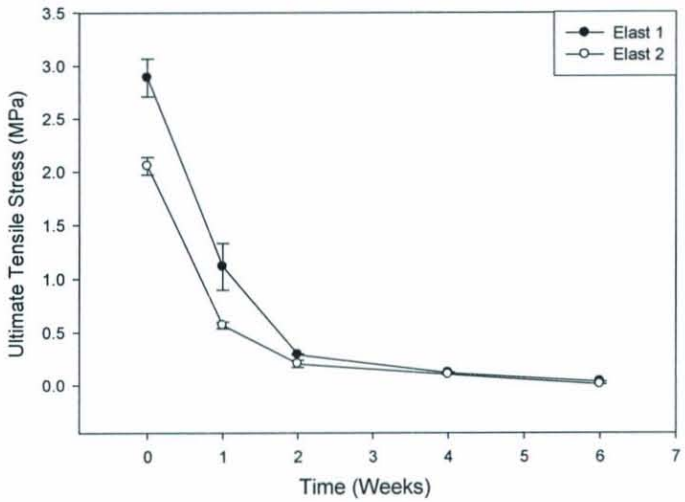

Figure 3.9 Change in ultimate tensile stress (maximum stress) with time.

In general, polymer erosion can be classified into homogenous or bulk erosion, and heterogeneous or surface erosion.[40] However, both types are extremes and the degradation mechanism of polymers is often characterized by a combination of both.[31] In a previous study by Schliecker et al., it was demonstrated that the degradation of a poly(diethyl tartarate)-co-(isopropyliden tartarete) polymer mainly proceeds via bulk erosion. The polytartrate implant is characterized by a rapid mass loss within a short period of time occuring after a definite lag phase without remarkable mass loss.[31] This behaviour is similar to the POT elastomers, which showed a lag time of two weeks. (figure 3.10).

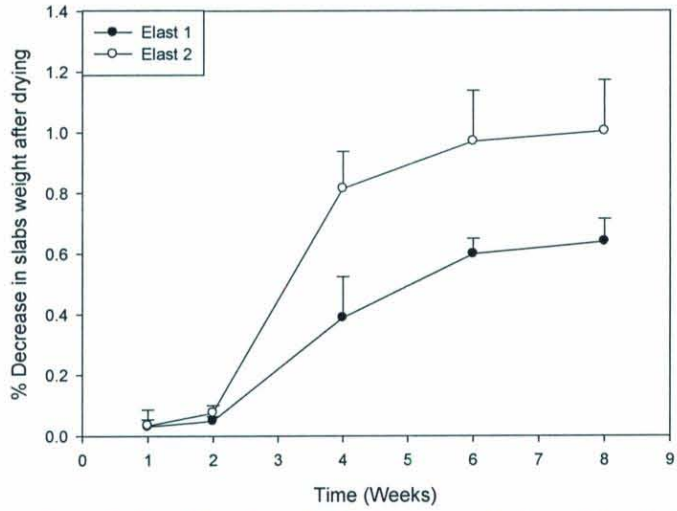

Figure 3.10 Change in weight of the tested elastomers with time after drying.

The changes in the extension ratio, λ_b, for the slabs with time are reported in Table 3.5. As expected, a decrease in the λ_b values accompanied the use of a higher amount of BCP and the resulting higher crosslinked density.

Table 3.5 Summary of the changes in the extension ratio values with time for the tested slabs. Values are mean ± (standard deviation).

Time	**Elastomers Tested**	
(Weeks)	**Elastomer 1**	**Elastomer 2**
0	1.34 (0.05)	1.46 (0.06)
1	1.30 (0.03)	1.36 (0.01)
2	1.31 (0.02)	1.45 (0.05)
4	1.37 (0.02)	1.54 (0.02)
6	1.66 (0.05)	1.67 (0.05)

During the first week of the study, there was a decrease in the extension ratio for both elstomers, which may be due to the initial water uptake. After the first week, the λ_b values increased for both elastomers. Elastomer 1, the more highly crosslinked elastomer, had lower values than elastomer 2. This behaviour is consistent with the mechanical properties tested in the study. The loss of mechanical properties over the incubation period for elastomer 1 and elastomer 2 were directly related to the hydrophilicity of the material. The more hydrophilic the material, the easier it was to lose the mechanical properties.[38]

Since the crosslinked density is directly proportional to the strength but inversely proportional to the degradation rate of POT elastomers, the properties of the elastomer were tailored by adjusting the amount of the crosslinking. Flexibility can be conferred on the elastomers by varying the amount of crosslinker. The results show that POT elastomers are degradable copolymers and that the degradation rate can be modulated by changing the ratio of BCP crosslinking agent.

PH Changes in the Degradation Media Over Time: This experiment was carried out to monitor the change in pH during the degradation process. The medium was not changed during the whole testing period, there were no sink conditions, to assess whether there were any changes in the pH of the medium due to the released products into the medium. As shown in Figure 3.11, the pH of the degradation solution decreased as the degradation process proceeded. The appearance of the drastic pH changes with the

different elastomers was parallel with the observable changes in the appearance of the elastomers, attributable to a faster degradation rate.

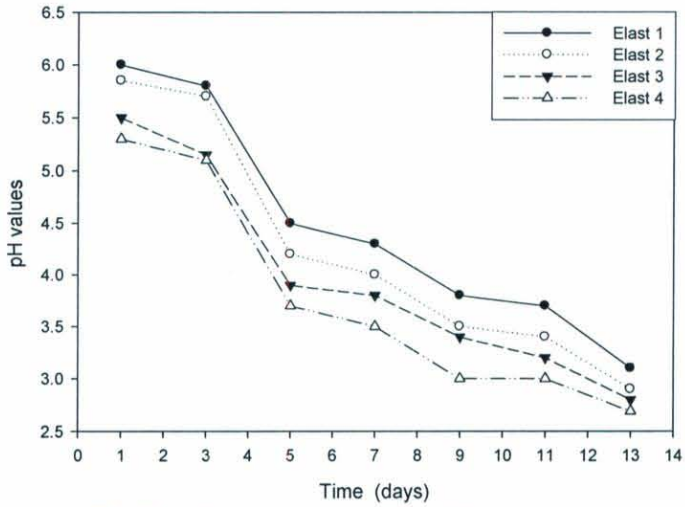

Figure 3.11 Change in pH of the degradation media with time.

In parallel with an increase in water absorption, the pH value of the degradation medium started to decrease. This is likely the result of the increase of monomers bearing the acidic carboxyl group of L-tartaric acid in the medium. The hydrophilicity of the polymer increases due to the formation of free hydroxylic and carboxylic end groups. As a consequence, the acidic monomer and oligomer products start to diffuse into the surrounding medium and decrease the pH value.

Elastomers 1 & 2 showed the smallest pH change after it reached only a pH of 3.5 by day 10. Fortunately, END can survive stable and remains active within this pH environment, and, sink conditions would be assumed in the human body.

3.5 CONCLUSIONS

A series of novel biodegradable polyester elastomers were successfully synthesized and characterized. A crosslinking agent, BCP, was used to change the crosslinking densities, swelling and the mechanical properties of the elastomers. A consistent correlation was established between the mechanical properties and the amount of BCP added into the polymer matrices. The *in vitro* degradation study showed that the higher the amount of BCP, the slower the degradation. The original mechanical properties were diminished with longer degradation times. The new elastomers follow a bulk hydrolysis degradation pattern and demonstrate promising applications in tissue engineering and the development of implantable drug delivery systems.

The effect of the crosslinking density on elastomers by the addition of an external source of crosslinking agent, BCP, was investigated. However, there are other factors that affect the characteristics of elastomers. The use of different ratios of the monomers, with or without BCP can be investigated. Future experiments could be conducted to focus on the monitoring the molecular weight, the molecular weight distribution, the hydrophilic/hydrophobic character, and thermal characterization of the elastomers during the *in vitro* degradation study.

As a final observation, the elastomer crosslinking was performed under elevated temperature, which is not feasible for most drugs and certainly not for protein drugs; Therefore, it was necessary to find a method that does not require high temperatures in

the preparation of the elastomer. As a result, a non-thermal and photocuring method was developed to prepare a crosslinked elastomer to use for drug delivery.

3.6 REFERENCES

1. Sodian, R.; Sperling, J. S.; Martin, D. P.; Egozy, A.; Stock, U.; Mayer, J. E., Jr.; Vacanti, J. P. Fabrication of a trileaflet heart valve scaffold from a polyhydroxyalkanoate biopolyester for use in tissue engineering. *Tissue Eng 2000, 6, 183-188.*

2. Sodian, R.; Loebe, M.; Hein, A.; Martin, D. P.; Hoerstrup, S. P.; Potapov, E. V.; Hausmann, H.; Lueth, T.; Hetzer, R. Application of stereolithography for scaffold fabrication for tissue engineered heart valves. *ASAIO J 2002, 48, 12-16.*

3. Sodian, R.; Fu, P.; Lueders, C.; Szymanski, D.; Fritsche, C.; Gutberlet, M.; Hoerstrup, S. P.; Hausmann, H.; Lueth, T.; Hetzer, R. Tissue engineering of vascular conduits: fabrication of custom-made scaffolds using rapid prototyping techniques. *Thorac. Cardiovasc. Surg. 2005, 53, 144-149.*

4. Yang, C.; Sodian, R.; Fu, P.; Luders, C.; Lemke, T.; Du, J.; Hubler, M.; Weng, Y.; Meyer, R.; Hetzer, R. In vitro fabrication of a tissue engineered human cardiovascular patch for future use in cardiovascular surgery. *Ann. Thorac. Surg. 2006, 81, 57-63.*

5. Diez, S.; Tros, d., I Versatility of biodegradable poly(D,L-lactic-co-glycolic acid) microspheres for plasmid DNA delivery. *Eur. J Pharm. Biopharm. 2006, 63, 188-197.*

6. Tang, G. P.; Guo, H. Y.; Alexis, F.; Wang, X.; Zeng, S.; Lim, T. M.; Ding, J.; Yang, Y. Y.; Wang, S. Low molecular weight polyethylenimines linked by beta-cyclodextrin for gene transfer into the nervous system. *J Gene Med. 2006, 8, 736-744.*

7. D'Souza, R.; Mutalik, S.; Udupa, N. In Vitro and In Vivo preparation evaluations of bleomycin implants and microspheres Prepared with DL-poly (lactide-co-glycolide). *Drug Dev. Ind. Pharm. 2006, 32, 175-184.*

8. Ekholm, M.; Helander, P.; Hietanen, J.; Lindqvist, C.; Salo, A.; Kellomaki, M.; Suuronen, R. A histological and immunohistochemical study of tissue reactions to solid poly(ortho ester) in rabbits. *Int. J Oral Maxillofac. Surg. 2006, 35, 631-635.*

9. Chorny, M.; Mishaly, D.; Leibowitz, A.; Domb, A. J.; Golomb, G. Site-specific delivery of dexamethasone from biodegradable implants reduces formation of pericardial adhesions in rabbits. *J Biomed. Mater. Res. A 2006, 78, 276-282.*

10. Yang, J.; Webb, A. R.; Pickerill, S. J.; Hageman, G.; Ameer, G. A. Synthesis and evaluation of poly(diol citrate) biodegradable elastomers. *Biomaterials 2006, 27, 1889-1898.*

11. Chia, S. L.; Gorna, K.; Gogolewski, S.; Alini, M. Biodegradable elastomeric polyurethane membranes as chondrocyte carriers for cartilage repair. *Tissue Eng 2006, 12, 1945-1953.*

12. Qiu, H.; Yang, J.; Kodali, P.; Koh, J.; Ameer, G. A. A citric acid-based hydroxyapatite composite for orthopedic implants. *Biomaterials 2006, 27, 5845-5854.*

13. Yang, J.; Motlagh, D.; Webb, A. R.; Ameer, G. A. Novel biphasic elastomeric scaffold for small-diameter blood vessel tissue engineering. *Tissue Eng 2005, 11, 1876-1886.*

14. Kang, Y.; Yang, J.; Khan, S.; Anissian, L.; Ameer, G. A. A new biodegradable polyester elastomer for cartilage tissue engineering. *J Biomed. Mater. Res A 2006, 77, 331-339.*

15. Younes, H. M.; Bravo-Grimaldo, E.; Amsden, B. G. Synthesis, characterization and in vitro degradation of a biodegradable elastomer. *Biomaterials 2004, 25, 5261-5269.*

16. Wang, Y.; Ameer, G. A.; Sheppard, B. J.; Langer, R. A tough biodegradable elastomer. *Nat. Biotechnol. 2002, 20, 602-606.*

17. Chandra, R.; Rustgi, R. Biodegradable polymers. *Progress in Polymer Science 1998, 23, 1273-1335.*

18. Alla, A; Rodriguez-Galfin, A.; De llarduya, A.M.; Mufioz-Guerra, S. Degradable poly(ester amide)s based on L-tartaric acid. *Polymer 1997, 38, 4935-4944.*

19. Olson, D. A.; Gratton, S. E.; DeSimone, J. M.; Sheares, V. V. Amorphous linear aliphatic polyesters for the facile preparation of tunable rapidly degrading elastomeric devices and delivery vectors. *J Am. Chem. Soc. 2006, 128, 13625-13633.*

20. Huang, S. J.; Ho, L. H.; Hong, E.; Kitchen, O. Hydrophilic-hydrophobic biodegradable polymers: release characteristics of hydrogen-bonded, ring-containing polymer matrices. *Biomaterials 1994, 15, 1243-1247.*

21. Pitt, C. G.; Hendren, R. W.; Schindler, A.; Woodward, S. C. The enzymatic surface erosion of aliphatic polyesters. *Journal of Controlled Release 1984, 1, 3-14.*

22. Palmgren, R.; Karlsson, S.; Albertsson, A. Synthesis of degradable crosslinked polymers based on 1,5-dioxepan-2-one and crosslinker of bis--caprolactone type. *Journal of Polymer Science Part A: Polymer Chemistry 2000, 35, 1635-1649.*

23. Liu, Q.; Tian, M.; Ding, T.; Shi, R.; Zhang, L. Preparation and characterization of a biodegradable polyester elastomer with thermal processing abilities. *J. Appl. Polym. Sci. , Appl. Polym. Symp. , 2005, 98, 2033-2041.*

24. Xie, D. L.; Chen, D.; Jiang, B.; Yang, C. Z. Synthesis of novel compatibilizers and their application in PP/nylon-66 blends. I. Synthesis and characterization. *Polymer 2000, 41, 3599-3607.*

25. Michel M..; Bitritto, J. P.; George, M. B.; Samuel, J. H.; James, R. K. Synthesis and Biodegradation of polymers derived from alpha hydroxy acids. *Journal of Applied Polymer Science: Applied Polymer Symposium 1979, 35, 405-414.*

26. Sarvestani, A. S.; Jabbari, E. Modeling and experimental investigation of rheological properties of injectable poly(lactide ethylene oxide fumarate)/hydroxyapatite nanocomposites. *Biomacromolecules. 2006, 7, 1573-1580.*

27. Kimura, M.; Fukumoto, K.; Watanabe, J.; Takai, M.; Ishihara, K. Spontaneously forming hydrogel from water-soluble random- and block-type phospholipid polymers. *Biomaterials 2005, 26, 6853-6862.*

28. Rosenblatt, Joel and Han (Bridgewater, NJ Kataria Ram L. Polymer coated microparticles for sustained release. *Ethicon, Inc. Somerville NJ. 10/183,260[United States Patent 7101566]. 2006. United States. Ref Type: Patent*

29. Hurrell, S.; Cameron, R. E. The effect of initial polymer morphology on the degradation and drug release from polyglycolide. *Biomaterials 2002, 23, 2401-2409.*

30. Jeong, S. I.; Kim, B. S.; Lee, Y. M.; Ihn, K. J.; Kim, S. H.; Kim, Y. H. Morphology of elastic poly(L-lactide-co-epsilon-caprolactone) copolymers and in vitro and in vivo degradation behavior of their scaffolds. *Biomacromolecules. 2004, 5, 1303-1309.*

31. Schliecker, G.; Schmidt, C.; Fuchs, S.; Kissel, T. Characterization and in vitro degradation of poly(2,3-(1,4-diethyl tartrate)-co-2,3-isopropyliden tartrate). *J Control Release 2004, 98, 11-23.*

32. Lu, L.; Peter, S. J.; Lyman, M. D.; Lai, H. L.; Leite, S. M.; Tamada, J. A.; Uyama, S.; Vacanti, J. P.; Langer, R.; Mikos, A. G. In vitro and in vivo degradation of porous poly(DL-lactic-co-glycolic acid) foams. *Biomaterials 2000, 21, 1837-1845.*

33. Mao, H. Q.; Shipanova-Kadiyala, I.; Zhao, Z.; Dang, W.; Brown, A.; Leong, K. W. Biodegradable poly(terephthalate-co-phosphate)s: synthesis, characterization and drug-release properties. *J Biomater Sci Polym Ed 2005, 16, 135-161.*

34. Quaglia, F.; Vignola, M.; De Rosa, G.; La Rotonda, M.; Maglio, G.; Palumbo, R. New segmented copolymers containing poly(epsilon-caprolactone) and etheramide segments for the controlled release of bioactive compounds. *J Control Release 2002, 83, 263-271.*

35. Huang, S. J.; Ho, L.; Hong, E.; Kitchen, O. Hydrophilic-hydrophobic biodegradable polymers: release characteristics of hydrogen-bonded, ring-containing polymer matices. *Biomaterials 1994, 15, 1243-1247.*

36. Jayachandran, K. N. Synethesis of dense brush polymers with cleavage grafts. *Eur. Polym. J. 2000, 36, 743-749.*

37. Laschewsky, A.; Rekai, E. D.; Wischerhoff, E. Tailoring of stimuli-rewponsive water-soluble acrylamide and methacrylamide polymers. *Macromol. Chem. Phys 2001, 202, 276-286.*

38. Katarzyna Gorna, S. G. Biodegradable polyurethanes for implants. II. In vitro degradation and calcification of materials from poly(-caprolactone)-poly(ethylene oxide) diols and various chain extenders. *Journal of Biomedical Materials Research 2002, 60, 592-606.*

39. Yang, J.; Webb, A. R.; Ameer, G. A. Novel Citric Acid-Based Biodegradable Elastomers for Tissue Engineering. *Adv. Mater. 2004, 16, 511-516.*

40. Goepferich, A. Mechanism of polymer degradation and elimination. *In Handbook of Biodegradable Polymers; A.Domb, J. K. D. W., Ed.; Amsterdam, 1998; pp. 451-471.*

Chapter 4. Synthesis, Characterization and *In Vitro* Osmotic Release Studies of Pilocarpine Nitrate and Endostatin from a New Photo-crosslinked Biodegradable Elastomer.

4.1 ABSTRACT

Purpose: To prepare and characterize a novel family of ultraviolet (UV) crosslinked biodegradable poly(octanediol-tartarate) (POT) elastomers and to test the effect of drug loading, particle size, device geometry, and polymer properties on the *in vitro* release of the water soluble drug, pilocarpine nitrate (PN) and endostatin (END) from these novel elastomers.

Methods: An aliphatic polyester prepolymer was first synthesized via the polycondensation reaction of L-tartaric acid with 1,8-octanediol at 140 °C for one hour under vacuum to form the POT prepolymer. The purified prepolymer was reacted stepwise with acryloyl chloride (ACRL) and the purified acrylated poly(octanediol-tartarate) (APOT) prepolymer was then mixed with an UV initiator and subjected to UV light to form the photocurable elastomer. All the prepared products were characterized using proton nuclear magnetic resonance (^{1}H-NMR) spectroscopy, fourier transform infrared spectrometry (FT-IR), and differential scanning calorimetry (DSC). For *in vitro* release studies, PN powder of three different particle sizes was mixed with APOT to achieve a 10% w/w loading. Lyophilized END, with trehalose and bovine serum albumin (BSA), was mixed with APOT to achieve the same w/w loading. Each mix was poured into glass moulds and subjected to photo-crosslinking. PN prepared devices were

immersed in scintillation vials with the three different media. END prepared devices were immersed in small scintillation vials containing phosphate buffer solution. Release of PN was detected using UV analysis, however, the END was quantified using a rhEND ELISA kit. The percent release for both drugs was plotted versus time.

Results: ^{1}H-NMR and infrared analysis confirmed the purity and structure of the prepolymer. Thermal analysis of the acrylated prepolymer reported a semicrystalline structure with a corresponding glass transition temperature (Tg) of -10.8°C and a melting endotherm at 53.4°C. The final photo-crosslinked POT elastomers were amorphous and have a Tg of -4.4°C. The release profiles showed that, contrary to reported studies, devices formulated with the same volumetric loading and smaller drug particle size released drug faster than the devices with a larger particle size. It was also shown that osmotic release contributed to the linear release pattern of PN from the new POT elastomers. The elastomers also followed a bulk degradation mechanism with no significant weight loss during the period of study.

Conclusions: Novel biodegradable photo-crosslinked POT elastomers were successfully prepared and characterized, and are suitable for implantable sustained release delivery of hydrophilic drugs.

4.2 INTRODUCTION

The use of biodegradable polymers in tissue engineering,[1-5] gene therapy[6,7] and drug delivery systems[8-10] has inspired the desire to develop new biodegradable elastomers.[11-13] It is desirable that biodegradable elastomers designed for such applications show a homogenous degradation profile and keep their dimensional stability during the drug release period.

One strategy to prepare elastomers involves the preparation of prepolymers, then thermally crosslinking those prepolymers using different biocompatible crosslinkers such as BCP to produce elastomers.[14] However, the preparation involves the use of solvents, such as DCM or acetone, and elevated temperatures, which would prevent it from being used as a delivery vehicle for thermo-sensitive therapeutic agents such as proteins and hormones.

In the previous chapter, the synthesis and characterization of thermoset amphiphilic elastomers as potential biomaterial for biomedical applications was reported. BCP was used to crosslink a semicrystalline prepolymer prepared by polymerizing L-tartaric acid with 1,8-octanediol and stannous 2-ethylhexanoate as a catalyst. This method resulted in biocompatible biodegradable polyester elastomers, but a polymerization temperature of 120 °C was required in the thermal curing process. Such high temperatures would hinder the use of these prepared elastomers for delivering heat sensitive protein drugs and hormones that denature at high temperatures.

In an attempt to enable the loading of thermosensitive drugs into elastomeric matrices, photo-polymerization was used. Photo-polymerization has been utilized to synthesize biodegradable hydrogels and elastomers for several biomedical applications such as drug delivery systems.[15,16] This technique involved the preparation of prepolymers with photosensitive termini which can undergo free radical polymerization and formation of photocured elastomers in the presence of a photoinitiator and ultraviolet (UV) light. This promising technique would present a number of benefits and advantages over thermal polymerization for the synthesis of biodegradable elastomers. First, it avoids the use of heat for the crosslinking process as it can be carried out at room temperature. Second, the photocuring process is rapid and proceeds in a matter of minutes. Third, it is a solvent-free process. Finally, the photocured elastomers can be customized with different crosslinking densities and mechanical properties by changing the number of photosensitive termini in the prepared acrylated prepolymers. Elastomers synthezied by this method would enable the incorporation of heat labile drugs such as proteins. There are many applications for photo-crosslinking elastomers in the biomedical field.[17-20]

Elastomers can be used for the drug delivery of osmotically active and water-soluble drugs. It is well accepted that the osmotic activity of the drugs is a major component of the drug release from such a device.[15,21,22] Many researchers have focused on the different factors that affect the mode and the rate of release from those new delivery systems.[15,22-24] It was demonstrated that the osmotic activity, concentration, and the particle size of the therapeutic agents or excipients, the degradation rate of the

polymer, and the characteristic of surrounding media play important roles that affect the release profiles of the biodegradable polymeric devices.[14,15,22,24-26]

Volumetric loading plays an important role in the release of the drug from an elastomeric monolith matrix. When the monolith system is loaded above the percolation threshold, that is to say, the drug particles dispersed in the polymer matrix are interconnected with one another, the release of the drug will not be controllable. Upon immersion of such a device into an aqueous medium, the water-filled pores that are formed as water is imbibed from the surface of the device replaces the active agent that leaches out into the medium and the release becomes non-constant and diffusionally controlled.[25] To control the osmotic and constant release of the solute from the device, the drug loading must be kept below the percolation threshold, which is approximately 30 to 35%.[23,25,27]

Osmotically active drug release from an elastomeric device is outlined briefly in scheme 4.1. Stage 1: By immersion of the drug loaded device into an aqueous medium, water vapour starts to diffuse into the elastomeric matrix and begins to dissolve the highly osmotic encapsulated solid drug particles. Stage 2: More dissolution occurs and the drug capsules start to swell and exert an osmotic pressure on the surrounding elastomeric matrix. Stage 3: Microcracks are formed due to the high osmotic pressure, and the dissolved drug is forced out of the drug capsule, through the microcracks in the elastomer into the releasing medium. This ruptures and microcracks process continues in a layer by layer fashion until complete degradation of the elastomer has occured.

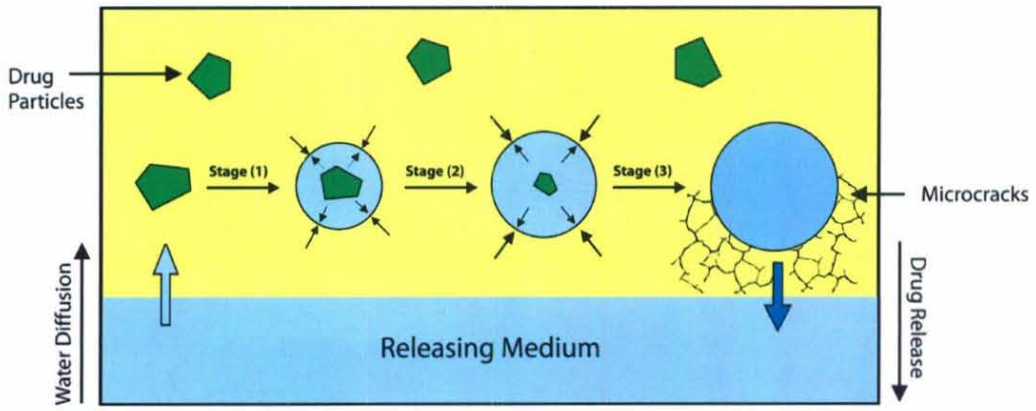

Scheme 4.1 This diagram represents the stages of the osmotic release of one drug particle within the elastomeric matrix. The particles close to the elastomer releasing medium interface will be released first. The process occurs in a serial layer by layer fashion.

The release of a drug by an osmotic mechanism has several advantages; the two main advantages being that it provides a continuous release and the rate of release can be controlled by the manipulation of excipients. Additionally, the biodegradable polymers degrade into small biocompatible monomers and can be excreted via normal excretion processes in the body, thereby avoiding a surgical removal step. In view of the challenges of administration of therapeutic doses of END, as described in chapter 2, the use of a biodegradable device having an osmotic release mechanism would circumvent many of the obstacles to the delivery of END.

Implantable biodegradable polymeric devices would provide a unique practical means of localizing angiogenic inhibitors such as END at a tumor site. The strategy of using a polymeric controlled delivery device would reduce the amount of protein needed, relative to systemic administration, to achieve a similar angiogenic inhibition. However, for protein drugs,

polymers have drug stability issues during polymer degradation because of the acidic moieties released which have an affect on the protein stability.

Three series of experiments are described in this chapter. First, details of the synthesis, photocuring and characterization of a novel biodegradable elastomer is provided. This new elastomer has potential for use as an implantable device for the delivery of therapeutic agents and protein drugs. A series of photocured elstomers with varying amounts of acryloyl chloride were prepared by means of the following steps. (i) Thermal synthesis of an aliphatic POT ester prepolymer using 2-ethylhexanoate as a catalyst; (ii) conversion of the terminal hydroxyl groups to vinyl groups by an acrylation reaction; and (iii) photocuring of the acrylated POT using 2,2-dimethoxy-2-phenyl-acetophenone (DMPA) as the photoinitiator. The resulting elastomers were characterized for structure and purity. The photocured elastomer having optimal photo-crosslinking was chosen for loading the therapeutic agents. Pilocarpine Nitrate (PN) was used as a model drug in place of END, as END is very expensive.

Second, the release profile of a highly osmotic agent such as PN from the novel elastomer was determined. In another experiment, PN was also co-formulated with trehalose. These experiments were designed to examine the effects of osmotic activity, particle size of the drug, the device geometry and the surrounding media on the release profile.

Finally, an osmotic release study of END from the photocured elastomer was carried out. END lypholized particles were incorporated into the acrylated prepolymer solution and the system was solidified into an elastomeric drug matrix by photocuring using ultra-violet light.

Trehalose and BSA were lyophilized with rhEND to produce a homogenous mixture. The excipients, trehalose and BSA, were used to maintain the bioactivity of END during the photo-crosslinking reaction. In addition, the END release was driven by the osmotic pressure generated by the dissolved trehalose co-lypholized with the END.

In summary, this novel elastomer which is biodegradable, and has desirable amphiphilic properties, is photo-crosslinked, and it is suitable to deliver protein drugs. The formulations of both PN and END were altered by incorporation of trehalose to increase the osmotic activity. The outcome was the development of a new local drug delivery system for a therapeutic protein.

4.3 MATERIALS AND METHODS

4.3.1 Materials

L-tartaric acid and 1,8-octanediol and other chemicals used in the synthesis and purification of elastomers including, stannous octoate, acetone, acryloyl chloride, triethylamine, and 4-dimethylaminopyridine, chloroform, ethyl ether, ethyl acetate, the long-wave UV (LWUV) initiator, 2,2-dimethoxy-2-phenyl-acetophenone, pilocarpine nitrate salt (PN), (+) trehalose, and serum bovine albumin (BSA) were all obtained from Sigma-Aldrich (Canada). Recombinant human Endostatin and the ELISA kit were purchased from Perprotech Canada, and R&D Systems, respectively.

4.3.2 Preparation of 1:1 Poly(Octanediol-L-Tartaric) Ester Prepolymer (POT)

The detailed method of synthesis and characterization of non-acrylated prepolymers were reported in Chapter 3. The schematic representation of the steps is repeated below.

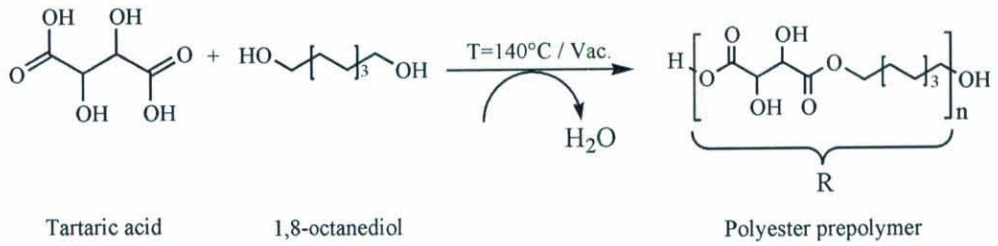

Tartaric acid 1,8-octanediol Polyester prepolymer

Scheme 4.2

4.3.3 Synthesis of the Acrylated POT Prepolymer (APOT)

Based on the number of hydroxyl terminals in the POT prepolymer, two moles of acryloyl chloride were used to react with one mole of POT prepolymer to form APOT prepolymer. The synthesis is summarized as follows. In a three neck round bottom flask, 20 gm of POT (0.016 mole) was dissolved in 200 ml of acetone on a magnetic stirrer using a magnetic stir bar. The flask was sealed using a rubber septum and flushed with argon gas. This step was repeated every 30 minutes. The flask was then immersed in an ice bath ($0^{o}C$), after which 10 mg of 4-dimethyl aminopyridine (DMAP) were added as a catalyst. A stepwise addition of 0.032 mole of each of acryloyl chloride (ACRL) and triethylamine (TEA) were added over a period of 12 hours at $0^{o}C$. The reaction was then continued at room temperature for another 12 hours. The final solution was filtered to remove the triethylamine hydrochloride salt formed during the reaction. The polymer

solution was concentrated using a rotary evaporator and further purified via dissolution in chloroform, filtered, precipitated in cold anhydrous ethyl ether, and then dried in the fume hood under vacuum for 2 days. ^{1}H-NMR, DSC, and FT-IR were used to characterize the purity of the final product and the disappearance of OH groups as a result of the formation of the vinyl groups at the arm terminals of the APOT prepolymer.

4.3.4 Ultra Violet-Crosslinking of Acrylated POT Prepolymer

Thirty percent weight / volume (%w/v) of 2,2-dimethoxy-2-phenyl-acetophenone (DMPA) in acetone was prepared to form the UV initiator solution. In a small test tube, 50 μl of the UV initiator solution was added to 1 gm of acrylated POT. The viscous solution was mixed well using a vortex mixer and poured into a cylindrical glass mould (6 mm diameter x 10 mm length). The sample was then exposed to UV light at a distance of 5 cm at room temperature for 5 minutes using a BLAK-RAY long wave ultraviolet lamp model B-100 AP of 21,700 $\mu W/cm^2$ relative intensity. The elastomer formed was then removed from the mould. The crosslinked polymer was dried in the fume hood for one day to ensure complete evaporation of any remaining acetone and kept in the desiccator under vacuum until required for analysis and characterization. A schematic presentation of the preparation process is shown in scheme 4.3.

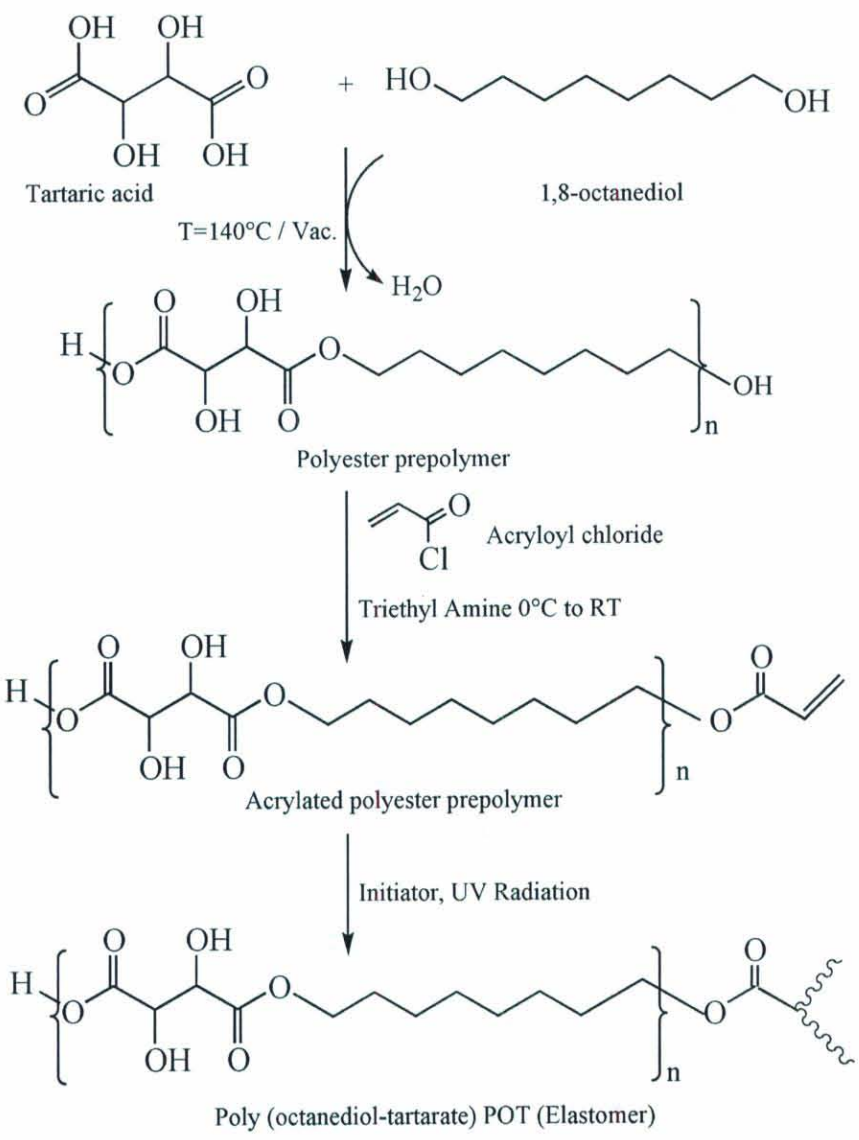

Scheme 4.3

4.3.5 Polymer Characterizaitons

Proton NMR of the acrylated POT was run in acetone-d_6 using a Bruker AVANCE 500MHz Spectophotometer. The chemical shifts in parts-per-million (ppm) for the generated spectra were referenced relative to tetramethylsilane (TMS, 0.00 ppm) as the internal reference.

Fourier transform infrared (FT-IR) spectra were obtained at room temperature using a Bruker TENSOR 27 Fourier transform infrared spectrometer. The acrylated POT prepolymer samples were prepared and poured over a zinc/selenium crystal. The infrared data was analyzed using Opus Bruker Optik version 4.0 software.

The thermal properties of the elastomers and APOT prepolymers were characterized using a Seiko 210 DSC attached to a cooling system. The sample (5-8 mg) was placed in an aluminium pan and was run at the heating rate of 10 °C/min using two cycles. From ambient temperature to -60°C to 150°C to -60°C to 150°C, with the glass transition temperature (Tg) was measured from the second heating cycle. The DSC instrument was calibrated using indium and gallium standards. The enthalpies, glass transition temperatures, and melting endotherm were determined using the internal DSC analysis program.

4.3.6 Preparation of Pilocarpine Nitrate (PN) Loaded Tablets and Cylinders

UV initiator solution (30% w/v of DMPA in acetone, 500 µl) was added to 10 gm of the APOT prepolymer. The resulting viscous clear yellow solution was mixed until homogenous. Three different particle sizes were prepared by sieving the PN powder through 45, 100, and 300 µm meshes. A 10 percent weight / weight (% w/w) PN loading was achieved by adding 1 gm of each particle size of the micronized powder to the mix. The thick suspension was then mixed using a vortex mixer for 1 minute. The product was poured into glass moulds of 10 mm diameter x 3 mm length for the tablet moulds, and 6mm diameter x 10 mm length for the cylinder moulds. The moulds were exposed to UV

light as previously described. The photo-crosslinked elastomers were then removed from the moulds by breaking and peeling the glass to get the final tablet and cylindrical devices loaded with the PN salt. Each device was weighed. When a 1:1 mix of PN and Trehalose were used to load the elastomeric monolithic systems, first both powders were dissolved in water to get an intimately mixed solution. Water was then removed using a Freezone model 77530 freeze dryer, operating at -48°C and 36 X 10^{-3} mbar. The resulting powder was seived through a 100 μm mesh sieve to obtain the final micronized mix. The drug content in all elastomeric tablet or cylinder devices was calculated based on 10% w/w which corresponds to approximately 14.4 percent volume / volume (% v/v), which is below the percolation threshold. However, % w/w is used as it is directly measured and % v/v is calculated indirectly.

4.3.7 *In Vitro* Release Study of PN and UV Analysis

The prepared monolith tablets and cylinders with different particle sizes (45 μm, 100μm, and 300μm), loaded with 10% w/w PN with or without trehalose were subjected to *in vitro* release studies using phosphate buffer saline (PBS) of pH 7.4 as a release medium. Furthermore, tablets and cylinders with 100 μm particle size PN with 10% w/w were subjected to *in vitro* release studies using DW, PBS, and 3% NaCl as release media. Three samples of each device were put into 40 ml amber scintillation vials filled with a pre-selected dissolution medium. The vials were attached to the Glas-Col rugged culture rotator. The rotator was set at a 30% rotation speed and placed in an oven at 37°C. The release medium was replaced with fresh medium to ensure sink conditions and a constant osmotic pressure driving force. The release media were replaced over a period of 24 days

or until a 100% cumulative release was achieved. Solutions withdrawn were filtered and the concentrations were determined by an ultraviolet method of analysis at a maximum wavelength of 216 nm using a MILTON ROY Spectronic 601 UV/VIS spectrophotometer.

4.3.8 Lypholization of Protein with Excipients

Human recombinant Endostatin (rhEND) was co-lyophilized with trehalose and BSA. Trehalose and BSA at a ratio of 1:1 w/w were used, while the END amount remained 500 ng and to achieve a final amount of 10 % w/w in each device. To prepare the lyopholized protein, the excipient was added as a solid to aliquots of the protein solution and stirred gently at room temperature until dissolution was complete. The solution was then filtered with a 0.22 μm low protein binding filter to remove any particulate. The filtered solution was subjected to a cycle of freeze drying at -48°C and 36 X 10^{-3} mbar for 36 hours to obtain the lyophilized product. The lyophilized product was ground into powder using a mortar and pestle and sieved through a 220 μm to 300μm mesh.

4.3.9 Preparation of Protein Loaded Elastomer Slabs

Lyophilized powder was mixed with a polymer containing the photoinitiator (0.25 gm of APOT prepolymer + 12.5 μl of 30% w/v of 2,2-dimethoxy-2-phenyl-acetophenone in acetone). This suspension was poured into Teflon rectangular moulds of 6mm x 5 mm x 1.5 mm, and then exposed to UV radiation for 5 minutes to crosslink the prepolymer. After crosslinking, the drug loaded slabs were removed from the moulds and dried in the

fume hood overnight. The drug content in each elastomeric slab was calculated based on 10% w/w (corresponding to an approximate 14.4% v/v) to ensure that the loading was well below the polymer percolation threshold of 30-35%.

4.3.10 *In Vitro* Release Study and Quantitative Analysis of the Protein

The release study was carried out by immersing the protein loaded elastomeric slabs in small scintillation vials containing 2 ml sterile PBS with pH = 7.4. The vials were attached to the Glas-Col rugged culture rotator. The rotator was set at a 30% rotation speed and placed in an oven at 37 °C. The release medium was removed at pre-determined time intervals and replaced with fresh buffer to ensure sink conditions and constant osmotic pressure driving force. The collected samples were divided into aliquots, and frozen at -80°C for subsequent analysis of concentration using a rhEND ELISA kit.

4.4 RESULTS AND DISCUSSION

Preparation and Characterization of a Photocured Elastomer: The aliphatic polyester POT prepolymer with two hydroxyl groups at the terminals was prepared using solvent free polymerization of 1,8-octanediol and L-tartaric acid at 140 °C in the presence of 2-ethylhexanoate as a catalyst. The full synthesis procedure and characterization was reported in chapter 3.

The photo-polymerization reactions were conducted with different photo-polymerizable end groups for the purpose of UV-photo-crosslinking.[28,29] The acrylation method was selected because it possesses a high reactivity with photo-polymerization conducted in the order of

minutes.[26] Moreover, the final elastomers degrade into acrylic acid which is extensively metabolized into water soluble end products that are safely washed out and excreted by the kidney without bioaccumulation.[30] For these unique properties, the terminal hydroxyl groups in the previously prepared POT were subjected to an acrylation process[15,24,26] using acryloyl chloride for the purpose of replacing the OH groups at the terminal of the aliphatic POT chains with unsaturated vinyl terminals. These acrylated terminals can undergo crosslinking via UV photo-polymerization technology in the presence of DMPA as a photoinitiator.

In order to optimize the amounts of acryloyl chloride required to undergo the complete acrylation process of the hydroxyl group terminals of the POT prepolymer, different molar ratios of acryloyl chloride were reacted with the POT prepolymer as shown in Table 4.1.

Table 4.1 Acrylated POT synthesized by using different amount of acryloyl chloride to react with POT prepolymer.

Acrylated POT Code	**POT (mol) / Acryloyl chloride (mol)**
POT-0.0	1.0 / 0.0
POT-0.5	1.0 / 0.5
POT-1.0	1.0 / 1.0
POT-2.0	1.0 / 2.0

The FT-IR spectra for the acrylated prepolymers are shown in Figure 4.1. It is clear that by increasing the molar ratio of the acryloyl chloride to POT, the intensity of the corresponding OH stretching at (3500) cm^{-1} decreased with concomitant increase in

the formation of vinyl group terminals which are indicated by the appearance of the new C=C stretching peak at (1690) cm^{-1}.

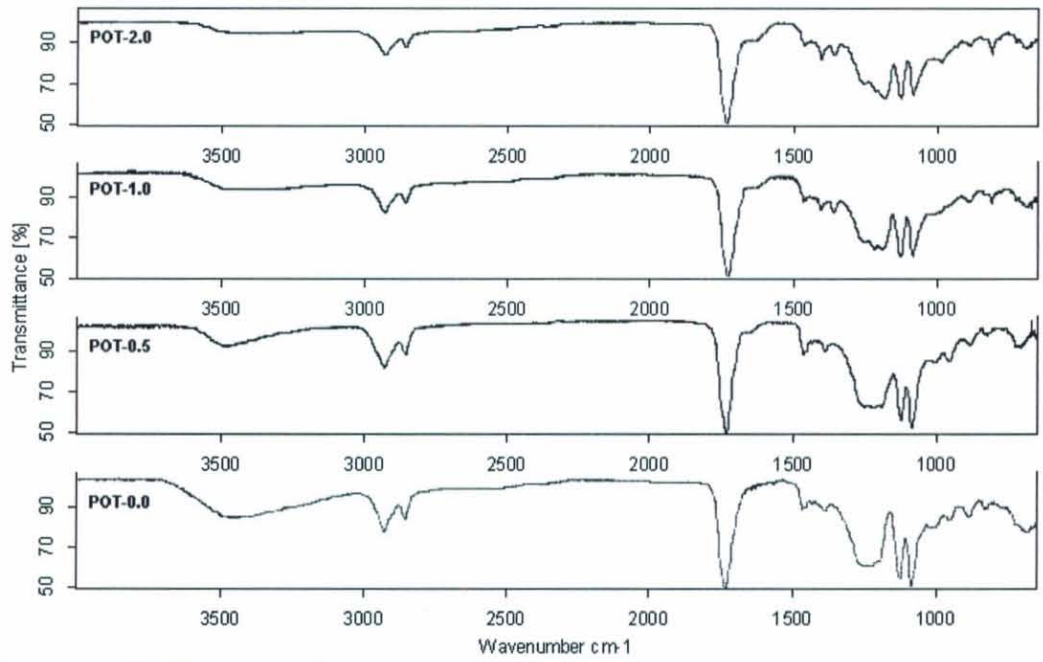

Figure 4.1 FT-IR spectra of the acrylated POT prepolymers reacted with different molar ratios of acryloyl chloride.

FT-IR spectra showed that the complete disappearance of the OH stretching was taking place with acrylated POT-2.0 compared to the OH stretching peak in the case of non-acrylated POT-0.0. This observation can be observed more clearly in Figure 4.2.

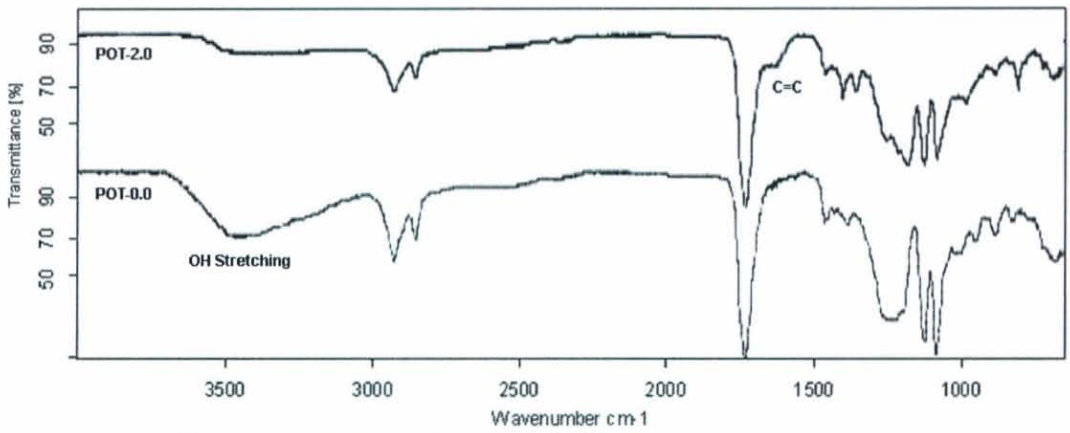

Figure 4.2 FT-IR spectra of POT before and after acrylation process.

The calculated conversion percentage of the hydroxyl groups to the corresponding vinyl groups were measured using the following equation :[31]

$$\% \text{ Conversion} = 100 - \left(\left[\frac{\left(\frac{AUP_{OH}}{AUP_{C=O}} \right)_{APOT}}{\left(\frac{AUP_{OH}}{AUP_{C=O}} \right)_{POT}} \right] \times 100 \right)$$

Where AUP_{OH} is the area under the peak of the OH stretching at (3500) cm^{-1} and $AUP_{C=O}$ is the area under the peak for C=O stretching at (1734) cm^{-1}.

As shown in table 4.2, there was no significant difference between the calculated percentage of conversion compared to the theoretical values. In general, it was obvious that the optimum amounts of acryloyl chloride used for the acrylation of POT prepolymer was one mol of acryloyl chloride to one mol of OH in the polyester POT prepolymer and resulted in a conversion percentage of 96 %.

Table 4.2 Area under the peak for OH and C=O stretching for POT and acrylated POT and % conversion of the terminal hydroxyl to the vinyl groups.

Acrylated prepolymer	AUP (OH)	AUP (C=O)	AUP (OH) / AUP (C=O)	Calculated % Conversion	Theoretical % Conversion
POT-0.0	4651	4588	1.017	0	0
POT-0.5	3452	4612	0.749	26	25
POT-1.0	2333	4561	0.512	49	50
POT-2.0	164	4345	0.038	96	100

The acrylation process and further purification was confirmed using ^{1}H-NMR spectroscopy. The acrylated groups were represented by the peaks of acryl protons between 5.9 and 6.1 ppm for OCHC=CH_2 (*cis*), and 6.4 and 6.5 ppm for OCHC=CH_2 (*trans*) as shown in Figure 4.3.

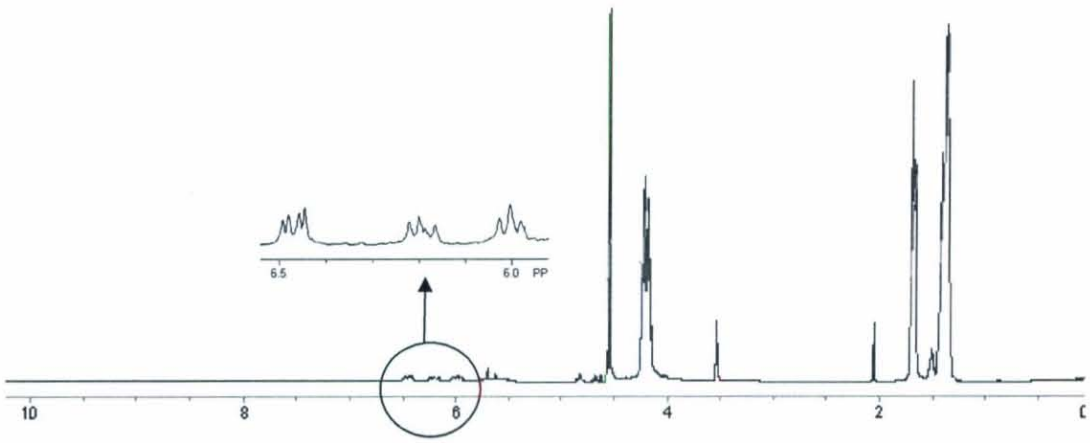

Figure 4.3 ^{1}H-NMR of the acrylated POT prepolymer.

The thermal analysis of the acrylated POT prepolymer using DSC demonstrated a semicrystalline structure with a melting endotherm at 53.4°C and with a glass transition (Tg) of -10.8°C. However, the POT-2.0 elastomer showed that it has no melting endotherm, indicating that the final product was an amorphous photoset elastomer with a Tg of -4.4°C, which is well below body temperature.

The photo-crosslinking process was initiated using DMPA as a photoinitiator. DMPA was chosen because it possesses many desirable properties. It is a highly reactive photoinitiator which accelerates the crosslinking reaction. It is biocompatible and has low toxicity on living tissues. It has good initiation efficiency and a low amount of unreacted initiator remains in the photocured polymer.[32,33]

Photocured elastomers were produced after 5 minutes of exposure of the acrylated POT prepolymer to LWUV light at a distance of 5 cm. The polymerization was rapid, the crosslinked network had formed and was confirmed by immersion of the elastomers in DCM. The elastomers swelled, but did not dissolve. This behaviour can be used as an indication that crosslinking has occurred.

The elastomer with the highest amount of crosslinking (POT-2) was used for the drug release studies, as all the hydroxyl groups were converted to photosensitive termini, and therefore would provide the highest degree of crosslinking density.

Drug Release Studies: The original purpose of the project was to load the angiogenic inhibitor protein, END, into a novel biodegradable elastomeric polymer at a volumetric loading well below the percolation threshold and to achieve a prolonged, sustained, and osmotic release of the END. The intension was to determine the conditions for the development of an optimal release profile by monitoring the effect of factors that govern the release such as particle size, surrounding medium, device geometry, and the osmotic activity of the incorporated excipients with the protein. For economic reasons, this determination was initially carried out using Pilocarpine Nitrate salt (PN) as a peptidomimetic, hydrophilic, water soluble and therapeutic drug. When the optimal conditions were determined, the END osmotic release study was carried out.

PN was selected because it is a peptidomimetic drug with reasonable osmotic activity, the concentration in the releasing media can easily be measured using UV analysis, and it is an inexpensive drug. The stability of PN in the three used media, PBS, DW, and 3 % NaCl, was tested and showed no significant changes during a one-week period.

The goal was to develop an osmotically controlled drug release system. Iso-osmotic (PBS), hypo-osmotic (DW) and hyperosmotic (3% NaCl) releasing media were used to determine the degree of osmotically controlled release of drug from the elastomer. The osmolalities of these releasing media, as well as PN and the excipient trehalose are reported in table 4.3

Table 4.3. Osmolality of PN solution and release media.[31]

Solution	Osmolality (mOsm/kg)
Deionized Water	20
Phosphate Buffer Saline (PBS) of pH= 7.4	280
3 % NaCl	919
Saturated Pilocarpine Nitrate	791
Trehalose	1524

Influence of Particle size on drug release: Figures 4.4 and 4.5 show the release profiles of PN of different particle sizes, 45, 100, and 300 μm, respectively, from tabular and cylindrical devices in PBS media. It was noted that the release profiles consist of three distinct regions. A predominant burst release which lasted for the first 24 hours accounting for 40% release of the loaded drug. This portion resulted from the drug particles dispersed at or close to the surface of the devices. The burst amount in the two devices was almost the same. This initial burst segment was similar to many biodegradable polymers.[34-37] The initial burst release was followed by a slower sustained and constant release period that lasted up to 10 days. This constant release segment is due to both diffusion and osmotic phase and accounted for 30-40% release of PN. The further increase in the release rate was due to the degradation of the elastomers.

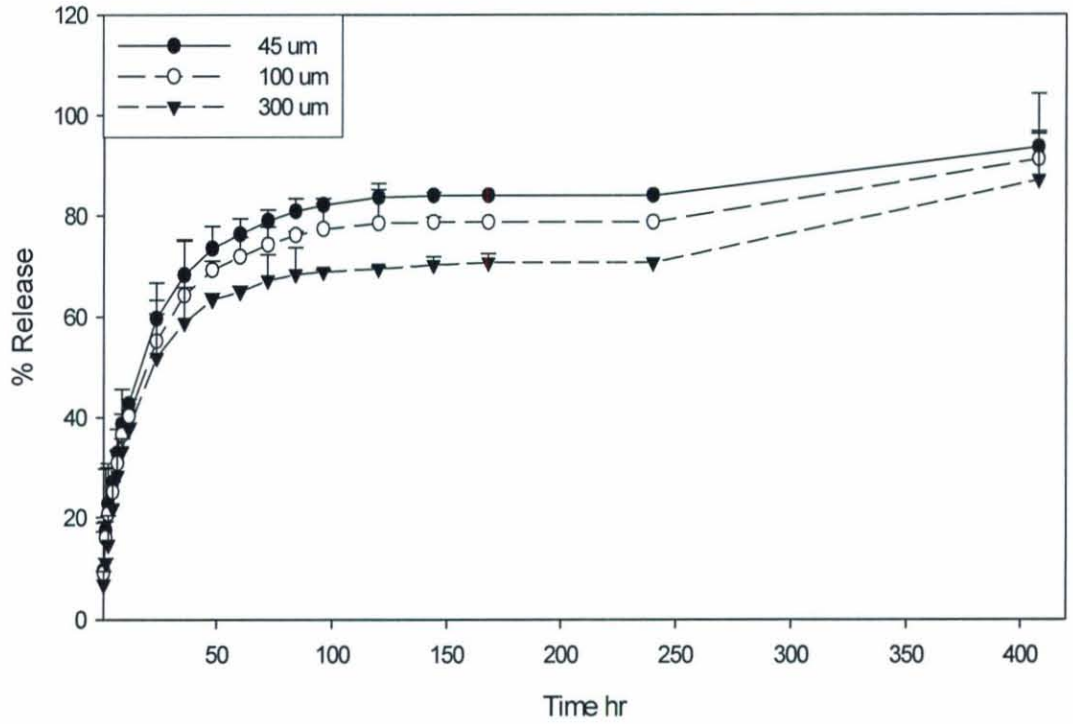

Figure 4.4 Cumulative percent PN released from 10 % w/w loaded tablet devices with different particle sizes in PBS medium at 37 °C.

The high release during the first and second phase of the release profiles can be attributed to the hydrophilicity of both the polymeric network and the PN salt. It should be noted that these experiments were performed under highly-accelerated *in vitro* degradation processes that increased the high degradation rate of these hydrophilic elastomers.

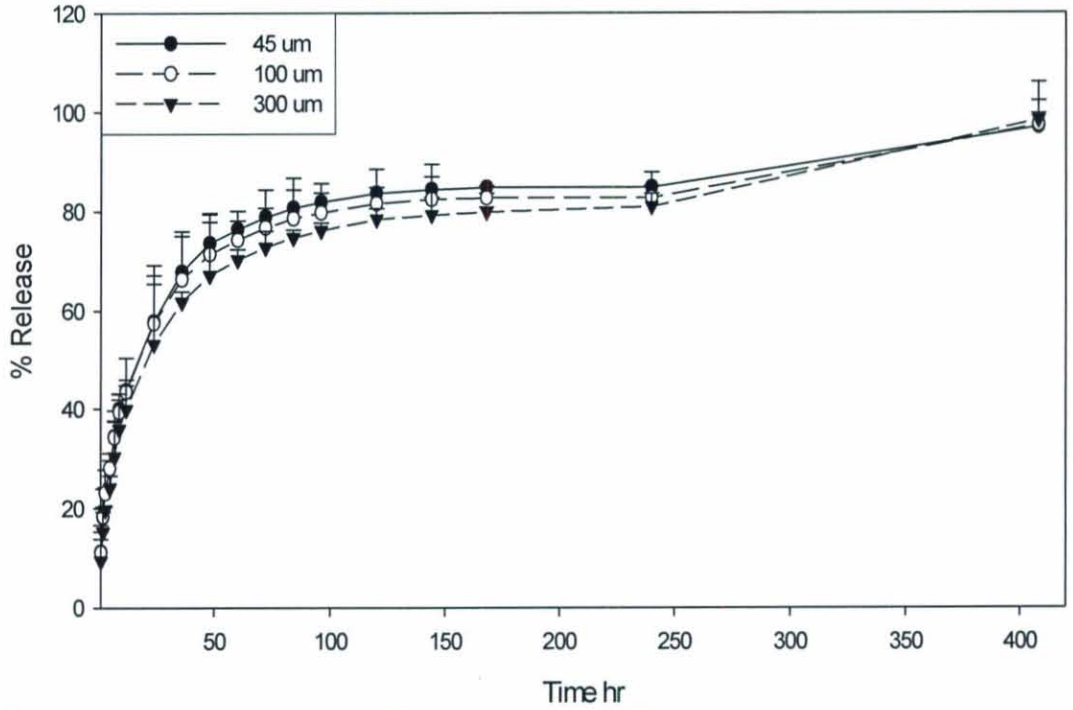

Figure 4.5 Cumulative percent PN released from 10 % w/w loaded cylinder devices with different particle sizes in PBS medium at 37 °C.

The release profiles of the devices formulated with the same volumetric loading but with smaller drug particle sizes released drug faster than those devices with larger particle sizes. This phenomenon can be attributed to the fact that the small particle sizes dissolve more rapidly and require less water vapour to rupture the capsules. Furthermore, the shorter distances between the drug particle layers would lead to a shorter time to rupture the encapsulated drug particles within the elastomeric matrix. As shown in Figures 4.4 and 4.5, there was no significant difference between the release profiles of the tabular and cylindrical devices. Clearly, the device geometry did not play a major role in the release of the PN.

Influence of Osmolality of the Releasing Media on Drug Release: The effect of the release media on the release rate of the tabular and cylindrical network is shown in Figures 4.6 and 4.7 respectively. It was noted for the three different dissolution media that the constant release phases started from day 2 up to day 10 for both the tabular and cylindrical devices and were within the same range. This indicates that one release mechanism is controlling the release of PN from the these networks, regardless of the release medium used.

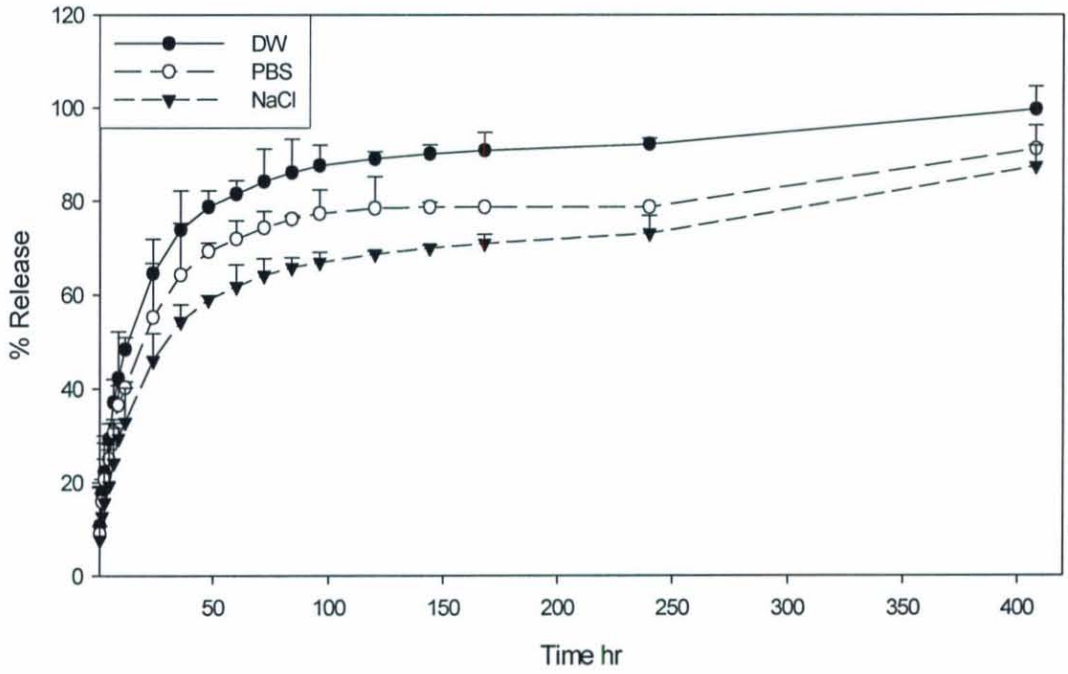

Figure 4.6 Cumulative percent PN released from 10 % w/w loaded tablet devices of 100μm particle size in different osmotic media at 37 °C.

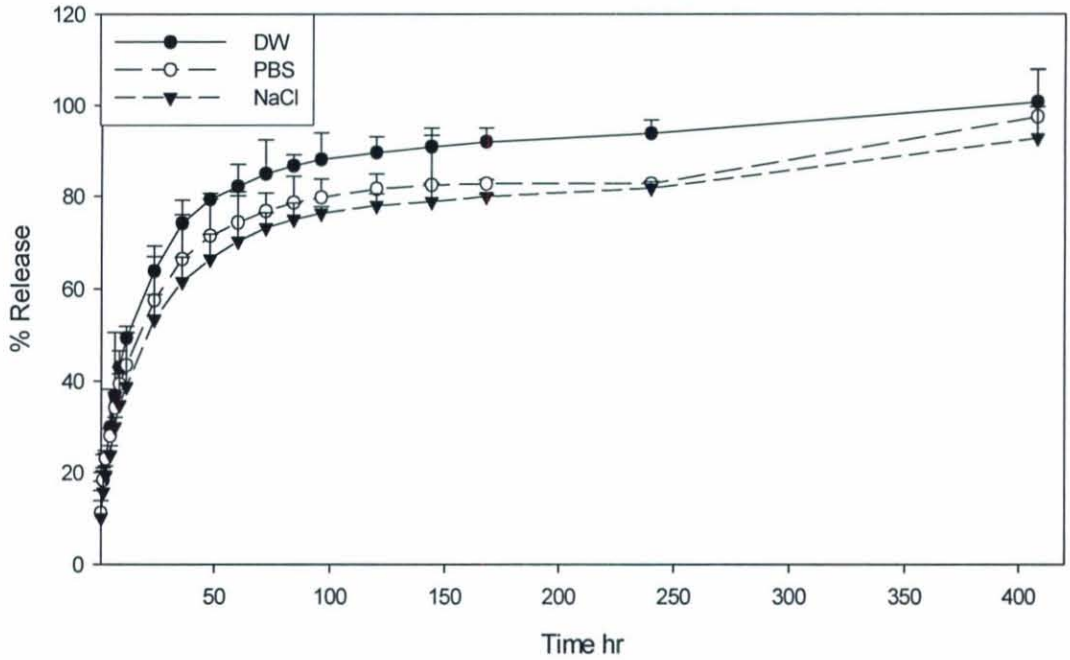

Figure 4.7 Cumulative percent PN released from 10 % w/w loaded cylinder devices of 100μm particle size in different osmotic media at 37 °C.

The osmotic activity of the NaCl media (919 mOsmol/Kg), is higher than that of a saturated PN solution (791 mOsmol/Kg). No osmotic release occurs under these conditions. The profile of drug release in 3% NaCl is due to the degradation of the elastomer. The increase in the amount of the drug released into the PBS medium is due to an osmotic effect, as the osmotic activity of the PBS medium (280 mOsmol/Kg) is lower than that of saturated PN solution. Even more drug was released when the the medium was deionized water.

The predominant mechanism of drug release was degradation with an additional osmotic effect when the releasing medium had a lower osmolality than a saturated PN solution. The osmotic effect when the releasing medium was PBS was more clearly seen

in the tablet than the cylinder. This difference might be attributed to differences in the surface area of the two devices.

One of the successful strategies utilized to maintain the stability and activity of therapeutic proteins is to coformulate them with stabilizing agents such as trehalose and mannitol.[24] Such a strategy would offer protection to the protein from aggregation. PN, as a model for a protein drug, was formulated with trehalose to study the effect of this osmotically active agent on the release rate. Two polymeric devices with tabular and cylindrical geometries were loaded with a 1:1 ratio of trehalose and PN with a total weight fraction of 10% w/w with a 100 μm particle size.

.

Figures 4.8 and 4.9 show the release profiles from tabular and cylindrical devices in PBS at pH = 7.4. The addition of the high osmotic excipient, trehalose, resulted in an increased release rate in all phases. More than 50% was released in the initial burst, within the first day, with the balance of the 85% total release being released within 5 days. The increase in the release of PN was greater in the tablet than the cylinder.

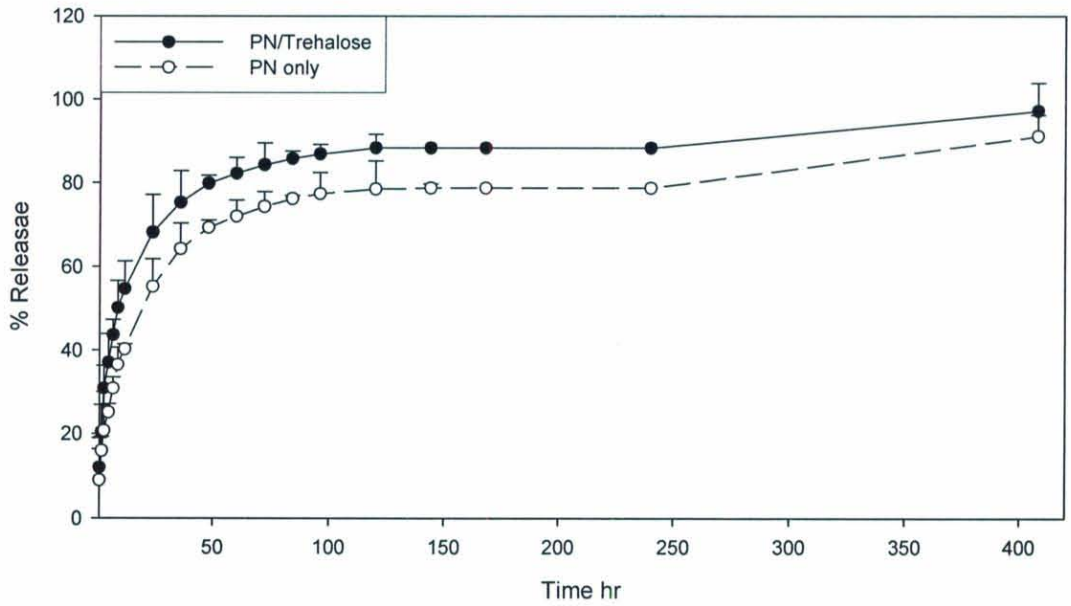

Figure 4.8. Cumulative percent PN released from 10 % w/w loaded tablets of 100 μm particle size with or without trehalose in PBS medium at 37 °C.

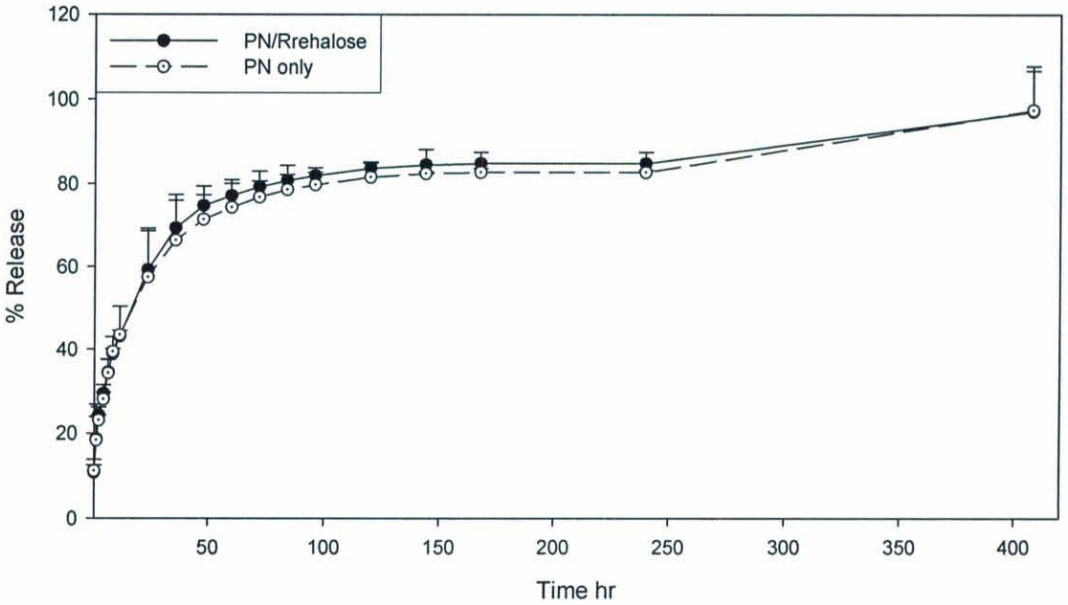

Figure 4.9. Cumulative percent PN released from 10 % w/w loaded cylinders of 100 μm particle size with or without trehalose in PBS medium at 37 °C.

Based on the above observations, it is evident that the osmotic release mechanism plays a role in the release kinetics of PN since the incorporation of the highly osmotic release agent, trehalose, increased the amount of drug in the tabular device until all the drug that was loaded was released. There was no significant additional release of drug in the presence of trehalose in the cylinders.

Release of rhEND from the Elastomer Formed from POT-2: The above experiments were carried out to establish the conditions for the release of END from the elastomer. The main problem in the incorporation of proteins in a polymer delivery device is the protein aggregation that occurs during the loading step. Excipients were used in the formulation to prevent such a problem.

Trehalose was shown to be a good stabilizer of proteins,[89] and, as was shown above, increased the release of a peptidomimetic drug from the elastomer. It was expected that trehalose would act to stabilize END and increase the amount of END released from the polymer.

Bovine serum albumin (BSA) was also shown to be a powerful lyoprotectant for proteins. This effect is attributed to its role in the inhibition of the pH drop that occurs during lyophilization in a buffer and inhibition of the protein adsorption to the surface.[38] In addition, it would protect the protein from the acidic monomers formed from the degraded polymer within the releasing medium. Therefore, lyophilization in the presence of trehalose and BSA would provide the best protection for END during the device

preparation and the protection would extend during the release in the releasing medium. In addition these two excipients would block the exposure of END to the generation of free radicals in the solution and to UV radiation during photo-crosslinking.

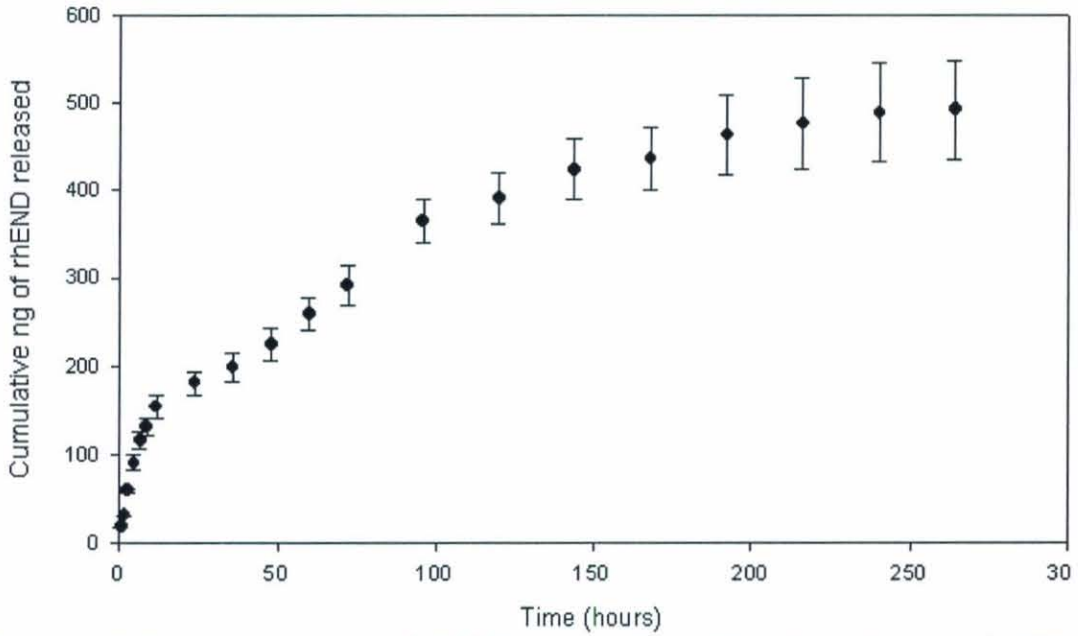

Figure 4.10. Cumulative amount of rhEND released from 10% w/w loaded slabs in PBS medium from a slab at 37 °C detected using ELISA assay from stored frozen aliquots. Values are mean ± (standard deviation).

Figure 4.10 shows the release profile for rhEND from a slab of the elastomer in PBS. The slabs were used in this experiment instead of the tablets because of economic considerations. The release profile consists of three distinct phases. The initial burst release segment occurred during the first 9 hours of the release study and accounted for 30% of the release of END. This initial phase was followed by a slower, linear, constant, and sustained release for 5 days and accounted for an additional 20% of the release of the drug. Finally, the last release segment of the profile was attributed to polymer degradation

and was extended for another week until the remainder of the drug particles were released.

The release profile was distinctly different from that of PN. The difference might be due to the presence of BSA or the geometry of the delivery system since the slabs were smaller and thinner. Also, the two drugs were different, one was a peptidomimetic drug and the other was a protein. Further experiments would need to be carried out to determine the reasons for the differences.

4.5 CONCLUSIONS

A solvent free polymerization was carried out using a 1:1 ratio of L-tartaric and 1,8-octanediol to produce a polyester POT prepolymer. The acrylation reaction was started by adding different ratios of ACRL to convert the terminal OH groups into photosensitive vinyl termini. Higher amounts of ACRL used in the reaction resulted in an increase in the percentage conversion with an approximate complete conversion achieved when 2 moles of ACRL were used to react with 1 mole of POT prepolymer.

A release study of PN (10% w/w loading) from monolithic tablets and cylinders of the prepared photocured elastomers was carried out. The release profiles were divided into three release phases in which the second linear release phase was a mix of osmotic release and diffusion but mainly dominated by a degradation mechanism which was obvious during the last phase of the release. The release profile was unchanged when PN was co-formulated with trehalose, but more drug was released. Upon using this excipient,

a larger fraction of PN was released during the initial burst phase, then the release became linear until complete PN release was achieved. In this situation, osmotic release contributed to drug release. Our results show that smaller particle sizes are released more rapidly from photocured devices as compared to drug particles of larger sizes. In addition, the osmolality of the releasing medium has an effect on the release rate, however, geometrically different designs do not play a significant role on the release of PN from these two different devices.

The objective of this study was to use the photocured elastomer for the delivery of END. The study demonstrated that the device has a potential to be utilized in delivery of END in constant and sustained release fashion, but only for a short period of time. Therefore, continuation of this work would be to extend the time period of release by incorporation of hydrophobic oligomers to decrease the degradation rate of the polymer, while maintaining the effect of the excipients on the activity and stability of END.

This novel biodegradable elastomeric drug delivery vehicle can be considered a potential drug delivery device for proteins other than END. Further studies concentrated with END activity, conformational changes and possible denaturation and aggregation of the END particulates are required.

4.6 REFERENCES

1. Yang, C.; Sodian, R.; Fu, P.; Luders, C.; Lemke, T.; Du, J.; Hubler, M.; Weng, Y.; Meyer, R.; Hetzer, R. In vitro fabrication of a tissue engineered human cardiovascular patch for future use in cardiovascular surgery. *Ann. Thorac. Surg.* 2006, *81,* 57-63.

2. Sodian, R.; Fu, P.; Lueders, C.; Szymanski, D.; Fritsche, C.; Gutberlet, M.; Hoerstrup, S. P.; Hausmann, H.; Lueth, T.; Hetzer, R. Tissue engineering of vascular conduits: fabrication of custom-made scaffolds using rapid prototyping techniques. *Thorac. Cardiovasc. Surg.* 2005, *53,* 144-149.

3. Sodian, R.; Loebe, M.; Hein, A.; Martin, D. P.; Hoerstrup, S. P.; Potapov, E. V.; Hausmann, H.; Lueth, T.; Hetzer, R. Application of stereolithography for scaffold fabrication for tissue engineered heart valves. *ASAIO J* 2002, *48,* 12-16.

4. Sodian, R.; Sperling, J. S.; Martin, D. P.; Egozy, A.; Stock, U.; Mayer, J. E., Jr.; Vacanti, J. P. Fabrication of a trileaflet heart valve scaffold from a polyhydroxyalkanoate biopolyester for use in tissue engineering. *Tissue Eng* 2000, *6,* 183-188.

5. Wintermantel, E.; Mayer, J.; Ruffieux, K.; Bruinink, A.; Eckert, K. L. [Biomaterials, human tolerance and integration]. *Chirurg* 1999, *70,* 847-857.

6. Diez, S.; Tros, d., I Versatility of biodegradable poly(D,L-lactic-co-glycolic acid) microspheres for plasmid DNA delivery. *Eur. J Pharm. Biopharm.* 2006, *63,* 188-197.

7. Tang, G. P.; Guo, H. Y.; Alexis, F.; Wang, X.; Zeng, S.; Lim, T. M.; Ding, J.; Yang, Y. Y.; Wang, S. Low molecular weight polyethylenimines linked by beta-cyclodextrin for gene transfer into the nervous system. *J Gene Med.* 2006, *8,* 736-744.

8. D'Souza, R.; Mutalik, S.; Udupa, N. In Vitro and In Vivo preparation evaluations of bleomycin implants and microspheres Prepared with DL-poly (lactide-co-glycolide). *Drug Dev. Ind. Pharm.* 2006, *32,* 175-184.

9. Ekholm, M.; Helander, P.; Hietanen, J.; Lindqvist, C.; Salo, A.; Kellomaki, M.; Suuronen, R. A histological and immunohistochemical study of tissue reactions to solid poly(ortho ester) in rabbits. *Int. J Oral Maxillofac. Surg.* 2006, *35,* 631-635.

10. Chorny, M.; Mishaly, D.; Leibowitz, A.; Domb, A. J.; Golomb, G. Site-specific delivery of dexamethasone from biodegradable implants reduces formation of pericardial adhesions in rabbits. *J Biomed. Mater. Res. A* 2006, *78,* 276-282.

11. Chia, S. L.; Gorna, K.; Gogolewski, S.; Alini, M. Biodegradable elastomeric polyurethane membranes as chondrocyte carriers for cartilage repair. *Tissue Eng* 2006, *12,* 1945-1953.

12. Qiu, H.; Yang, J.; Kodali, P.; Koh, J.; Ameer, G. A. A citric acid-based hydroxyapatite composite for orthopedic implants. *Biomaterials* 2006, *27,* 5845-5854.

13. Wang, Y.; Ameer, G. A.; Sheppard, B. J.; Langer, R. A tough biodegradable elastomer. *Nat. Biotechnol.* 2002, *20,* 602-606.

14. Younes, H. M.; Bravo-Grimaldo, E.; Amsden, B. G. Synthesis, characterization and in vitro degradation of a biodegradable elastomer. *Biomaterials* 2004, *25,* 5261-5269.

15. Gu, F.; Younes, H. M.; El Kadi, A. O.; Neufeld, R. J.; Amsden, B. G. Sustained interferon-gamma delivery from a photo-crosslinked biodegradable elastomer. *J Control Release* 2005, *102,* 607-617.

16. Missirlis, D.; Kawamura, R.; Tirelli, N.; Hubbell, J. A. Doxorubicin encapsulation and diffusional release from stable, polymeric, hydrogel nanoparticles. *Eur. J Pharm. Sci* 2006, *29,* 120-129.

17. Gu, F.; Younes, H. M.; El Kadi, A. O.; Neufeld, R. J.; Amsden, B. G. Sustained interferon-gamma delivery from a photo-crosslinked biodegradable elastomer. *J Control Release* 2005, *102,* 607-617.

18. Gu, F.; Neufeld, R.; Amsden, B. Osmotic-driven release kinetics of bioactive therapeutic proteins from a biodegradable elastomer are linear, constant, similar, and adjustable. *Pharm. Res* 2006, *23,* 782-789.

19. Gu, F.; Neufeld, R.; Amsden, B. Sustained release of bioactive therapeutic proteins from a biodegradable elastomeric device. *J Control Release* 2007, *117,* 80-89.

20. Gu, F.; Neufeld, R.; Amsden, B. Maintenance of vascular endothelial growth factor and potentially other therapeutic proteins bioactivity during a photoinitiated free radical cross-linking reaction forming biodegradable elastomers. *Eur. J Pharm. Biopharm.* 2007, *66,* 21-27.

21. Amsden, B. Review of osmotic pressure driven release of proteins from monolithic devices. *J Pharm. Pharm. Sci* 2007, *10,* 129-143.

22. Gu, F.; Neufeld, R.; Amsden, B. Osmotic-driven release kinetics of bioactive therapeutic proteins from a biodegradable elastomer are linear, constant, similar, and adjustable. *Pharm. Res* 2006, *23,* 782-789.

23. Amsden, B.; Cheng Y-L A generic protein delivery system based on osmotically rupturable monoliths. *J Control Release* 1995, *33,* 99-105.

24. Gu, F.; Neufeld, R.; Amsden, B. Sustained release of bioactive therapeutic proteins from a biodegradable elastomeric device. *J Control Release* 2007, *117,* 80-89.

25. Amsden, B.; Cheng Y-L; Goosen, M. F. A. A mechanistic study of the release of osmotic agents from polymeric monoliths. *J Control Release* 1994, *30,* 45-56.

26. Amsden, B. G.; Misra, G.; Gu, F.; Younes, H. M. Synthesis and characterization of a photo-crosslinked biodegradable elastomer. *Biomacromolecules.* 2004, *5,* 2479-2486.

27. Amsden, B.; Cheng Y-L Enhanced fraction releasable above percolation threshold from monoliths containing osmotic excipients. *Journal of controlled release* 1994, *31,* 21-32.

28. Matsuda, T.; Mizutani, M. Molecular Design of Photocurable Liquid Biodegradable Copolymers. 2. Synthesis of Coumarin-Derivatized Oligo(methacrylate)s and Photocuring. *Macromolecules* 2000, *33,* 791-794.

29. Ichimura, K.; Akita, Y.; Akiyama, H.; Kudo, K.; Hayashi, Y. Photoreactivity of Polymers with Regioisomeric Cinnamate Side Chains and Their Ability To Regulate Liquid Crystal Alignment. *Macromolecules* 1997, *30,* 903-911.

30. Changez, M.; Koul, V.; Dinda, A. K. Efficacy of antibiotics-loaded interpenetrating network (IPNs) hydrogel based on poly(acrylic acid) and gelatin for treatment of experimental osteomyelitis: in vivo study. *Biomaterials* 2005, *26,* 2095-2104.

31. Younes, H. M. New Biodegradable Elastomers for Interferon Gamma Delivery. 2002. Faculty of Pharmacy and Pharmaceutical Science, University of Alberta. Ref Type: Thesis/Dissertation

32. Quinn, C. P.; Pathak, C. P.; Heller, A.; Hubbell, J. A. Photo-crosslinked copolymers of 2-hydroxyethyl methacrylate, poly(ethylene glycol) tetra-acrylate and ethylene dimethacrylate for improving biocompatibility of biosensors. *Biomaterials* 1995, *16,* 389-396.

33. Choi, S. I.; Christensen, M. B.; Fredin, N.; Pitt, W. G. Swellable coatings for hearing aid applications. *J Biomater Appl.* 2005, *20,* 123-135.

34. Choi, S.; Kim, S. W. Controlled release of insulin from injectable biodegradable triblock copolymer depot in ZDF rats. *Pharm. Res* 2003, *20,* 2008-2010.

35. Lemmouchi, Y.; Schacht, E.; Lootens, C. In vitro release of trypanocidal drugs from biodegradable implants based on poly(epsilon-caprolactone) and poly(D,L-lactide). *J Control Release* 1998, *55,* 79-85.

36. Kranz, H.; Bodmeier, R. A novel in situ forming drug delivery system for controlled parenteral drug delivery. *Int. J Pharm.* 2007, *332,* 107-114.

37. Sharifpoor, S.; Amsden, B. In vitro release of a water-soluble agent from low viscosity biodegradable, injectable oligomers. *Eur. J Pharm. Biopharm.* 2007, *65,* 336-345.

38. Wang, W. Lyophilization and development of solid protein pharmaceuticals. *Int. J Pharm.* 2000, *203,* 1-60.

Chapter 5.

5.1 Summary

The main objective was to emphasize the need to design a new local delivery system to produce a sustained release of END within the therapeutic window of the drug. Initial steps towards this goal have been achieved by incorporating END with other osmotic excipients as solid particles into a photocured elastomer which allowed the protein to release at a controllable rate into a localized area.

Goal: The review of the literature focused on the evaluation of the different drug delivery systems and the routes of administration for END, as a therapeutic protein for cancer treatment. Long term, site localized and sustained release of END is a very desirable goal in order to maximize the therapeutic outcome of the drug and at the same time to minimize the side effects due to the exposure of the other body parts to the inhibitory effect of this powerful angiogenesis inhibitor.

Thermal Preparation of Elastomers and Characterization: A solvent free polymerization of 1:1 L-tartaric acid and 1,8-octanediol to form a semicrystalline POT prepolymer was carried out. The reactive prepolymer that was formed was thermally crosslinked with different ratios of 2,2-bis(ε-caprolactone-yl)-propane (BCP) using stannous octanoate (SnOct) as a catalyst to prepare crosslinked elastomers. All the polymer products were thermally, chemically, and mechanically characterized. Accelerated *in vitro* degradation studies were conducted. These studies demonstrated a

direct correlation between the loss of mechanical properties with time, and confirmed that bulk hydrolysis was the predominant mechanism of polymer degradation. As a final observation, the elastomer crosslinking was traditionally performed under elevated temperature, which is not feasible for most drugs and certainly not for protein drugs; therefore, it was necessary to find a method that does not require high temperatures in the preparation of the elastomer. It was decided to develop a non-thermal and photocuring method to prepare a photo-crosslinked elastomer to be used for delivery of END.

Photo-crosslinked Preparation of Elastomers and Drug Release Studies: An aliphatic polyester prepolymer was synthesized via a polycondensation reaction of L-tartaric acid with 1,8-octanediol to form a POT semicrystalline prepolymer. The purified prepolymer was reacted stepwise with acryloyl chloride (ACRL) and the purified acrylated poly(octanediol-tartarate) (APOT) prepolymer was then mixed with a UV initiator and subjected to UV light to form the amorphous photocurable elastomer. For *in vitro* release studies, PN powder of three different particle sizes was mixed with APOT to achieve a 10% w/w (approximately a 14.4% v/v) loading. Lyophilized END with trehalose and bovine serum albumin (BSA) was also mixed with APOT to achieve the same volumetric loading. Prepared devices were used to conduct release studies. The release profiles showed that devices formulated with the same volumetric loading and smaller drug particle size released drug more rapidly than the devices with a larger particle size. It was also shown that osmotic release was a contributing mechanism governing the linear release pattern of PN from the new POT elastomers. The study demonstrated that the device has a potential to be utilized in the delivery of END or any

other hydrophilic protein drug in a constant and sustained release fashion, but only for a short period of time. Further modifications to the elastomer will be required to extend the period of sustained release. Using different ratios of L-tartaric with 1,8-octanediol and/or changing the photosensitive termini of the prepolymer may change the crosslinking density. That may slow the degradation process and increase the period of the drug release.